# MICRO-STRUCTURE ANALYSIS OF PLANT TISSUES

Edited by

Krystyna Konstankiewicz, Artur Zdunek
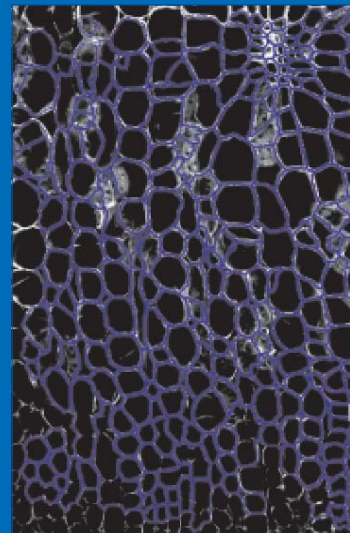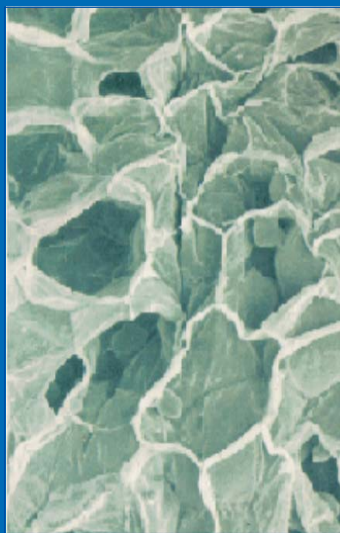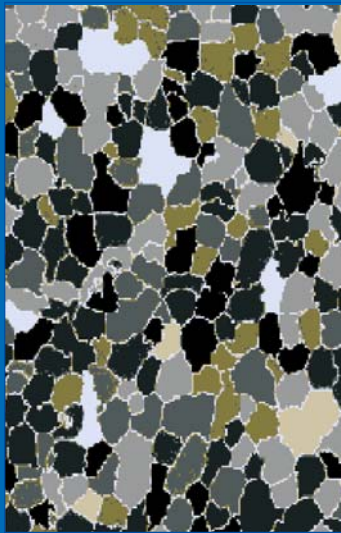
Centre of Excellence for Applied Physics
in Sustainable Agriculture AGROPHYSICS
ul. Doświadczalna 4, 20-290 Lublin, Poland

Institute of Agrophysics of the
Polish Academy of Sciences
ul. Doświadczalna 4, 20-290 Lublin, Poland

MICRO-STRUCTURE ANALYSIS OF PLANT TISSUES

EDITORS:
Krystyna Konstankiewicz
Artur Zdunek

Lublin 2005

PREFACE

The subject matter of research conducted by the Department of Agricultural Materials in Institute of Agrophysics PAS in Lublin concerns one of the most important problems of contemporary agriculture, related to the quality of agricultural production. High quality product means "health food", the production of which minimizes the hazard of interference with the natural environment, the product itself being under constant control and protection. Studies in this field require increasing amounts of knowledge on the object studied itself and on its behavior under a variety of effects. Contemporary food processing industry needs raw materials of high quality, homogeneity and stability of properties, meeting specific requirements for oriented utilization. Among many factors that influence on quality and utilization of agricultural plant product one of the most important is its micro-structure. The micro-structure means here cellular skeleton of a tissue. However, the problem that we still face up is how to quantify the micro-structure. For last 10 years we have been intensively worked on it. Our goal is to develop efficient computer method of micro-structure quantification. In order to do this, we have adopted microscopic techniques and sample preparation methods known in biology and material sciences. However, the first conclusion of our research was that a real plant tissue requires individual and original treatment. Being aware of that, we are still improving and extending our methods to new microscopes and new materials.

This book is a state-of-art of our approach to the problem. More than 10 years experience with microscopy and image analysis has allowed presenting in this book how to obtain image of plant tissue and how to analyze it in order to quantify the micro-structure of plant tissues. Each part of this book was written by other author, researcher in the Department of Mechanics of Agricultural Materials, an experienced specialist at the topic presented. The first chapter gives overview of our approach to the problem. The goal of following chapters was presenting principles of a few microscopes that can be used for micro-structure quantification. This part was written by daily users of the microscopes. To prepare next Chapter we have invited one of the most word wide famous specialists at image analysis Prof. Leszek Wojnar. He was so kind to present tips and tricks with deep scientific interpretation of digital visualization

and image analysis. The next chapter focuses on application of image analysis to images of plant tissues obtained by conventional and confocal microscopes. This part is a summary of research conducted in the Department of Mechanics of Agricultural Materials.

We hope that the book will be a source of knowledge about microscopes and image analysis for students and researchers interested in application of these methods to improving and controlling quality of plant food products.

Editors

Krystyna Konstankiewicz
Artur Zdunek
Institute of Agrophysics PAS
Department of Agricultural Materials

6

1. THE GOAL OF IMAGE ANALYSIS OF PLANT TISSUE MICRO-STRUCTURE

Krystyna Konstankiewicz[*]

1.1. Material studies in modern agriculture

The latest research programs, also those of the European Union, adopt - as the primary objective of studies - scientific progress generating knowledge with significant impact on the practical implementations. Among this group of research problems one should include work concerning the knowledge and control of the material properties of numerous media.

Highly developed technologies in particular require increasing amounts of knowledge concerning the properties of materials. This is true also with relation to agricultural materials, used both for direct consumption and for industrial processing. In both cases we face increasing demands concerning the quality of the raw material and the final product, as well as the monitoring of material properties throughout the process of production.

Meeting the stringent quality requirements concerning agricultural materials and products may facilitate their entry and stable position in the globalized world market. Coping with this challenge is difficult in view of the extreme competitiveness of the market and the complex legislative procedure concerning new products. Especially high requirements are created for the increasingly popular healthy ecological food, which is related to the observation of stringent standards and to the implementation of the methods of precision agriculture. All the regulations concerning healthy food are extremely restrictive and enforce more and more detailed monitoring of all material properties and of the conditions under which the materials are produced. This is exemplified by the European regulations that restrict access to the market for genetically modified organisms – GMO – that are commonly accepted in other countries.

A product is of good quality if it has a suitable set of properties that can be controlled, even in a continuous manner. One of the solutions for the problem of material quality control can be provided by constant monitoring, ensuring

---
[*] Krystyna Konstankiewicz, Professor
Institute of Agrophysics, Polish Academy of Sciences
ul. Doświadczalna 4, 20-290 Lublin 27, Poland
e-mail: konst@demeter.ipan.lublin.pl

the traceability of properties of raw materials as well as products at every stage of processing, including the conditions of growth and storage.

Traceability as an intrinsic aspect of product quality control means the assurance of the possibility of tracing back through the history of the raw material and the product with records of changes in all their properties to determine and maintain their characteristic features. This is a very difficult and costly task, especially in the situation of growing customer and consumer expectations concerning the stability of prices throughout the production path. This approach means an enormous challenge not only for the researchers but also for the engineering solutions for continuous recording and processing of huge amounts of data, especially as the expectations concern not only the knowledge of the product quality but also information on the flexible modification of the production process, including the economic dimension.

Determination of the quality of raw materials and products involves determinations of characteristic physical values, representative both for a single object and for a bulk of objects, in an objective, repeatable and, best of all, automated manner. In the case of agricultural raw materials and products, work on the improvement of traceability is difficult, mainly due to their extensive biological diversity and to the need of consideration of a large number of factors resulting from the complex environmental conditions of cultivation and growth. In most cases, experimental materials of such complexity require the development of original methods of measurement, preceded with fundamental studies, as there is no possibility of satisfactory adaptation of measurement systems commonly used in studies on other materials. Also, the newly developed methods of study require constant modifications and improvement due both to the rapid development of measurement techniques and to the changing cultivar requirements related to the assigned purpose of agricultural raw materials and products.

1.2. Structure as a material feature

One of the fundamental physical features characterizing materials studied is the structure that has a decisive effect on other properties of the materials, e.g. physical, chemical, or biological.

Material studies have a long tradition backed with practical experience in the field of production of a great variety of materials. One of the fundamental laws in the science of materials is that two materials with identical structures have identical properties irrespective of the manner in which the structure was formed. Quantitative description of the structure of a material studied can, therefore, provide the basis for comparison of different objects or for recording changes

within an object, caused e.g. by a technological process, storage, or resulting from the non-homogeneity of the material. On the other hand, knowledge on the effect of structure on the properties of materials can be utilized for the control of technological processes in order to obtain materials with required properties and also for designing completely new materials.

However, practical utilization of structural studies is possible only when their results are presented with the help of numbers. In the practical and common application description of the type of better-worse is insufficient. It was the need for utilization of structural studies that spurred the creation of quantitative methods of structure description that were then developed as stereological methods and now constitute a separate branch of knowledge. The rapid development of theoretical stereology in recent years is related mainly with the development of techniques of observation of microstructure and of analysis of the obtained information.

In the case of plant materials we deal with cellular structure of considerable non-homogeneity and instability with frequent areas of discontinuity of relatively large dimensions. The morphology of their structure is a derivative of numerous factors, such as plant variety, object size and shape, type of tissue, method of cultivation, climatic conditions, time of harvest, post-harvest processing, storage conditions. Such materials are especially susceptible to a variety of effects, e.g. mechanical, thermal, which often result in structure changes that may subsequently cause numerous processes lowering the quality of the product. Among the agricultural plant materials, soft tissues are especially susceptible to structure changes and to various kinds of damage. In many cases, an additional factor conducive to the occurrence of structure changes is high moisture content of the medium. Due to the "delicate" structure of the objects studied, even the preparation of samples for observation and analysis may present considerable problems. Especially when the study is concerned not just with the input status of the structure, but also changes that occur in the structure as a result of various effects.

1.3. Observation of plant tissue structure

The problem of quantitative description of the cellular structure of agricultural plant materials is related to the selection of a suitable method for the acquisition of images of the structure, preferably in its natural condition without any preparation, and then for the recording and analysis of the images obtained.

The continually perfected methods of microscopy permit the observation of structure under magnification, and digital techniques of image recording allow the analysis of information contained in the images obtained. The broad array

of various types of microscopes available, e.g. optical, confocal, electron, acoustic, X-ray, with the abundance of accessories, optional equipment and software that provide routine operation with very good results for a variety of materials, create extensive possibilities also for the research on plant tissue. However, while the selection of suitable equipment is not an easy task, it is frequently of decisive importance for the success of solving a given problem, and can help economize on both the time and the cost of studies. The most important is the definition of the objective of the study, i.e. concentration on the significant elements of the structure with the exclusion of unnecessary details and assurance of methodological correctness. For example, the application of initial preparation of specimens, from simple slicing to fixation of structure, may introduce disturbance to the structures observed, which has to be taken into consideration in subsequent stages of the study and in the formulation of conclusions.

In the study of the physical properties of plant tissue methods are sought for obtaining such an image of the tissue structure that will clearly show cell walls which determine the dimensions of the whole cell. The arrangement of cells on the surface observed provides information on the spatial organization of elements of the structure, and also on possible changes to the structure, resulting from processes under study. Studies as well as comparative observations of plant tissue require numerous measurements, therefore there is a growing tendency of employing computer methods for the purpose. For images with good quality, analysis can be conducted automatically with the help of professional dedicated software.

Images of structure for computer analysis should be of good quality, and primarily with very good contrast. Elements of structure that are of interest should be clearly identifiable, countable and measurable. This is not an easy task in the case of plant tissue that has little colour and sometimes is even transparent and, additionally, due to the high content of water, subject to rapid drying and deformation during observation.

Quantitative description of cellular structure requires the development of suitable methods for the study of a given object. Even with very good procedures, however, the experience and knowledge on the part of the observer is essential for proper interpretation of information contained in structure images.

1.4. Analysis of plant tissue structure images

The use of image analysis software may seem an easy task, especially in the situation of easy access to professional software and to encouraging results for other materials. However, it turns out that the task is a complex one and requires experience and knowledge not only about the object itself, but also about methods of obtaining images, their acquisition and processing, and – finally – analysis. In spite of the continual advances in specialist knowledge concerning image analysis and, sometimes, the resultant problems with its understanding, it is absolutely indispensable at a basic level for every user in order to avoid errors that may result in irreversible effects at the final stage of formulation of conclusions. Similar problems are faced by everyone who undertakes the study of the cellular structure of plant tissue. The authors of this monograph also had to face similar problems in their work, but they also have already some practical experience.

Several years ago, at the Laboratory of Mechanics of Plant Materials, we started work on the quantitative description of cellular structures of plant media. Many times in our work we made use of the achievements of stereology – a totally different branch of science but very much open to new research challenges. Thanks to the high activity of the Polish Stereological Society we could take advantage of specialized publications, conferences and workshops, as well as of individual consultations that facilitated for us the understanding of very difficult problems of stereology. It was during the 6th European Congress of Stereology in Prague in 1993 that we established cooperation with the creators of an original confocal microscope which met our expectations related to the observation of cellular plant structures – from a thin slice specimen under the surface of a transparent object, in natural state without initial preparation, in real time, with the possibility of 3D reconstruction of the structure. The equipment set that was developed then is still in use and, in spite of the increasing competitiveness of numerous newer types of microscopes, still fulfils its function well.

To date, in our research we have also been using a confocal laser microscope permitting the observation of selected elements of the structure thanks to suitable staining of specimens, a classical optical microscope for the observation of cellular structure of fixed specimens in transmitted light, and also a scanning electron microscope for qualitative estimation of the structures under observation.

The microscope images obtained are used primarily for the study of the geometric features of the cellular skeleton as the fundamental characteristic of the structure of plant tissues. The parameters determined that quantitatively describe the size and shape of cells as well as their distributions, permit the identification

of the relation between the structure and other properties of the medium, and can also be used in modelling the structure of plant tissue.

We are grateful to Professor Leszek Wojnar for his unfailing support and understanding of our complex problems of the cellular structure of agricultural plant media and for being the author of the chapter which provides a lucid introduction to the difficult problems of image analysis.

All the presented methods of obtaining microscope images – confocal microscopes: TSRLM and CSLM and the optical and electron microscopes – as well as analyses of the images are the results of work of the Group for the Mechanics of Agricultural Materials. Studies in the field of quantitative description of the structure of plant media are continued and up to date information on their results are presented on our website: www.mam.lublin.pl

2. MICROSCOPES AND SAMPLE PREPARATION

2.1. Optical Microscope

Marek Gancarz[*]

Microscope is a device for the generation of magnified images of objects or their detail parts, invisible to the naked eye. The images can be viewed directly (conventional optical microscope), photographed (microphotography), projected straight onto a screen (projection optical microscope) or converted (TV optical microscope).

The first microscope was built by a Dutch optician, van Jansen (Fig. 2.1), around 1595. It was a very simple device which permitted the observation of yeast cells.
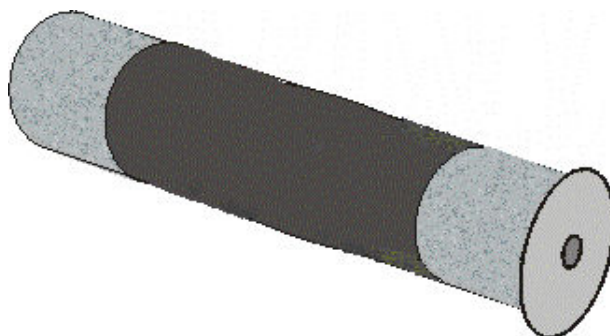

Fig. 2.1. *The first microscope built by van Jansen around 1595.*

In March, 1625, the word „microscope" was used for the first time – in a letter from one of the scientists to the Italian Prince, Federigo Cesie.

[*] Marek Gancarz, MSc
Institute of Agrophysics, Polish Academy of Sciences
ul. Doświadczalna 4, 20-290 Lublin 27, Poland
e-mail: marko@demeter.ipan.lublin.pl

The most dynamic development of the microscope took place in the second half of the 17th century. The first microscopes gave low magnification ratios (up to x60), due to the imperfect lenses of those times. Using just such a microscope with a magnification ratio of only x40, the English scientist Robert Hooke discovered, around 1665, the cellular structure of living organisms. The design of the microscope already resembled the microscopes of the present day (Fig. 2.2), [9, 13, 14].
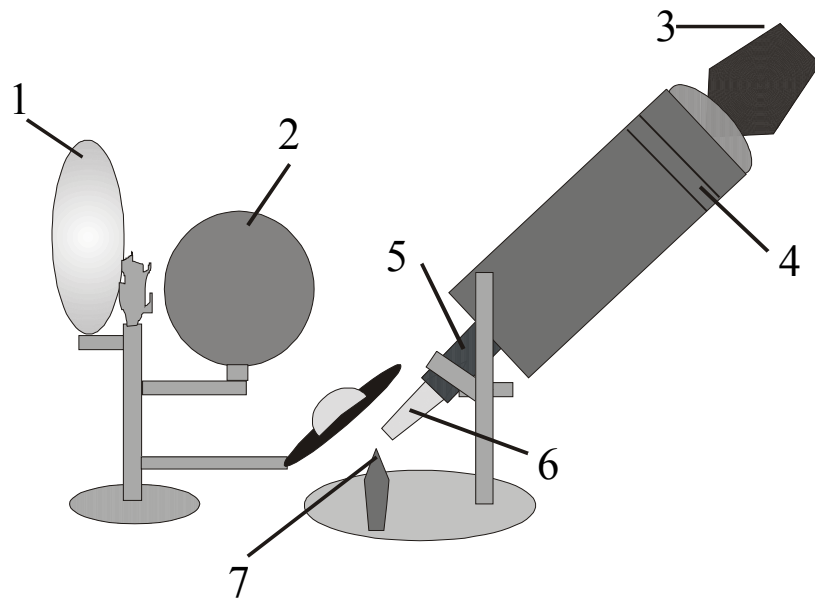
Fig. 2.2. *Schematic of the microscope built by Robert Hooke, 1 – oil lamp, 2 – water flask, 3 – eyepiece, 4 – barrel, 5 – focusing screw, 6 – objective, 7 – specimen holder.*

The microscope had already two separate optical systems – the objective and the eyepiece.

The Dutch naturalist and merchant, Antony van Leeuwenhoek, designed an improved microscope using very short focal length lenses with high precision grinding (for the times). The microscope gave x270 magnification, although its height was 5 cm, and had only one lens. In September, 1674, he informed the Royal Society in London that with the help of the microscope that he built himself ha was able to observe „*very small living creatures*". He was the first man to see bacteria [3, 6, 13, 14].

Possibilities created by the microscope spurred on further work aimed at its improvement. In the 17th century, Giuseppe Campini introduced the dual

14

focusing mechanism permitting the adjustment of distance between the slide and the objective lens, and between the objective lens and the eyepiece; then Divini designed a microscope with a compound objective lens built of two plano-convex lenses. In the same period of time, another contribution to the progress of optical microscopy was made by Bonani who employed a revolutionary zooming mechanism permitting correct focusing on the slide, and designed a two-lens condenser [13, 14].

In the second half of the 18th century, the microscope was equipped with achromatic lenses designed by John Dollond (England) and Joseph von Fraunhofer (Germany). Achromatic lenses (built of a combination of different kinds of glass) were used as early as mid 17th century in building telescopes. However, attempts at employing such lenses in microscopes failed due to the low quality of glass used for their manufacture. Progress in the field, combined with the art of joining lens components with Canadian balm, resulted in the creation, in 1826, of the first microscope with achromatic lenses by Lister and Tulley (Fig. 2.3), [3,6,12].
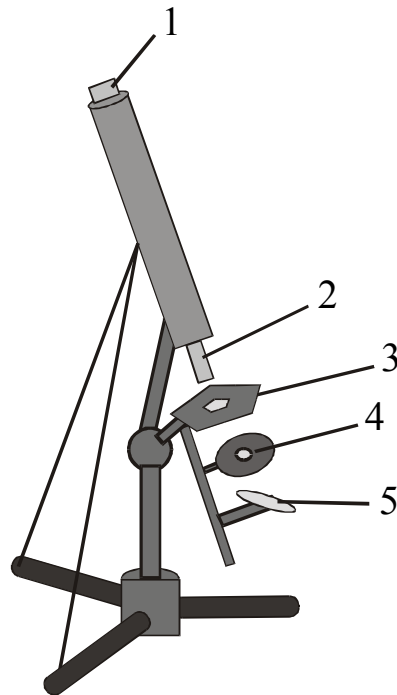

Fig. 2.3. *Schematic of Lister's microscope, one of the first achromatic microscopes - ca. 1826r, 1 – eyepiece, 2 – achromatic objective lens, 3 – stage, 4 – condenser, 5 - mirror.*

In 1830, Lister published the theoretical foundations for building achromatic lenses. His ideas were then employed by other microscope designers [3,14]. Moreover, Giovanni B. Amici discovered a method for the elimination of spherical aberration through the application of a suitable combination of lenses. The two discoveries permitted the building of multi-lens objective lenses and condensers which gave greater magnification ratios while retaining high optical correctness level. In 1827, Amici invented the immersion lens [12,14]. Also in 1872 the German physicist, Ernst Abbe, equipped the microscope with a lamp [13]. At the beginning pf the 20th century the optical microscope was capable of magnification ratios of about x2000. In 1931, a team of German physicists headed by Ernst Rusk (who was awarded the Nobel Prize for that work, in 1986), designed the electron microscope, a usable version of which was built in 1938 by the Siemens company. The microscope permits magnification ratios of the order of x250,000. In 1942, C. Magnan (France) invented so-called proton microscope, the theoretical capabilities of which reach to the level of x5000,000 magnification ratio; in practice, however, its performance is no better than that of the electron microscope. In 1956, the American Ervin W. Mueller designed an ion microscope for examination of the structure of metallic blades, permitting magnification ratios of the order of several million. In 1962, E.N. Leith and J. Upatnieks designed and built a lens-less holographic optical microscope [3, 6, 12, 13, 14].

In spite of the tremendous progress in the field of microscopy, work is continued on better still and more modern microscope designs, yielding better and better effects of observation.

2.1.1. Principle of optical microscope

The structure of the optical microscope utilizes two systems – the optical system, used for illumination of the object observed and for image magnification, and the mechanical system, the function of which is to ensure correct positioning of the particular components of the optical system. The key aspect is stability, mutual parallelism and concentricity of the optical system components. Fig. 2.4 presents the structure of the optical microscope.
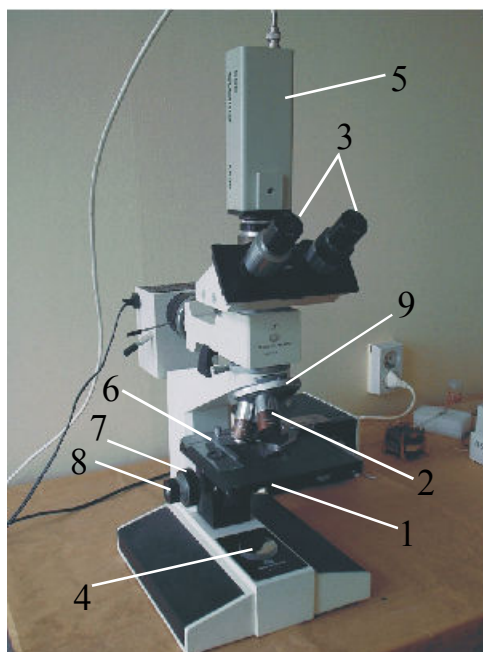
Fig. 2.4. *The structure of the optical microscope: 1 – condenser, 2 – objective lens, 3 – eyepiece, 4 – mirror or lamp, 5 – CCD camera, 6 – moving or mechanical stage with knobs for slide position control in the XY plane, 7 – coarse adjustment knob, 8 – fine adjustment knob, 9-revolving nosepiece (with objective lenses).*

2.1.2. Optical elements

Illumination system: in ordinary microscopes it will be a mirror; it can also be a simple lamp with a reflecting surface, or a sophisticated illumination system with a collector, position adjustment, individual power supply with voltage regulation, etc.

Condenser: the condenser lenses concentrate the light coming from the mirror on the object (specimen) under observation. The image generated in the microscope is magnified and reversed with relation to the actual object. The microscope magnifies also the angle of view of the object under observation.

Immersion: filling the space between the slide and cover and the objective and condenser with a liquid.

Objective lenses: systems of lenses receiving the light from the slide and generating its magnified image.

Body tube: - the tube in which the objective and the eyepiece are installed and where the image is generated.

Eyepiece attachment: it mounts the eyepieces and changes the direction of light from vertical to more sloping and more comfortable for the observer. The eyepieces can be monocular (in simpler types of microscopes) or binocular, permitting comfortable and easy observation with both eyes, which is important not just from the viewpoint of ergonomy, but also for the health of the observer, as binocular eyepieces can be provided with tube spacing adjustment (to match the distance between the observer's eye pupils) and with dioptric adjustment (on one of the eyepiece tubes) for correction of differences between the eyes of the observer, and, finally, the attachment can be equipped with a camera adapter (for either a conventional or a digital camera). In the latter case it may be a so-called tri-ocular attachment, or a dedicated camera adapter. Stereoscopy – a microscope with a binocular eyepiece attachment is not the same as a 3D microscope. In 3D microscope the image reaching each of the eyes of the observer is different; the observer has the impression of the image having depth. In the binocular microscope the image in both eyepiece tubes is the same. 3D microscopes, for design reasons, usually operate on overall magnification ratios (objective x eyepiece) below 100x.

Eyepiece lenses: they permit visual observation of the objects, at the same time magnifying the image generated by the objective lens of the microscope with the additional possibility of correcting optical defects of the images from the objective.

Images generated in the microscope are magnified and reversed with relation to the actual object under observation. The microscope magnifies also the angle of view of the object studied. The magnification ratio of the microscope is equal to the product of the magnification ratios of the objective and the eyepiece.

The application of mirror lenses in the optical microscope permits increasing of the distance between the objective and the object viewed, and allows the microscope to be equipped with additional accessories – heating or refrigeration chambers and micro-manipulators. The basic parameters characterizing the optical microscope are the magnification ratio and the resolution. Maximum usable magnification is determined by the resolution which in turn is limited by the diffraction of light. The resolution of a microscope increases with increasing aperture and decreasing wavelength of light [3, 4, 5, 7, 8].

2.1.3. Mechanical elements

Microscope body: it ensures the rigidity of the whole microscope structure. The more rigid and heavier the structure, the better for the quality of observation. The design of the microscope body determines whether the adjustment of the distance between the objective and the object viewed (focusing) is achieved by upwards and downwards movements of the stage or of the body tube (together with the objectives, eyepieces and other elements mounted on it). The former solution is better and dominates in more modern microscopes. It ensures constant eyepiece height, which is important from the viewpoint of ergonomy. But also, and more importantly, it eliminates a basic shortcoming of the traditional design in which focusing is achieved through tube movements. In that case the moving element had frequently considerable weight, which resulted in the phenomenon of autonomous downward slide or "float". To counteract that phenomenon, special resistance was designed into the screw controlling the vertical movement of the tube, but, irrespective of the adjustments, the tendency to "float" appeared with time. Modern designs eliminate that problem through the application of the moving stage solution.

Stage: it serves for securing the slide and permits slide movements within the X-Y plane. Depending on its technical design, its vertical movements can be used for adjustment of the distance between the objective and the object viewed (focusing). There are also special purpose stages, e.g. the rotary stage used for observation in polarized light.

Coarse and fine adjustment screws: they serve for the adjustment of the distance between the objective and the object viewed. Depending on the design of the microscope, the adjustment screws will raise and lower either the stage or the tube with the objectives. The fine adjustment screw is usually provided with a micrometric scale. In such a case the screw can also be used to measure the thickness of the object under observation. Thickness values measured with this technique do not correspond directly to the readings from the micrometric scale.

Parafocality: in newer designs of microscopes (from the middle of the 20th century) we find what is called the parafocal system. This means that different objectives have almost identical focal length with different magnification ratios, i.e. once we focus on the object viewed with one objective, another objective (with another magnification ratio) can be selected without the need to refocus, or, perhaps, with the need for just a slight focus adjustment. In older designs, change of objective requires significant corrections of the distance between the objective and the object viewed.

Revolving nosepiece: the objective lenses of the microscope are set in a revolving disc. Rotating the disc permits easy selection of objective lenses and thus selection of the magnification ratio used.

Tube: the space between the objective and the eyepiece attachment, in which the image is formed. In older microscope designs, the length of the tube was standardized at 160mm (Zeiss and many others) or 170mm (Leica and few others) and objectives were designed to suit one or the other tube length (tube length is engraved on the objectives). In newer designs, from the end of the 20th century, the principle of the so-called "optics to infinity" is used, and suitable objectives with the symbol of infinity engraved on their casings.

Illumination system: made up of a mirror directing light onto the slide. In more sophisticated microscopes it comprises a special lamp, with a collector system. Illumination of the object viewed is an extremely important element of microscopy observations.

Mechanical system of the condenser: it permits adjustment of the condenser position along the vertical axis. In more advanced microscopes it also allows the condenser to be centered relative to the optical axis of the microscope. Some microscopes have a mechanical stop (brake) preventing the condenser from „driving" into the slide glass and damaging the slide [3, 4, 5, 6, 8].

Depending on the character of the study, the optical microscopes used are adapted for observations in different radiation bands – visible light, infrared, ultraviolet (in the latter two cases the images are viewed with the help of special image converters). Also, different methods of observation are applied – mainly the so-called "bright field method" (which permits the observation of particles reflecting or diffusing light; such a particle gives a dark image on a bright background), the „dark field method" (only light diffused on the particles reaches the objective; it is also possible to observe translucent objects with a refractive index different from that of the medium), and the method of phase contrast (for observation of translucent objects whose difference of thickness of refractive index is converted in the optical system into different levels of image brightness) and the interference method which is similar to the phase contrast method.

Design modifications and additional accessories permit observation both in light passing through the object viewed and in light reflected from the object, as well as adapt the optical microscope for special tasks, including, among others, observation of anisotropic objects (polarizing microscope), the study of fluorescent images of micro-objects illuminated with short-wave visible radiation, ultraviolet (optical fluorescence microscope), stereoscopic observations (optical stereoscopic microscope), and observation of particles with lateral dimensions much smaller than the theoretical resolution of the optical microscope (ultramicroscope). The invention of the laser permitted the design and construction of the scanning optical microscopes – reflecting and fluorescence, the Doppler optical microscope, the ellipsometric optical microscope, and others [4, 5, 7, 8].

20

2.1.4. Image generation in optical microscope

The basic optical system of the microscope is built of two converging lenses called the objective and the eyepiece. The object viewed is placed between the focal length f_1 and double the focal length $2f_1$ of the objective lens. Magnified, reversed and actual image A_1B_1 of the object is observed in the eyepiece which generates the virtual image A_2B_2 of the true image A_1B_1 (Fig. 2.5).
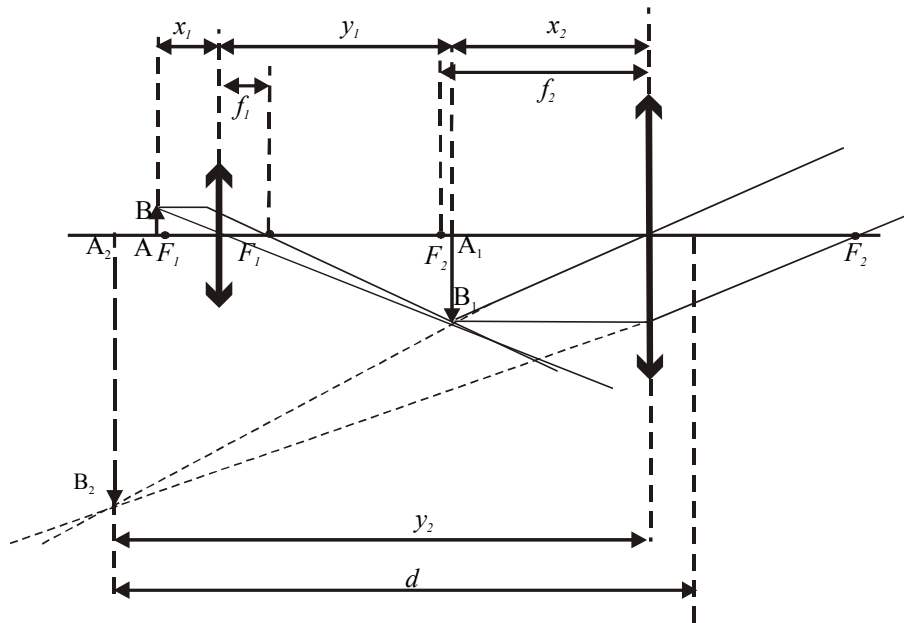
Fig. 2.5. *Image generation in the optical microscope.*

The magnification of the object p observed through the microscope is equal to the product of the magnification ratios of the objective p_{ob} and of the eyepiece p_{ok} and can be expressed with the formula (1):

$$p = p_{ob}\, p_{ok.} \tag{1}$$

The position of the object, **AB,** is selected so that its distance from the objective - x_1 – is approximately equal to the focal length of the objective - f_1, i.e.:

$$x_1 \approx f_1 \tag{2}$$

In turn, the image distance y_1 is approximately equal to the tube length l

$$y_1 \approx l \tag{3}$$

Therefore, the objective magnification ratio p_{ob}, in accordance with (2) and (3), equals:

$$p_{ob} = \frac{y_1}{x_1} \approx \frac{l}{f_1} \tag{4}$$

The true image A_1B_1, generated by the objective, is formed close to the focus, between the eyepiece focus and the eyepiece, so its distance from the eyepiece may be accepted as equal to the focal length of the eyepiece f_2, i.e.:

$$x_2 \approx f_2 \tag{5}$$

Distance y_2 of the virtual image A_2B_2 is approximately equal to d, then:

$$y_2 \approx d \tag{6}$$

where d – distance of image A_2B_2 from the eye of the observer (so-called "good vision" distance)

Therefore, the eyepiece magnification ratio can be expressed with the formula:

$$p_{ok} = \frac{y_2}{x_2} \approx \frac{d}{f_2} \tag{7}$$

And thus, in accordance with (1), (4) and (7) the total magnification ratio of the microscope, p, can be expressed with the formula:

$$p = \frac{d\, l}{f_1 f_2} \tag{8}$$

To obtain very high magnification ratios, microscopes are built with objectives and eyepieces having very short focal lengths. In such cases, the objectives and eyepieces are not single lenses but systems of several lenses [3, 4, 5, 6, 7, 8].

2.1.5. Resolution of the microscope

Image quality and the amount of information that can be obtained from the image depend not only on the objective and eyepiece used, i.e. on the magnification ratio, but first of all on what is known as the resolution of the optical system. The resolution of the microscope is the smallest distance between two points which can be perceived as discrete points in the microscope image. Resolution is expressed in terms of units of length. The smaller the distance, the better the resolution of the optical system and the more information can be extracted from the microscope image. In practice it means that the better the resolution the higher the magnification ratios that can be used. Resolution or resolving power is a feature of all devices generating images – not only of the light or optical microscope, but also of electron microscopes, telescopes, or monitors, though in the last case the resolution is expressed in another way.

Resolution is expressed by the formula (8):

$$d=0{,}61\lambda/A \tag{8}$$

where: λ – length of wave forming the image, A- numerical aperture of the microscope objective calculated according to the formula (9):

$$A= n \sin \alpha \tag{9}$$

where: n- refractive index of the light wave forming the image, characteristic for the medium contained between the specimen under observation and the objective lens, α – angle between the optical axis of the objective and the and the rim-most ray of light that enters the face lens of the objective with correct focusing of the system [4,5,7,8].

2.1.6. Variants of optical microscopes

Dark field: Microscopy in the so-called dark field permits the observation, in the specimen prepared, of particles with dimensions smaller than the resolution of the optical system. This kind of microscopy utilizes the phenomenon of diffraction of light rays falling on objects with very small dimensions. An example of such a phenomenon is the fluorescence of tiny particles of dust – they are invisible under normal conditions, but when they happen to get into a beam of sunlight, coming e.g. through a slot in the window curtain, the effect becomes noticeable. The condition for seeing the dust particles is looking at the light beam from the side, so it is viewed against a dark background. Dark field microscopy requires the application of a special condenser in which the central part of the lens is opaque and light passes through the specimen under observation

only at very acute angles. In this situation the light rays passing through the slide do not enter the objective; what does enter the objective is light deflected or reflected by particles contained in the specimen (Fig.2.6). The particles are then seen as small fluorescent dots against a darker background. The dark field method is used mainly for the observation of micro-organisms in body fluids [3, 8, 14].
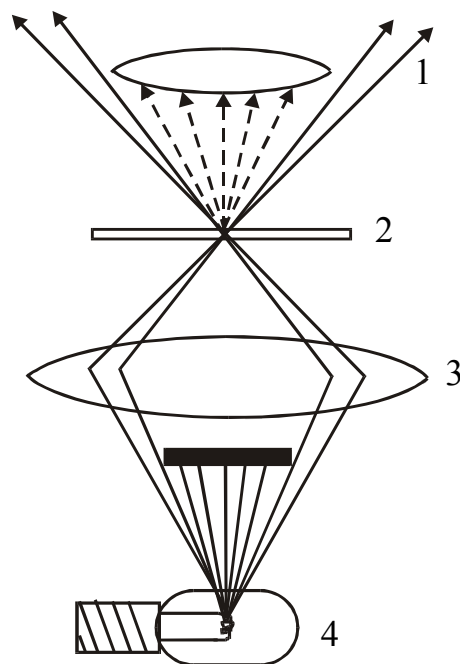
Fig. 2.6. *Image generation in dark field, 1 – objective lens, 2 – stage, 3 – condenser lens, 4 - light.*

Phase-contrast microscope: The retina of the human eye reacts to two out of three physical parameters of light wave – the length of the wave, perceived as colour, and its amplitude, perceived as the degree of brightness. The third parameter – phase – is not registered by the retina, although it is also subject to modification during the transition of light through the microscope slide. The various structures present in the specimen observed cause different shifts in the light wave phase. This phenomenon has been utilized in the design of the phase-contrast microscope, by introducing a special optical system that transforms the light wave phase shift into a change in its amplitude (Fig. 2.7), [4, 6, 14].

24
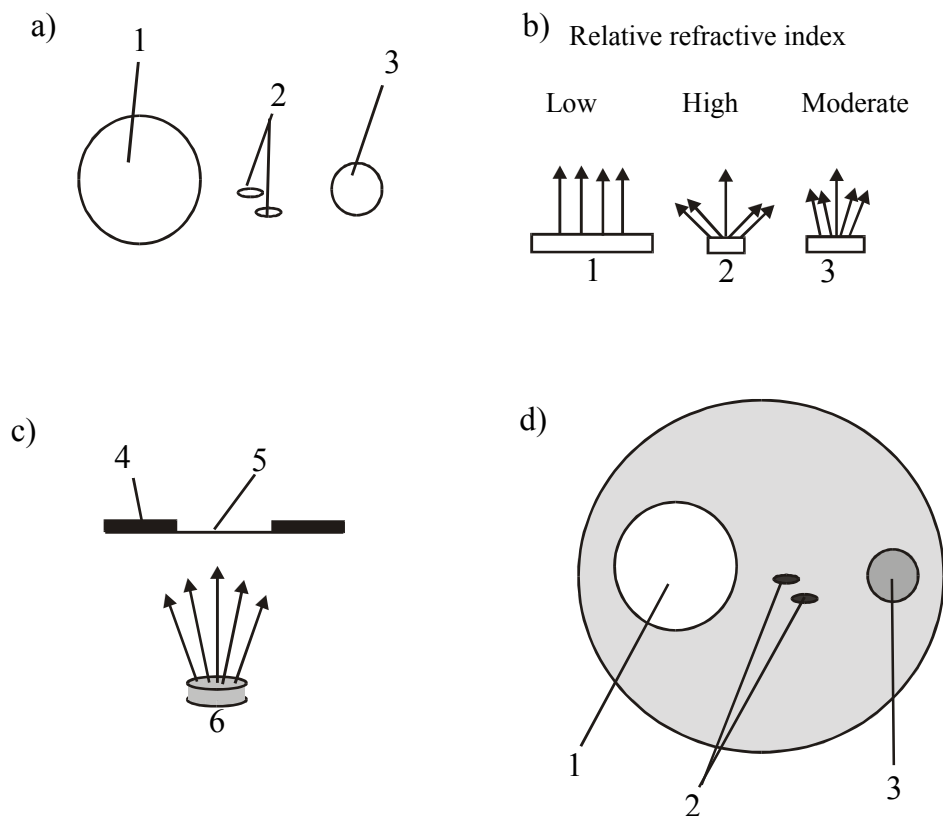
Fig. 2.7. *Image generation in the phase-contrast microscope: 1 – vacuole, 2 – granules, 3 – nucleus, 4 – outer edges retard light, 5 – centre allows light straight trough, 6 –specimen.*

Inside the condenser of the phase-contrast microscope there is an annular diaphragm which transforms the light beam emitted from the microscope lamp into a hollow cone of light rays. When the conical light beam passes through a specimen which acts as a diffraction grid, some of the light rays get deflected, while others pass in a linear manner. The structures of the specimen cause light ray deflection or phase shift. The objective of the microscope has an additional optical system (so-called phase plate) which causes uniform retardation or acceleration of the phase of linear light rays. Within the image plane interference of the two types of light rays occurs, during which the superposition of light rays with different phases causes the appearance of new waves with differentiated amplitudes. In this way, the structures in the specimen that cause

various degrees of light wave phase shift can be observed in a contrasted form. With the help of such microscopes one can observe much more cell organelle, even very small ones that are not visible in microscopes based on the bright field technique. The phase-contrast microscope permits also much clearer observation of some living processes of cells, such as cytoplasm movements [3, 4, 6, 8].

Interference microscope: This type of microscope operates in a manner similar to that of the phase-contrast microscope, i.e. transforms differences in the light wave phase into differences in light wave amplitude. The difference between the two types of microscope lies in the design of the optical system. Inside the condenser of the interference microscope is an optical system which separates the light beam into two components: 1 – light rays passing directly through the specimen, and 2 – light rays passing through the translucent area beside the specimen, i.e. the so-called reference light. On the other hand, the tube of the microscope has an optical system with reverse operation, i.e. combining the two beams into a coherent light beam. Interference takes place between the reference beam and the light rays deflected by the structures contained in the specimen. In view of the fact that the reference beam has constant characteristics, the optical system of the microscope not only contrasts the image, but can also be used for quantitative analysis of the dry mass of the structures under study and for the determination of the thickness of slices [3, 6, 8].

Polarizing microscope: Thus type of microscope incorporates two Nicole's prisms of polarizing grids built into the optical system, causing polarization of light. One of the prisms, the polarizing prism, is located between the lamp and the condenser. The other prism, the analyzing prism, is installed above the objective lens. The position of the analyser prism is fully adjustable through the possibility of its rotation. If the planes of polarization are set to parallel, polarized light passes freely through the analyser and reach the observer – the field of view is then bright. If the polarization plane of the analyzer is set perpendicular to the plane of the polarizer prism, light polarized by the polarizer prism does not pass through the analyzer and the field of view is dark. Such a positioning of the elements polarizing light in the microscope, i.e. prism crossing, permits observation of objects with the help of the polarizing microscope [4, 6, 7, 8].

2.1.7. Microscopy studies

Microscopy studies of biological objects are a very important element of studies aimed at acquiring knowledge on the world around us. Such studies, however, can only be conducted after specific conditions have been met. The first such condition is the transparency of the objects under study, due to the fact that observations are most often performed in transmitted light - Fig. 2.8 a and b. The cells walls are visible on the pictures but the focal plane and the out-of-focus areas above and below the focal plane can be seen.

a)

b)
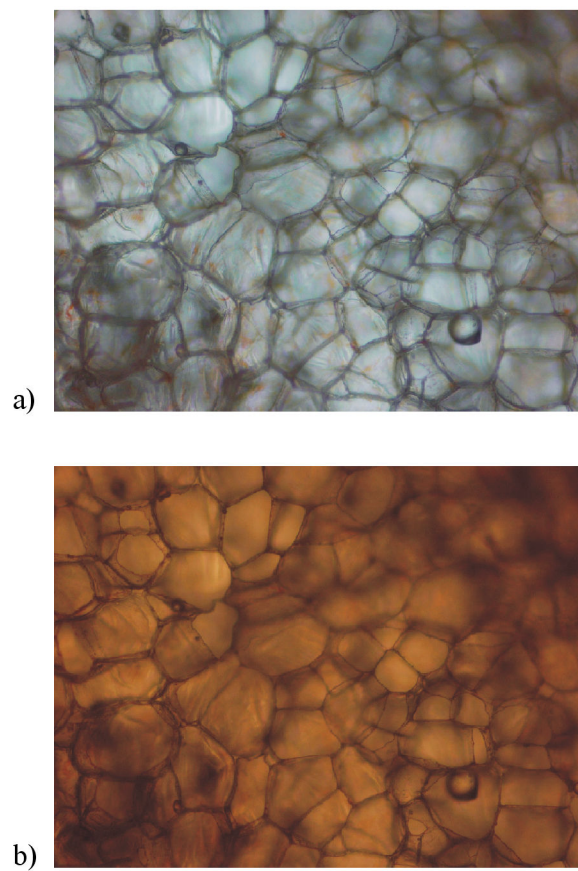
Fig. 2.8. *Image of carrot tissue structure obtained with OLYMPUS BX51 optical microscope with 10x magnification, observed in transmitted light: a) with the bright field technique, and b) with the dark field technique. The sample was 1mm thick.*

Studies involving the use of top lighting, on opaque objects, are performed only in exceptional cases. The structure under study can only be perceived by the observer when there is a contrast between the structure and its surroundings, and thus the existence of such a contrast in another condition that has to be fulfilled in microscopy studies. The last condition is that the object studied must be prepared in such way that it can be easily placed within the microscope field of view [1, 2, 3, 6, 7, 12].

Fig. 2.9 presents images of plant tissues obtained with the help of an optical microscope in transmitted light - a, c and d, and in reflected light – b.

a)

b)

c)

d)
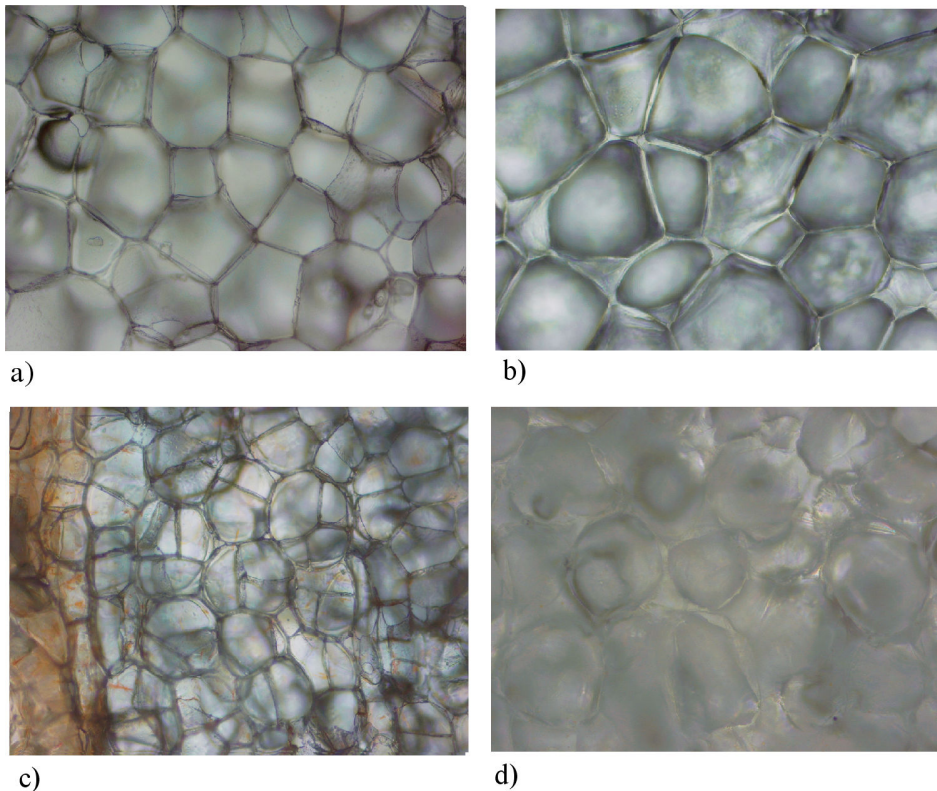
Fig. 2.9. *Images of plant tissue structures obtained with OLYMPUS BX51 optical microscope with 10x magnification: a) potato tuber inner core, b) potato tuber outer core (observed in reflected light), c) carrot, and d) apple. The samples were 1mm thick.*

The cells walls are visible on the photos. Only b photos show picture from the focal plane and the cells walls are good quality for analysis, on the a and c photos from the focal plane and out-of-focus areas above and below the focal plane can be seen but quality is not good for analysis. The d picture is bad quality for analysis.

28

One should take care, however, that the preparation of the specimen does not result in its losing its natural appearance. Very often it is difficult to avoid significant changes in the structure of living tissues in the course of their preparation (slicing with the microtome, maceration) or observation under the microscope, as the objects studied are placed in a drop of a liquid between the slide glass and the cover glass, where very soon unfavourable conditions may develop, causing structural changes to the object studied [1, 3, 6, 9,14].

Another aspect that does not permit observation of an object in its natural condition is its thickness. This problem becomes apparent in the microscope observations of objects made up of very soft tissues, for which there is a certain limit specimen thickness below which structural changes take place in the course of preparation. Therefore, in this case, the specimen should be prepared so that its structure undergoes the least change possible. This is facilitated by the process called the fixation. In some cases of fixation, the structure hardens to such a degree that further processing can be done without any risk of its causing changes to the object under preparation [1, 2, 6, 14].

Fixation of specimens to be studied: During the process of specimen fixation one should aim at obtaining an object that after fixation reflects as accurately as possible the appearance of the living material. Fixation should be performed, whenever possible, immediately after slicing off from the object studied. When immediate fixation is not possible, the specimen should be brought to the desired turgor by placing it in water. Also important is the size of the object, as it affects the rate of the fixing agent penetration into the specimen and the speed of penetration affects the chance of preventing changes to the specimen structure. The smaller the specimen, the faster the diffusion of the fixing agent into the specimen. The speed of diffusion depends also on the type of fixing agent used. For example, alcohol based fixing agents penetrate specimens the fastest. The preferred size of the object is also related to the character of the study – if the observations are to be concerned with the study of anatomy, the specimens can be larger than those for cytological studies. One should remember about the proper concentration of the solution, as it gets constantly diluted in the course of the process of fixation by the intracellular fluids, mostly water. To minimize the effects of dilution, the volume of the fixing solution must be greater than the volume of the specimen fixed by a factor of about 50 to 100.

The size of the specimen is determined with the help of special implements. Fig. 2.10 presents a guillotine-type device for specimen size determination, equipped with two blades fixed in parallel [1, 2, 7].
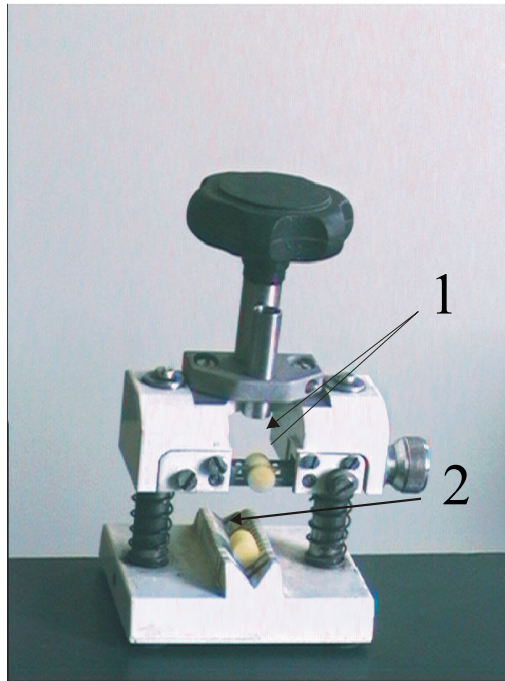
Fig. 2.10. *Specimen size determination, 1 – two parallel blades, 2 - specimen.*

The time of specimen fixation is affected by the temperature at which the process takes place. The higher the temperature, the faster the process and, therefore, the shorter the time of fixation. The selection of fixation temperature depends on the type of fixing agent used. Most fixation agents work the best at room temperature, but in the case of e.g. the Bounin Allen fixing agent better results of fixation are obtained at higher temperatures ($37\ ^OC$), while for the fixation of specimens for the study of chromosomes the temperature should be lowered even to about 4^OC. The course of the process itself depends also on the fixing agent used. The fixing agents may be solutions that precipitate proteins, or such that bind proteins. There is no possibility of using the same fixing agent for all the component elements of cells – only some of them are fixed by a given agent, and other components may be washed out from the specimen in the course of further preparation. In practice, two types of fixing agents are used – acidic and alkaline. Acidic fixing agents are most often used in microscopy, as they are not too difficult to use and further processing of the objects fixed, e.g. staining, can be fairly easy. Alkaline fixing agents are used very infrequently, as their application

may be difficult and the objects fixed can be hard to stain. However, there are fixing agents that provide fixing effects similar to those of acidic and alkaline agents combined. The choice of the fixing agent is determined by the type of object to be studied, and what kind of study is to be performed – anatomical studies or cytological analysis. In anatomical studies rapid action fixing agents are most often used, while fixing agents penetrating very slowly the specimens prepared are preferred in cytological studies. When deciding on the choice of a fixing agent, one should keep in mind what other operations are to be performed after the fixing, as some fixing agents preclude the application of some staining methods due to poor effects of staining or no staining effect at all [1, 3, 6].

The fixing agent may by composed of a chemically homogeneous liquid which is easy to apply, but may cause the appearance of artefacts. This can be avoided through the addition of another liquid to the fixing agent, that will minimize the undesirable effect of the agent. Therefore, solutions of several liquids are used as fixing agents, but also those, after some time, may react with one another and exert an unfavourable effect on the process of fixing. For this reason the fixation of the specimen must be effected before the onset of the reaction of fixing agent components. However, if for the fixation of a specimen we have to use a solution whose components react with one another faster than the process of fixation, the solution will have to be changed in the course of the fixing process [1, 2].

An important element of fixation is its time which depends on the type of tissue under study, the size of the specimen, and the fixing agent used. The depth of specimen penetration by the fixing agent can be determined by observing the change in the specimen colouring. If we are dealing with an object of considerable size, it should be incised. The object should remain in the fixing agent until all the reactions taking place in the process of fixation have run their course in the cells. With some fixing agents, the objects can be kept in them following the process of fixation, treating the agents as preservative or protective media. There are, however, also such fixing agents which, if we keep the object in them following the process of fixation, can cause damage to the object and in such a case the fixing agent should washed off the object once the fixing process has been completed. After the completion of the process of fixation, the active solution should be removed from the tissue through careful wash repeated several times. The rinsing of specimens from residues of fixing agents in the form of water solutions is most frequently done under running water, while fixing agents based on alcohol solutions should be washed out using alcohol at the same level of concentration [1, 2, 3, 6].

Fixed and washed material can be stored for long periods of time in preserving media, or subjected to further processing. The function of the

preserving media is to maintain the fixed structures in unchanged form. However, keeping fixed objects in preserving solutions for too long may reduce the susceptibility of the objects to staining [1, 2].

Observation in transmitted light under the optical microscope require the use of specimens with a certain thickness, as the object studied must be relatively transparent. To obtain the required specimen thickness, and therefore transparency, permitting microscope observation elements of structure interesting for the observer, the object must be sliced into thin layers using suitable methods of slicing describe below (Fig. 2.11).

a)

b)
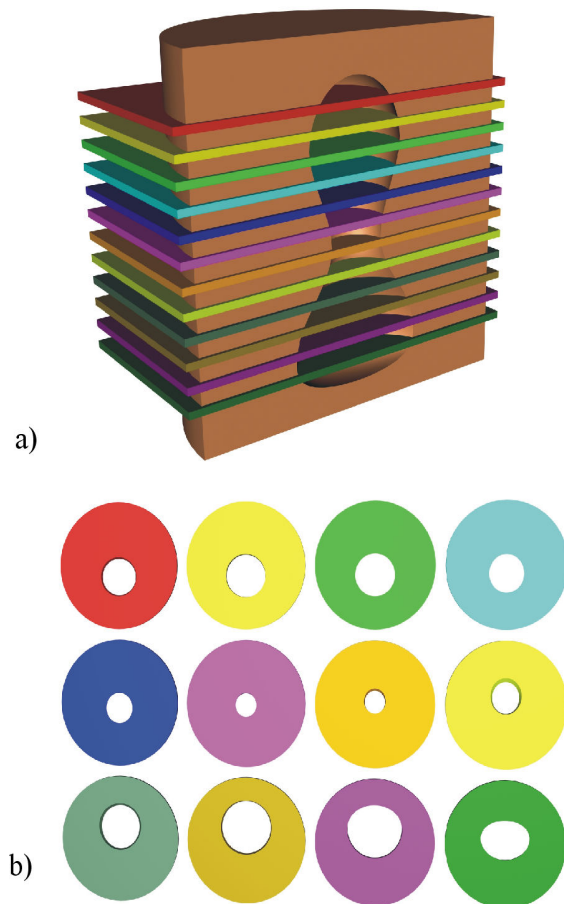
Fig. 2.11. *Schematic of the method of three-dimensional reconstruction of the gap: a) – method of specimen slicing with the help of the microtome, b) – fragment of the gap in the object obtained in each of the slices [11].*

Object slicing and application of slices onto the slide glass: The process of slicing can be divided into manual slicing and slicing with the help of specialized apparatus [1].

Manual slicing can be used in the case of objects with sufficient hardness. Certain living objects can be sliced without prior hardening (e.g. sprouts and leaves of higher plants), and when that is not possible, the material has to be hardened with 92% ethyl alcohol or FAA (formalin-alcohol-glacial acetic acid). Such a treatment permits the obtaining of required hardness in 24 hours, and if a material has been subjected to the FAA treatment and is still not hard enough, it should be placed in 92% alcohol and it should become hard enough in 24 hours. It should be kept in mind that subjection of a material to the effect of 92% alcohol for too long a period of time may make it brittle; this can be avoided by placing it in water for several minutes for softening. Manual slicing cannot be used with very hard objects, or with relation to such objects which require slicing to highly uniform thickness for subsequent 3D analysis of the object under study (Fig. 2.11), [1, 2,3, 6].

For this kind of slicing, special high precision devices are used, known as the microtomes (Fig. 2.12).

Fig. 2.12. Leica RM2155 microtome.

Material for slicing with a microtome should have a minimum hardness, uniform throughout the object volume in order to it was cut across not burst. Materials that can be sliced with a microtome without prior hardening include

fresh wood. Other, much softer objects, have to be hardened prior to slicing and sealed in a suitable medium that, penetrating the object, will fill it and cause it to become uniformly firm throughout its volume. The important aspect here is the proper choice of the medium – upon hardening it should have a hardness equal to or higher than that of the hardest element of the object. This creates the possibility of obtaining thinner slices. The choice of the sealing medium is related to the type of object and to the purpose of the study [1, 2].

The method of sealing that is most frequently used is sealing in paraffin. It is a simple method and gives good results, permitting slices with the thickness of about 5–30 μm to be obtained. The principal advantage of the method is the possibility of making a series of successive slices, which permits 3D reconstruction of the structure of the material. Objects, after fixation and washing, should be dehydrated by placing in a hygroscopic fluid (alcohol), and then in an intermediate medium that can mix with the dehydrating fluid and dissolves paraffin. It is a very frequent occurrence that objects become transparent in the course of this process. Then the object is transferred to liquid paraffin, heated to the required temperature, which permits paraffin to enter all those places that were formerly occupied by water, air or other elements. The object remains in paraffin until the paraffin solidifies. Once the paraffin has solidified, we obtain a solid transparent block which can be sliced. If the block is snow-white in colour, it may contain residues of the intermediate medium or other contaminants which will make the slicing difficult [1].

Prior to the actual slicing of a selected block, we glue it onto a block of wood or plastic for fixing in the grip of the adjustable head of the microtome. The block should not move or vibrate under the effect of the force applied, as this would preclude the obtaining of uniformly thick slices during the slicing. The next step in the process is the selection of a slicing blade for hardness number of material adequate and fixing it in the blade grip. Incorrect blade attachment may also result in non-uniform slice thickness. Both the adjustable head and the blade grip can be set at different angles to permit the selection of an angle that will be optimum for obtaining the best quality slices possible. The selection of the optimum angles is very difficult and requires several test slices to be cut but for soft material is about 2-3° and for hardness is 5° and more. Once the parameters of slicing have been set, we can proceed with slicing the object prepared. The product of slicing is a band of successive slices, joined with one another, which has to be pulled away in the course of the slicing process so it does not get wrapped on the blade or table and get damaged, 10–15 μm thick and 20°C are the best parameters. The band of individual slices is extremely delicate and the slices should be secured as soon as possible by attaching them to the slide glass. Some slices may roll during the slicing; in such a case they should be placed in distilled water which will cause

them to straighten out without damage. The method of slice attachment to the slide glass is highly important for subsequent storage of the material. For the slices to adhere well and not to get unstuck with time the slide glass used must be free of any dirt or contamination. It is best to glue the slice onto the slide glass with the help of a special cement. Most frequently used are the Haupt cement (gelatine with glycerine) or the Mayer cement (albumen with glycerine). A drop of the cement chosen is placed on the clean surface of a slide glass, and excess cement is removed by sliding our clean wrist over the slide glass surface. Excessive thickness of cement layer on the slide glass may prevent good adhesion of the slice or cause problems with subsequent slice staining. With slide glass prepared in the manner described, we place the slice band from the mcirotome on the slide glass. A very important aspect is the amount of water – it should be enough for the slices to float freely, as touching dry slide glass with a fragment of the slice will cause its adhesion to the glass and breakoff from the part of the slice that is still in water, and thus damage the slice. Too much water will cause its runoff from the slide glass, together with the slices, and thus also damage to the slices. Once the slices have been placed on the slide glass, the water has to be drained off with a piece of plotting paper by touching the blotting paper to a corner of the slide glass. Next the slide glass with the slice is placed on a bench heated to a suitable temperature, about $5^{O}C$ lower than the temperature of paraffin melting point, for the remaining water to evaporate. The cemented slices still contain paraffin which has to be removed. For this purpose we place the slide glasses for ten minutes in a developing tray filled with xylene. It should be kept in mind that a certain amount of xylene will dissolve a certain amount of paraffin, so the xylene in the developing tray should be changed at suitable intervals. The final effect of this procedure is slide glasses with attached specimen slices that can be used for observations or stored for later examination (Fig. 2.13), [1, 2, 6, 7].
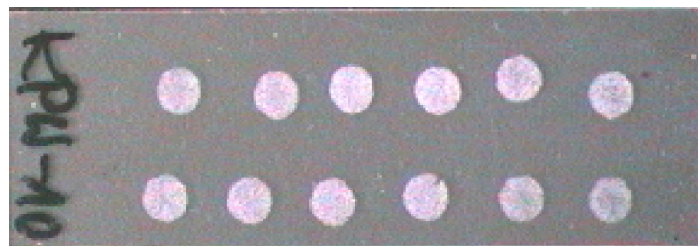

Fig. 2.13. Slide glass with attached slices of potato tuber parenchyma tissue

Slices prepared in this way can be used to obtain microscope images of the structure and damage to the structure, and 3D reconstruction of the structure (Figs 2.11, 2.14 and 2.15).

a)

b)
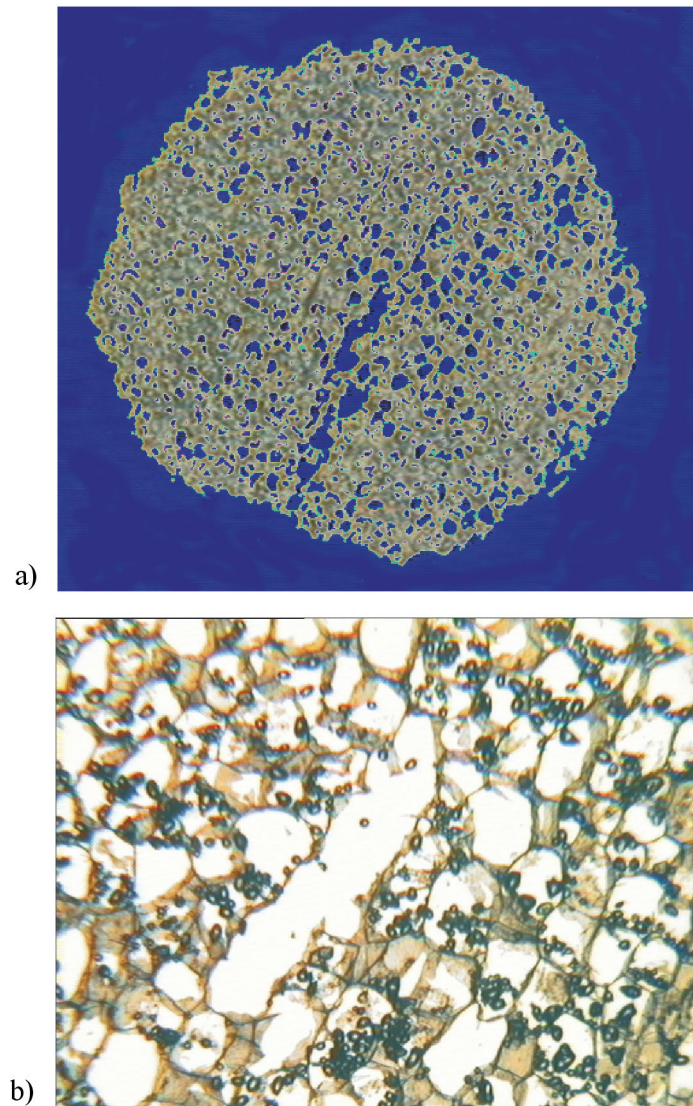
Fig. 2.14. *Image of the structure of potato tuber parencghyma tissue obtained with the Biolar EPI optical microscope, a – macro-scale image, magnification x10, b – micro-scale image obtained with the Plan 10/0.24 objective, [10].*
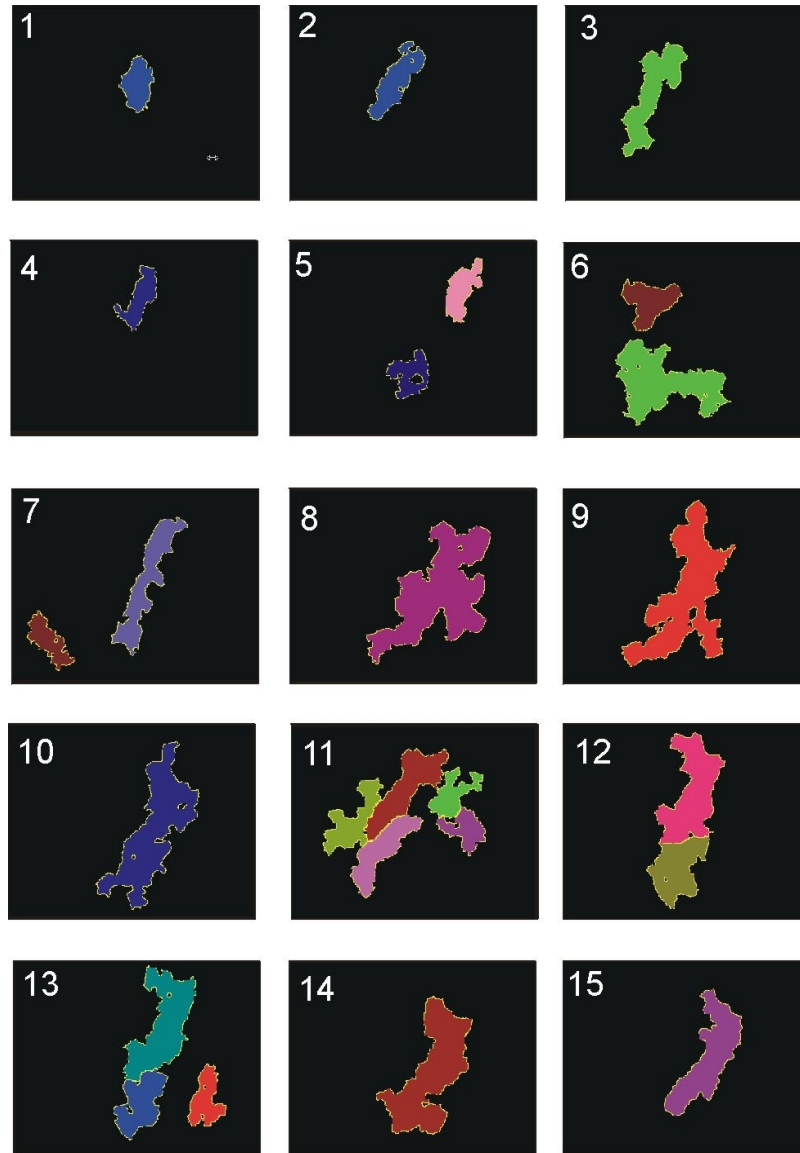
Fig. 2.15. *Reconstruction of the true image of a gap in the structure of potato tuber parenchyma tissue obtained with the Biolar EPI optical microscope with Plan 10/0.24 objective, following the performance of the procedure described above. 1 denotes the first slice and 30 the last slice in which the gap in the structure wad observed [9].*
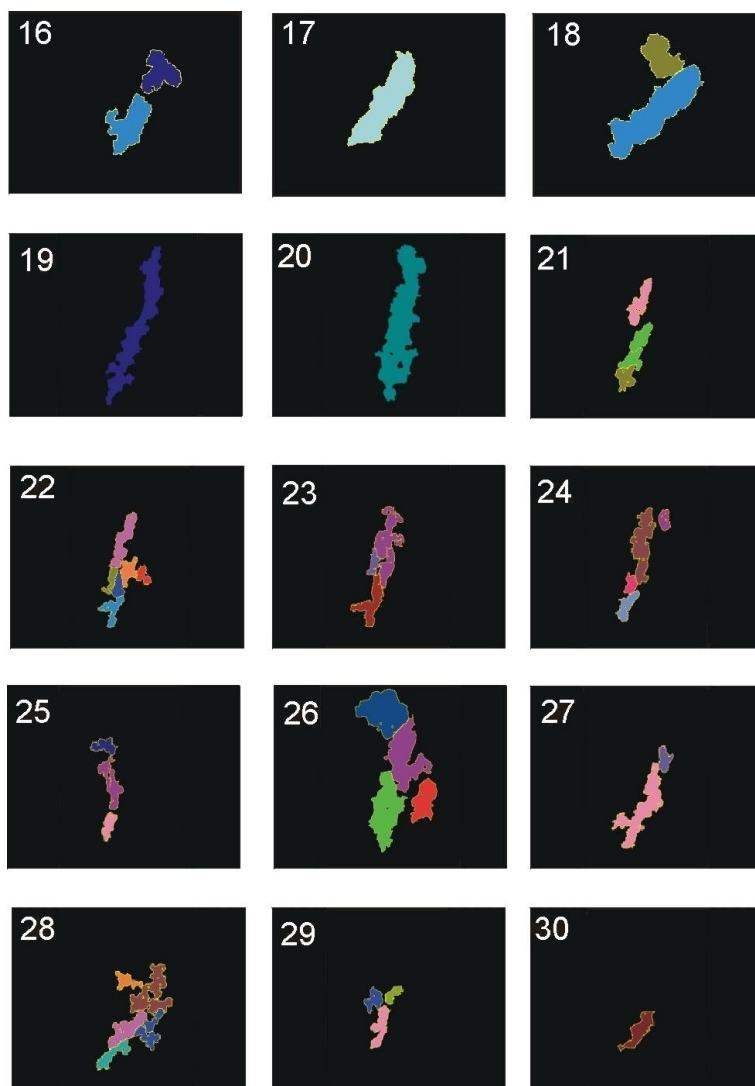
Fig. 2.15 - continued

Fig. 2.16 presents images obtained with the help of an optical microscope equipped with the Plan 20/0.4 objective using different methods of specimen illumination for showing differences on the same images.
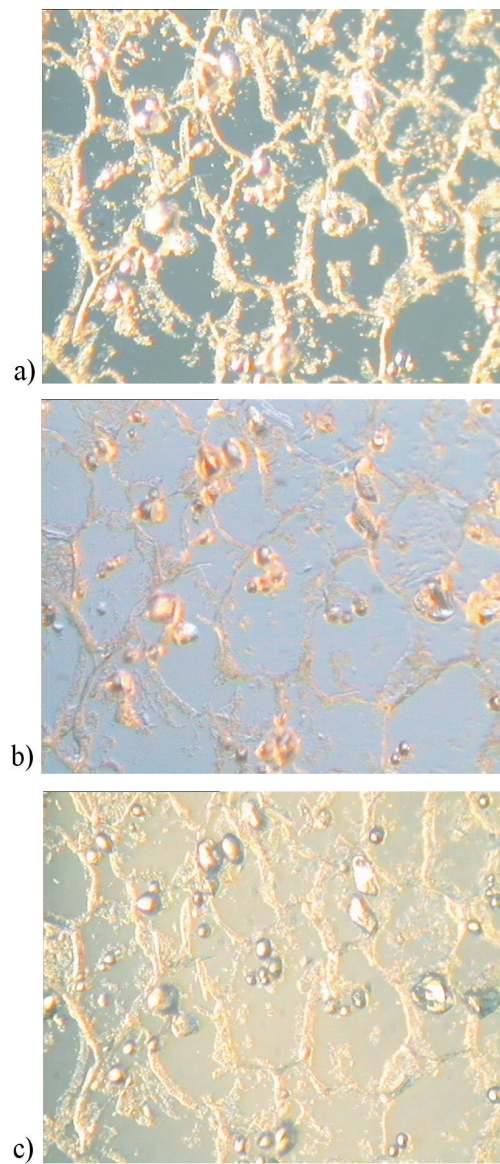
Fig. 2.16. *Images of the same part of the structure of potato tuber parenchyma tissue obtained with the Biolar EPI optical microscope with Plan 20/0.4 objective, using different methods of specimen illumination: a) – from above, b) – from the side, c) – from beneath.*

Staining: If the slices are to be stained, the next task is to remove xylene from the slices, as some of the dyes used for slice staining dissolve in fluids in which xylene does not dissolve. To achieve this, we place the slices for about 5 minutes in a developing tray filled with absolute isopropyl alcohol. After washing xylene out of the slices, they are placed for about 3 minutes in 92% denatured ethyl alcohol. The objective of slice staining is the obtaining of contrast between particular elements of the slice during the observation. Therefore, slices are immersed, for a specific period of time, in a solution of a staining agent, keeping in mind that there are dyes that stain only specific elements of the structure. The specimen can be immersed successively in several different staining agents to stain the structure elements of interest, obtaining multi-coloured contrast. Staining can be used not only for slices, but also for whole plants or their parts. Several different met5hods of staining can be distinguished [1, 2].

Progressive staining, in which the staining agent is applied as long as it takes for the object to attain the required intensity of staining [1].

Regressive staining, consisting in staining the object with uniform colour, then bleaching or decolouring in another liquid, in which the time of decolouring is different for the various elements of the structure; for this reason the process is also known as differentiation [1].

Simple staining - a process used with objects stained with one staining solution [1].

Compound staining is used for objects that require staining with a greater number of staining agents and has an application when making review specimens. Compound staining can be effected in two ways – with the staining solution being composed of two dissolved staining agents, then such staining is called concurrent staining, and with the staining agents being prepared separately, then we have successive staining. Fig. 2.17 presents images of the micro-structure of potato tuber parenchyma tissue, with starch granules having been stained prior to the observation, obtained with the help of the optical microscope. The starch granules are black and easy to detection [1].
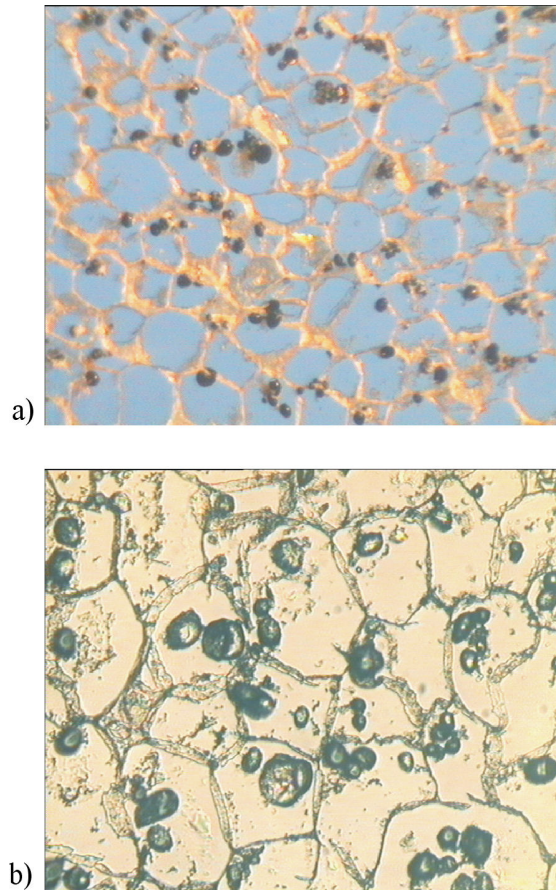
Fig. 2.17. *Images of the structure of potato tuber parenchyma tissue with stained starch granules, obtained with the Biolar EPI optical microscope with the following objectives: a) Plan 10/0.24 and b) Plan 20/0.4.*

It is possible to make a very large number of paraffin slices within a very short period of time. In such a case the slices should be placed on clean glass without any cement. After drying the slices, we proceed to remove the paraffin from the slices with xylene, and then to stain the slices, preferably with alcohol solutions of the staining agents, as this will permit avoiding the slices getting unstuck from the glass. Once the staining has been completed, the slices have to be dehydrated with alcohols, and then a little cyclone lake is placed on the slices. When it solidifies, the lake will form a hard film. When the lake film is hard, we can make incisions with a razor blade and pick film fragments with slices from the glass using a pair of pincers. The amount of lake used determined

the strength of the film and the possibility of subsequent microscope observation of the slices. The film with slices is then cut into suitable fragments and sealed in a solution of synthetic resin. The same method can also be used to remove important specimens from damaged slide glass and to place them on new ones for further storage or observations [1, 2, 3, 6, 7].

2.1.8. Prospects for the future of optical microscopy

Optical microscopy is a very important method used in studies on the biology of cells. This is shown by the great number of studies in which optical microscopes are used as the basic tools of research. A significant limitation of optical microscopy is the limit resolution of approximately 200 nm, below which no objects can be observed, such as ribosomes, viruses, or individual protein molecules. There are many unknowns at the level of light observed in optical microscopes, but in spite of this limitation optical microscopy should be accepted as a method necessary in the study of the surrounding micro-world.

REFERENCES

1. Gerlach D. 1972. Outline of botanical microscopy (in Polish). PWRiL, Warszawa.
2. Burbianka M., Pliszka A., Jaszczura E., Teisseyre T., Załęska H. 1971. Microbiology of food. Microbiological methods for the study of food products (in Polish). PZWL, Warszawa.
3. Litwin A., 1999. Foundations of microscopy techniques (in Polish). Wydawnictwo Uniwersytetu Jagiellońskiego, Kraków.
4. Meyer – Arendt J. R., 1979. Introduction to Optics (in Polish). PWN, Warszawa.
5. Jay Orear, 1999. Fizyka, WNT.
6. Pluta A., 1999. Foundations of microscopy techniques (in Polish). Wydawnictwo Uniwersytetu Jagiellońskiego, Kraków.
7. Przestalski S., 2001 Physics with elements of agrophysics and biophysics (in Polish), PWN, Warszawa.
8. Skorko M., 1973. Physics (in Polish) PWN Warszawa.
9. Pawlak K., Król A. 1999. Changes of the potato tuber tissue structure resulting from deformation (in Polish). Acta Agrophysica 24, 109-133.
10. Haman J., Konstankiewicz K. 1999. Damage processes in the plant cellular body (in Polish). Acta Agrophysica 24, 67-86.
11. Konstankiewicz K., Czachor H., Gancarz M., Król A., Pawlak K., Zdunek A. 2002. New techniques for cell shape size analysis of potato tuber tissue. 15th Triennal Conference of the European Association for Potato Research, Hamburg.
12. Francon, M. 1961. Progress in Microscopy. Pergamon Press: London (also Row, Peterson and Co.: Elmsford, NY.)
13. Gray P., 1964. Handbook of Basic Microtechnique. McGraw-Hill: New York.
14. http://www.discoveryofthecell.net/

2.2. Confocal Microscopy

Artur Zdunek[*]

2.2.1. Limitations of optical microscopy

The Confocal Microscope is one of the types of optical microscopes. Historically, optical microscopy initiated the rapid development of studies on the structure of biological materials at the level of tissues and cells. The classical optical microscope, however, has a number of limitations, such as:

1. Absolute limit of resolution d, determined by Abbe's Law, $d=1.22 \times \lambda_0 / (NA_{obj} + NA_{cond})$, where: λ_0 is the wavelength in vacuum, NA_{obj} and NA_{cond} are the numerical aperture of the lens and the condenser, respectively.

2. Limited contrast resulting from the natural properties of most biological materials. This limitation is less significant in direct observation, as an experienced observer can usually recognize and describe a given element of the micro-structure. The problem becomes more acute when the objective of the analysis is e.g. quantitative description of specific geometric features of the micro-structure using a computer. Additionally, for a series of images from various areas of the sample, the elements of the structure described should be clearly identified so that they can be effectively isolated from the images with the help of specific computer algorithms.

3. Information from the focal plane is interfered with by information from the out-of-focus areas above and below the focal plane (Fig. 2.18). This shortcoming is related to the one mentioned above. Out-of-focus fragments of the image reduce the contrast and cause problems e.g. in 3D reconstruction of the structure. Computer analysis of images in 2D is also difficult.

4. Complicated methods of sample preparation. Fig. 2.19 presents an example of the structure of potato tuber tissue after complex preparation which included dehydration in a series of alcohols, setting in paraffin, slicing and removal of paraffin. As can be noticed, e.g. cell walls look different in Fig. 2.18 than in Fig. 2.19. They are more arched in shape and are often undulating. Sample preparation procedures, and especially slicing, resulted in breaks or gaps in come of the walls. Therefore, it is not possible to state

[*] Artur Zdunek, PhD
Institute of Agrophysics, Polish Academy of Sciences
ul. Doświadczalna 4, 20-290 Lublin 27, Poland
e-mail: azdunek@demeter.ipan.lublin.pl

that the image of a structure after the preparation is a true representation of the structure in undisturbed tissue. It is obvious that any operation on the tissue, even just a slice through the structure, disturbs the true image of the tissue. However, we should aim at such a development of the sample preparation methods that would eliminate that phenomenon.
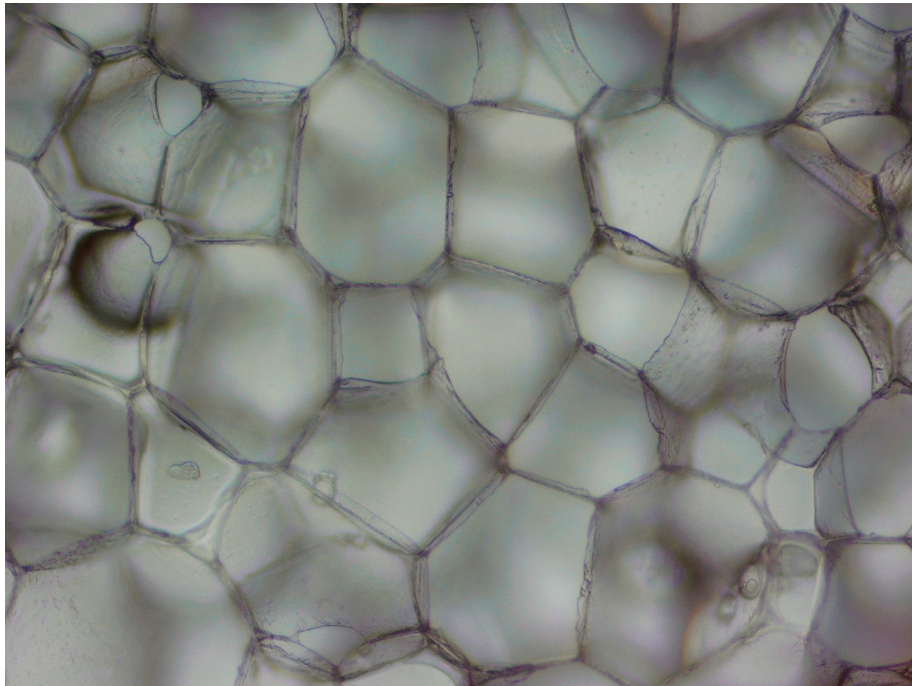

Fig. 2.18. *Potato tuber tissue. The image originates from an optical microscope with 10X magnification. The sample was 1mm thick and was sliced with a razor blade. The focal plane and the out-of-focus areas above and below the focal plane can be seen. This results in limited contrast and interference with information from the focal plane.*

For the above reasons the development of new types of microscopes, such the transmission electron microscope, the scanning electron microscope and the tunnel microscope caused the classic optical microscope to cease being the basic tool in the study of biological structures. However, the development of numerous procedures for sample staining and preparation helps maintain its usefulness in routine studies of various materials.
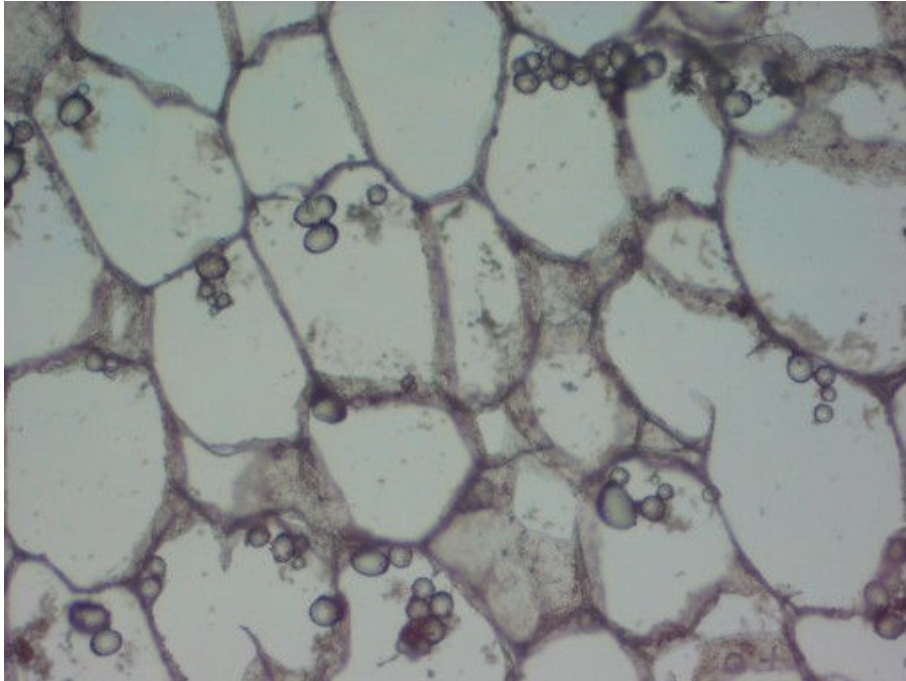
Fig. 2.19. *Potato tuber tissue. The image originates from an optical microscope with 10X magnification. The sample was 2 μm thick and it was sliced with a microtome after preparation: dehydration in a series of alcohols, setting in paraffin, slicing and paraffin removal. Focal place clearly seen; out-of-focus areas visible to a lesser degree than in Fig .2.18. The preparation caused breaks and deformation of cell walls.*

2.2.2. Confocal microscope principle of operation

The operating principle of the confocal microscope was presented to the patent office in 1957 by Martin Minsky, postdoctoral fellow at the Harvard University (Minsky 1957). In the design proposed by Minski, the conventional condenser was replaced with a lens identical to the main lens of the microscope. The original schematic of the microscope operation is presented in Fig. 2.20. Light (1) illuminating the object studied is limited by a diaphragm (2) located exactly in the optical axis of the microscope. Then the light passing beam is focused by the condenser (3) on the object viewed (4) located in the focal point. The second separation of the light takes place at the second diaphragm (6). This happens in such a manner that the light beam, having passed through the object viewed, is focused by the lens (5) in the plane of the second diaphragm (6). Then light coming from beyond the focal point (A) in the object viewed

is stopped by the diaphragm, so that the detector received only information from the area of interest. The important issue is for the diaphragms to be confocal with the plane of observation. The interesting and extremely important fact is the possibility of scanning and obtaining a secure field of view in two planes. Through movement of the object viewed in a plane perpendicular to the optical axis the x-y image is obtained, and movement of the object along the optical axis provides the z-axis image. One can also imagine combinations of movements in those directions and the obtaining of 2D and/or 3D images.
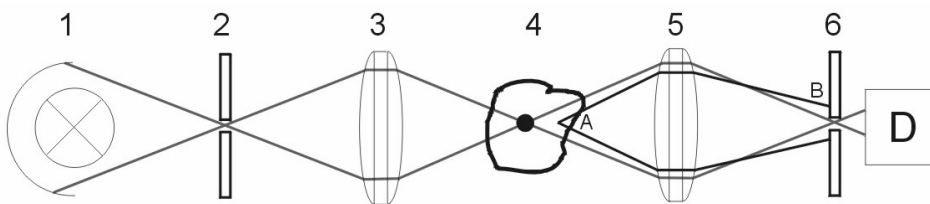

Fig. 2.20. *Schematic presentation of image generation in the optical microscope patented by Minsky. 1- light source, 2 and 6-confocal apertures, 3 - condenser, 4- object, 5-objective, D-detector, A- out of focal point, B- light stopped.*

Marvin Minsky proposed also another design of optical microscope, much more commonly used at present. In the design described above, light passed through the object studied, and the system was based on two identical lenses. In Minsky's second proposal, the microscope operated on the principle of epi-luminescence. Fig. 2.21 presents the original schematic of the microscope. Like in the first design, light is limited by the first diaphragm A_1, and then focused in the object studied, having passed through a semi-transparent mirror M_1. The original aspect here is that the object studied in placed on another mirror, M_2. Light reflected from the mirror passes through the same lens O and is reflected by the mirror towards another diaphragm, A_2, confocal with relation to the first one. This design has significant advantages over the first one, as it reduces the number of lenses used, which simplifies change of the magnification rate (change of one lens only) and permits the study of totally opaque objects (image from the surface of the object studied). In this design, also through moving the object studied, scanning is possible in any plane.
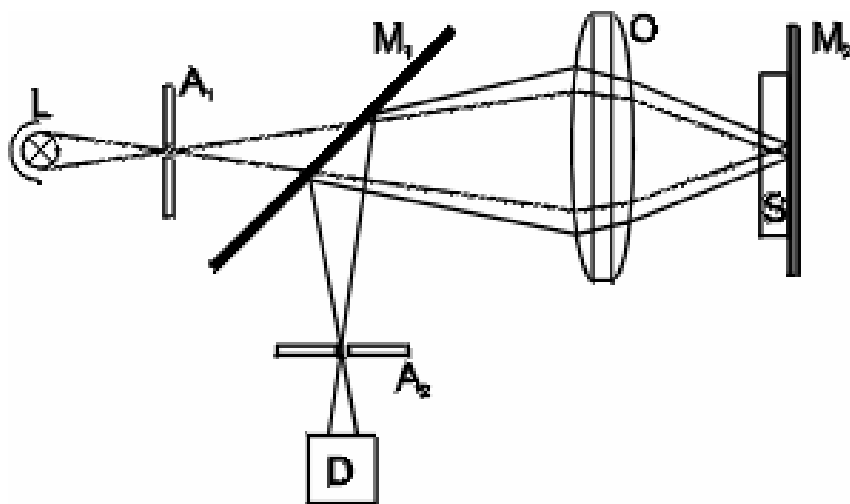
Fig. 2.21. *Confocal Microscope operating in the epi-luminescence mode (after Minsky 1957).*

In both designs, scanning the object with light was achieved by the object movements over short distance sections in a specific order. Changes in the luminance of the light reaching the photodetector were converted to electric current and displayed on an oscilloscope whose electron beam motion had to be synchronized with the sample movements. The magnification rate of the microscope was equal to the ratio of the electron beam motion amplitude in the oscillowcope to the sample movement amplitude. To explain the consequences of such a definition in the case of the confocal microscope, the Law formulated by Lukosz in 1966 can be employed. The Lukosz Law says that resolution can be increased through increasing the field of view (Lukosz 1966). Theoretically, the field of view can be infinitely large if scanning is employed. Therefore, placing an infinitely small diaphragm at an infinitely small distance from the object and performing a precision scan of the object one will be able to achieve, theoretically, enormous rates of magnification. The condition for this is to ensure accurate sample transport, comparable to the optical resolution of the microscope, or some other more sophisticated method of sample scanning.

One of the more important features of confocal microscopes is the separation of the planes located below and above the focal plane from the focal plane itself. In practice, however, it is not possible to make infinitely small (point-aperture) diaphragms, so the image is generated from a thin focal layer rather than from an actual focal plane. The larger the aperture, the thicker the focal layer.

The thickness of the focal layer is also related to the lens used (its numeric aperture, NA). For example, M. Petran (1995) reports, for the Tandem Scanning Reflected Light Microscope (TSRLM), that for an immersion lens of 40X 0.74 NA the image changes totally with every 5 μm focusing step in the Z axis, while for a 40X 1.3 NA lens – with every 1μm. Nevertheless, the difference in comparison to the image generated by the conventional optical microscope is notable. James B. Powley (1989) enumerates, among others the following advantages of the confocal microscope:

1. Reduction in the loss of image resolution resulting from light diffusion (improved contrast).
2. Increase in effective resolution.
3. Improvement in the signal-to-noise ratio.
4. Possibility of studying thick objects and light diffusing objects.
5. Possibility of theoretically unlimited extent scanning in the X-Y plane.
6. Scanning in the Z axis.
7. Possibility of electronic change of magnification rate.
8. Possibility of quantitative evaluation of the optical properties of the sample tested.

An example of the micro-structure of potato tuber tissue, obtained with the TSRLM confocal microscope (described below) is shown in Fig. 2.22. Comparing the image with that in Fig. 2.18, one can observe a distinct improvement in the contrast; the cell walls are visible as bright lines, while the interior of the cells is almost black. The image originates from a very thin layer of the tissue, hence such an optical section may also include cell membranes oriented in parallel or almost-parallel to the scan plane, visible as bright areas in the image. Such an image, due to its high contrast, is suitable for e.g. analysis of the geometric features of the mechanical skeleton of plant tissue.
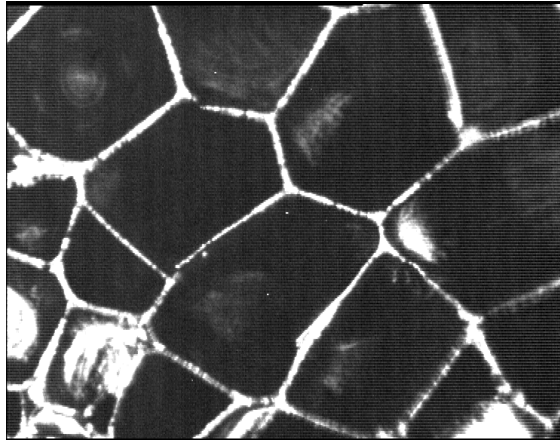
Fig. 2.22. *Potato tuber tissue. Image obtained with the TRSLM microscope (described further on in the text). Magnification 20X. Preparation: 1 mm sample sliced with a razor blade and washed with tap water.*

The advantages of the microscope listed above may be utilized provided adequate technical solutions are employed, especially in the aspect of scanning. Several scanning methods can be used:

1. Mechanical scanning through ordered movements of the sample. In Minsky's first design, the table on the sample was placed was induced to vibrate with the help of electromagnets. As has been mentioned above, this required extraordinary accuracy of the mechanical system. Therefore, in practice such system worked correctly only with low scanning speeds (Petran et al. 1995). Additionally, if the scan was to be non-linear, the computer had to linearize the image, most frequently by saving the image and replaying it later. The design in which the scanning process was realized through movements of the object scanned might not be suitable for the examination of objects changing in time, as the time needed for the scan to be completed could be as long as 100 seconds (Entwistle 2000).

2. Optical scanning through controlled movement of light beam over the object under observation. The scanning is effected through the movement of mirrors. The time of image acquisition is shorter than in the mechanical scan, at the level of 0.5-10 sec per image (Entwistle 2000).

3. Scanning with the help of the Nipkov's disc. This method, due to the speed of scaning (several to several dozen frames per second) will be described in greater detail (Pawle 1989, Petran et al. 1995, Wilson 1990).

2.2.3. Nipkov's disc

At the beginning of the 20th century, a young student from Berlin, Poul Nipkov, invented a method for the conversion of a 2D image into an electric signal that could be transmitted as a uni-dimensional signal (Nipkov 1884). In his solution, the image of an object was formed as a result of ordered scanning with the help of a disc with rectangular apertures arranged in so-called Archimedes spirals. The apertures are arranged at constant angle with relation to the centre of the disc, but their distance from the centre gradually decreases. A schematic diagram of Nipkov's disc is presented in Fig. 2.23 (Inoue 1986). Rotation of the disc at a constant speed generates, one by one, fragmentary images of the object in the form of light intensity pulses which are then recorded by the detector.
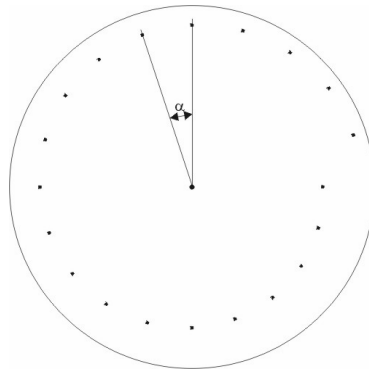
Fig. 2.23. *Archimedes spiral used by Nipkov for image scanning and conversion into a linear signal. The apertures in the disc are arranged at a constant angle to the disc centre while their distance from the centre decreases by a constant step (after Inoue 1986).*

2.2.4. Tandem Scanning Reflected Light Microscope-TSRLM

The above idea was put into practice for scanning in a confocal microscope isixties of the 20th century by Mojmir Petran (Egger and Petran 1967, Petran et al. 1968). For scanning the image of a sample, a greater number of apertures can be used (Fig. 2.24). It is also possible to employ a greater number of Archimedes spirals, which will provide the same number of scan cycle repetitions with one revolution of the disc. The important thing is for the number of the Archimedes spirals to be even. Each of the spirals has its equivalent (twin) on the opposite side of the disc. One side of the disc is used to limit the amount of light falling on the object, the other for the reflected light. The rotating disc plays two roles in the microscope – one is image scanning, the other to act as the confocal diaphragms. An important advantage of the application of Nipkov's disc,

in spite of the different original intentions of its creator, is the possibility of confocal image observation without any further electronic reconstruction. After the scanning, the image can be observed in the eyepiece of the microscope or recorded by means of any optical recording device.
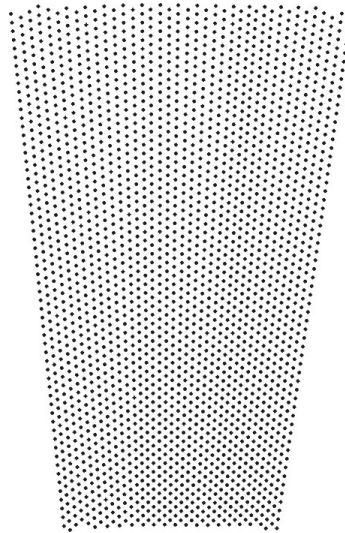

Fig. 2.24. *Fragment of Nipkov's disc used in the Tandem Scanning Reflected Light Microscope – TSRLM developed by Petran and Hadravsky.*

The microscope created by Petran and Hadravsky is known by the name of Tandem Scanning Reflected Light Microscope – TSRLM. The operating principle of the whole TSRLM is presented in Fig. 2.25. The Nipkov;s disc is made metal-coated foil 10μm thick, stretched on a frame with a diameter of 100mm (International Agr. 1995). The foil has 48,000 apertures located so that they form a ring 18 mm wide. Each aperture has a diameter of approximately 50μm. The apertures are arranged along Archimedes spirals so that every aperture has its twin on the opposite side of the disc centre. One side of the disc is illuminated with monochromatic light with a radius of 18 mm. The source of light is a mercury lamp. The light is directed onto the rotating Nipkov's disc with the help of a mirror and a collimator. After passing through the apertures of the disc, the light is directed, by means of system of mirrors, to the lens and, after being reflected from the object studied, returns through the same lens, passes through a light-splitting plate, and then again through the apertures of Nipkov's disc, but on the other side with relation of the axis of rotation. The image can be observed in the eyepiece or by means of a CCD camera installed on an additional image splitting element.
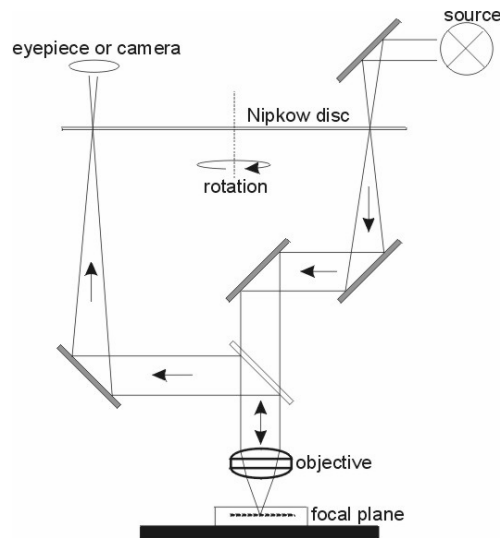
Fig. 2.25. *Schematic of the Tandem Scanning Reflected Light Microscope – TSRLM.*

Thanks to the high rotational speed of the Nipkov's disc (approx. 2,000 r.p.m.) and the absence of necessity of electronic reconstruction of the image after scanning, the image of the sample viewed can be observed in real time as the time of image generation is only about 20 ms. This is an extremely important feature in the study of living objects or objects changing in time. Additionally, most of the advantages of the original Minsky's patent, listed earlier on, hold true also for the design developed by Petran *et al.* Concentrating on plant tissues, one can emphasize the following features of the TSRLM from the view point of the study of such materials:

1. Possibility of observation of micro-structure from a thin layer in undisturbed object with preparation (e.g. living tissue or non-flat and non-polished surface)
2. Enhanced contrast.
3. Observation in real time.
4. Possibility of observation in layers beneath sample surface.

That last feature of the microscope appears to be highly useful in the next challenge that appears before the researchers, i.e. 3D reconstruction of the cellular structure of plant tissues. The tedious process of mechanical sectioning of samples may be replaced by optical sectioning. A major limitation here is the transparency of the test material. The depth of penetration depends also on the power of the light source and on the numeric aperture of the lens. Petran (1995)

estimated that for most animal tissues that depth is of the order of 0.2-0.5 mm. Our own experiments with plant tissues indicate similar values. The 3D reconstruction may be realized by making a series of X-Y scans with a specific step in the Z axis and computer compilation of images.

The confocal microscope, however, is not the perfect tool. The application of the Nipkov's disc has two fundamental shortcomings. The first is the possibility of light from reflected light from out of the focal plane to pass through the disc aperture. Another is the loss of light - 95-99% is blocked on the disc. In the confocal microscope, also in the TSRLM, the phenomenon of chromatic aberration occurs. This phenomenon, however, can be put to a good use. The application of a non-monochromatic source of light, such as the mercury lamp, permits the generation of an image which is a projection of the 3D surface of the sample observed. The image visible in the eyepiece is a colour image, thanks to the different angles of refraction of different colours of light when passing through the lens. For this reason the colours are related to the spatial position of the pixels (in CCD camera) along the Z axis, with the deepest regions corresponding to colours equivalent to the shorter wavelengths (Fig. 2.26). For the mercury lamp, the palette of colours observed is within the range from yellow to violet. Fig. 2.26 presents a visualization of the spatial reconstruction of a potato tuber cell which is the result of utilization of chromatic aberration.
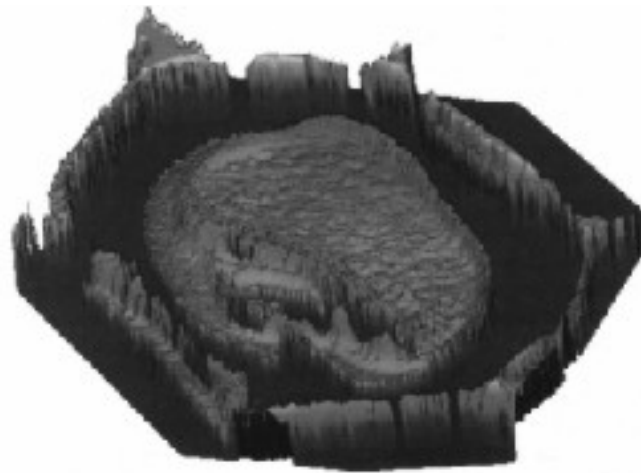

Fig. 2.26. *3D visualization of a cell of potato tuber tissue generated as a result of chromatic aberration in the TSRLM. The image was converted to grey. The brightest areas correspond to yellow, the darkest – to violet.*

2.2.5. Confocal Scanning Laser Microscope - CSLM

Another kind of confocal microscope is constituted by the laser microscopes. Like in the conventional design, the confocality of diaphragms makes the image to be obtained only from a specific layer in the object studied. However, the application of laser as the light source permits the utilization of the phenomenon of fluorescence.

The laws of quantum physics state that molecules may be in certain discrete states of energy. The energy or quantum state of a molecule is composed of energy levels of electrons, divided into sublevels related to the vibration and rotation of molecules. Fig. 2.27 presents schematically two energy levels in a molecule. From the basic state of S_0 the molecule can be excited to the higher energy level of S_1 by absorbing an electromagnetic wave with the frequency of ν which, multiplied by the Planck constant h is equal to the energy of transition between those energy (quantum) levels (the phenomenon of resonance occurs). The significant aspect of this that the frequency ν (or the wavelength λ) may only assume discrete values.
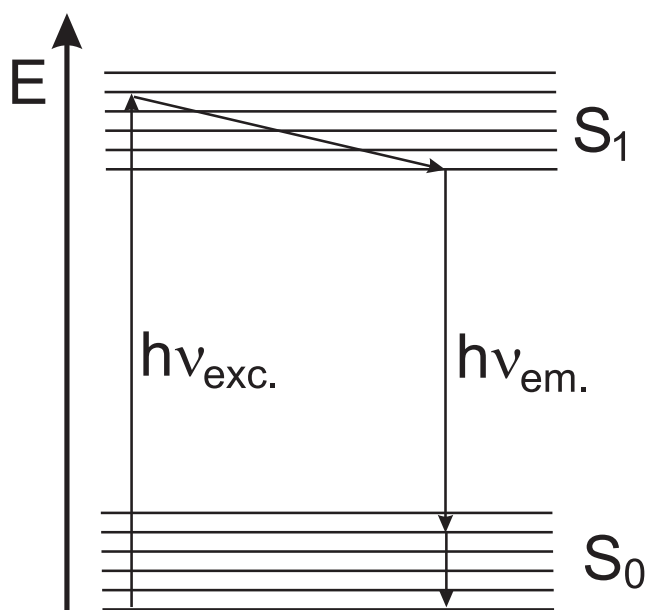
Fig. 2.27. *Jabłoński's diagram of molecule. Energy (quantum) levels S_0 and S_1 have sublevels related to the rotation and vibration of molecules. Absorption of wave occurs when the length of the wave corresponds to the energy of transition between the levels S_0 S_1. Emission occurs after a time known as the fluorescence time, during which partial dissipation of energy takes place.*

However, because of the broadening of the energy levels, the absorption spectrum does not have a discrete character but a continuous one, similar to the emission spectrum (Fig. 2.28). This happens especially with molecules of complex and long molecular chains, as their number of energy (quantum) levels is so high that electromagnetic waves can be absorbed within a very broad spectrum. The time of molecule "life" in the excited state is sometimes called the fluorescence time and usually lasts for about 1-5 ns. During that time transitions between sublevels take place in the excited state, i.e. energy dissipation occurs e.g. due to collision of molecules. Then the molecule returns to its basic energy state, emitting an electromagnetic wave of greater length. The emission spectrum is shifted with relation to the absorption spectrum towards greater wavelengths (Fig. 2.28). This is the so-called red-shift. Once the molecule has returned to its basic energy state, relaxation of energy may still occur between the sublevels.
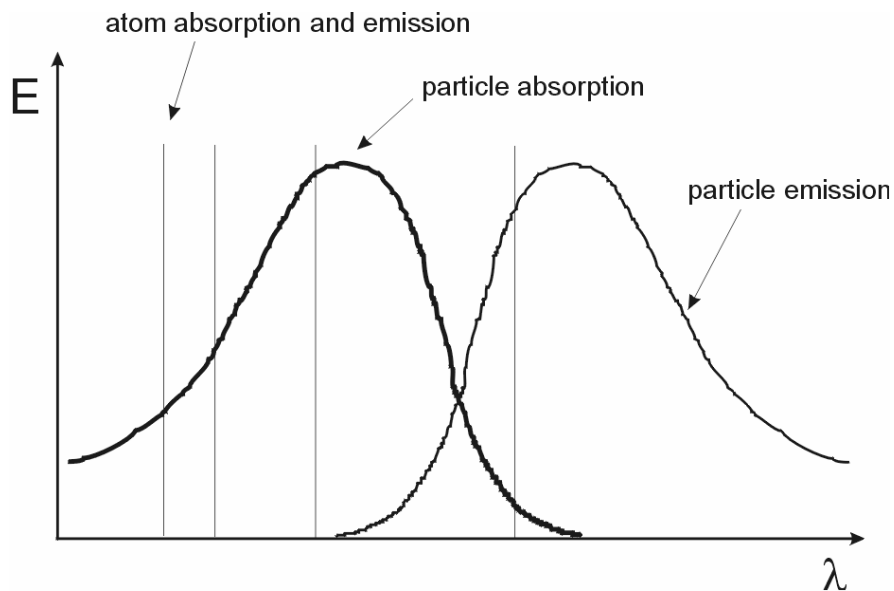
Fig. 2.28. Broadened spectra of molecular absorption and emission. The emission spectrum is shifted towards greater wavelengths. The absorption and emission spectra of a single atom coincide.

The phenomenon described above is utilized for the observation of specific elements of the micro-structure of plant and animal tissues. Through the use of various types of dyes, selected types of tissues can be stained or, more specifically, chemical compounds contained in those tissues. The resultant fluorescent image provides information concerning primarily the object of interest to the observer. Every day has a characteristic wavelength of emission and

excitation. Therefore, an additional condition is the application of a laser with wavelength corresponding to the excitation wavelength of a given dye. This, however, raises another problem, related to the fact that the excitation and emission spectrum of a dye has a certain width, is continuous, and has a maximum at a certain wavelength. Likewise the emission spectrum. This necessitates the application of suitable filters for the falling and emission light that transmit light with wavelengths corresponding to the absorption and emission maxima, respectively.

REFERENCES

1. Minsky M., 1957: U.S. Patent #3013467, Microscopy Apparatus.
2. Lukosz W., 1966. Optical system with resolving powers exceeding the classical limit. J. Opt. Soc. Am., 56, 1463-1472.
3. Petran M., Hadravsky M., Boyde A., 1995: The tandem scanning reflected light microscope. Int. Agrophysics, 9, 4, 275-286.
4. Pawley J.B., 1989: Handbook of biological confocal microscopy. Plenum Press. New York.
5. Entwistle A., 2000: Confocal microscopy: an overview with a biological and fluorescence microscopy bias. Quekett Journal of Microscopy, 38, 445-456.
6. Wilson T., 1990: Confocal Microscopy. Academic Press Limited, London.
7. Nipkow P., 1884: German Patent #30,105.
8. Inoue S., 1986: Video Microscopy. Plenum Press, New York.
9. Egger M.D., Petran M., 1967: New reflected-light microscope for viewing unstained brain and ganglion cells. Science 157, 305-307.
10. Petran M., Hadravsky M., Egger M.D., Galambos R., 1968: Tandem-scanning reflected-light microscope. J. Opt. Soc. Am. 58, 661-664.

2.3. Electron Microscopy

Andrzej Król[*]

The idea of substituting the beam of light generating the image in the optical microscope with a beam of electrons generating an image of their interaction with the specimen viewed was a natural consequence of the relation discovered by Ernst Abbe, according to which the maximum resolution of a microscope cannot exceed the value of a half of the length of the light wave used. Waves corresponding to electrons with energy of the order of 10^4 eV permit increasing the resolution of the electron microscope by a factor of $10^2 - 10^3$ as compared to the optical microscope. The first successful attempt at building such a microscope was made by a team of physicists, headed by Ernst Rusk, in 1931 (Nobel Prize in 1986). The first production transmission electron microscope (TEM) was made by Siemens at the end of the nineteen thirties. The first commercial microscopes of this type became available after the second world war. The idea of the scanning electron microscope (SEM) was first invented by Manfred von Ardenne (1938), but the practical implementation of the idea was not possible until electronic systems reached sufficient level of advancement in the nineteen sixties.

2.3.1. Operating Principle

With respect to the manner of image generation, the scanning electron microscope (SEM) is a reconstructive device. Certain close-to-surface features of the specimen viewed are represented as a function of its geometry. The focused beam of electrons pans the surface of the specimen, line by line, and the values of signals from the detectors are displayed on two monitors connected in parallel (Fig. 2.29). One of the monitors was used for observation of the specimen by the operator, and the other was photographed using a camera with lens and film parameters adapted to the task. In contemporary designs, signals from the detectors are transmitted to image cards integrated with a dedicated computer system. During the interaction of the focused beam of electrons with a very thin (~ 4 nm) layer on the surface of the specimen, a number of phenomena occur – backscattering of electrons of the incoming beam, emission of secondary electrons (Auger electrons), emission of photons of continuous and characteristic radiation, elastic effects (Fig. 2.30).

[*] Andrzej Król, MSc
Institute of Agrophysics, Polish Academy of Sciences
ul. Doświadczalna 4, 20-290 Lublin 27, Poland
e-mail: a.krol@demeter.ipan.lublin.pl

Fig. 2.29*. A scanning electron microscope (TESLA BS 340). Control monitor /1/. Monitor-camera unit /2/.*
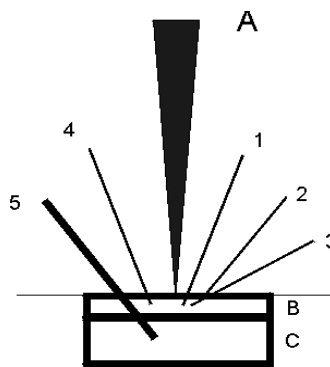

Fig. 2.30. *Schematic of primary electron beam /A/ interaction with the specimen material. Close-to-surface layer /B/. Deeper layer /C/ ~ 4 nm .Luminescence /1/. Reflected electrons /2/. Secondary electrons /3/. Continuous X radiation /4/. Characteristic X radiation /5 /.*

Due to the high vacuum inside the microscope chamber, specimens of materials of agricultural origin (fragments of tissues, kernels, soil, etc.) must be thoroughly dried using the method of lyophilization (freeze-drying) (Fig. 2.31) or critical point drying (Fig.2.32). Next, the specimens must be given the required electric conductivity through deposition of thin films of metals in sputter coaters (Fig.2.33), surface saturation with osmium oxides, or carburization.

Fig. 2.31. *Lyophilizing cabinet with accessories.*

Fig. 2.32. *Equipment set for critical point drying.*

Fig. 2.33. *Sputter coater with metallic coat thickness control (Au, Pt).*

2.3.2. Applications (examples)

The examples presented concern the application of scanning electron microscopy (SEM) in studies on the cellular structure of potato tuber tissue. The BS 340 microscope used has a large chamber that can accommodate specimens with surface areas of several dozen square centimetres, which permits taking photographs of preparations with a representative number of cells within the section plane. Specimen preparation was performed according to two methods. Two successive slices, 3 mm thick, were cut from the tuber of cv. Irga potato. Then square specimens, with the surface area of 1 cm^2, were cut from the slices, from near the inner core. Next, one specimen was prepared in a conventional manner, i.e. frozen, lyophilized, placed in a sputter coater and metal-coated (Fig.2.34a). The other specimen was subjected to preliminary dehydration in a series of acetone solutions with increasing concentrations, and then to the same procedure as in the case of the first specimen (Fig. 2.34b).

Comparing the images a) and b) we can see that the application of preliminary dehydration in acetone solutions causes a reduction in the number of defects resulting from specimen preparation. Examples of characteristic morphological details of the parenchyma tissue of potato tuber are presented in subsequent photos (Fig. 2.35, 2.36, 2.37) taken by means of the BS 340 SEM BS 340.

Fig. 2.38 presents an image of aggregates made up of starch granules. As we can see in image b), one small granule grew on the surface of a large one and it is rigidly attached to it. This may result in the initiation of a crack in case of a loading with the same orientation.


a)   b)
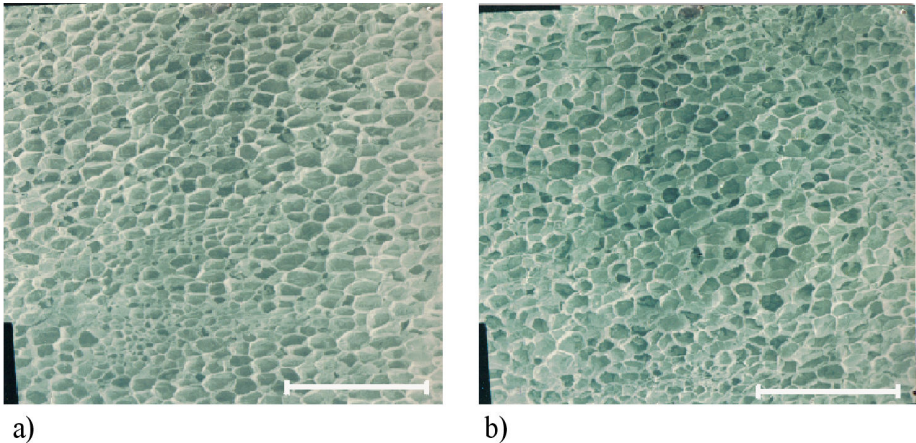
Fig. 2.34. *Specimen dehydrated in acetone solution, a) specimen subjected to direct freezing, b) Magnification - X 50. Bar 500 μm.*

a)   b)
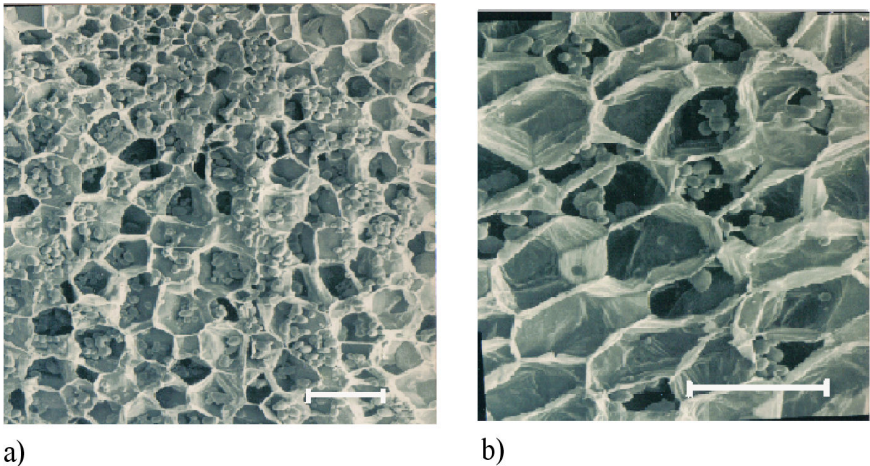
Fig. 2.35*. View of starch granules: specimen not washed, dried acc. to the triple point method. Magnification - X 100, a) Magnification - X 250, b) Bar 100 μm.*
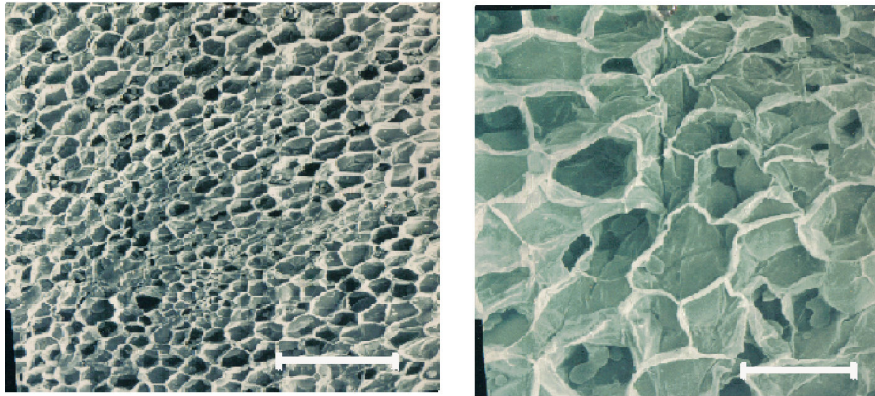
<center>a)</center>   <center>b)</center>

Fig. 2.36*. Image of a section of conducting bundles on the background of parenchyma tissue of the outer core. Bar 500 μm, a) Traces of damage to cell walls sustained in the process of specimen preparation (lyophilization). Bar 100 μm b).*
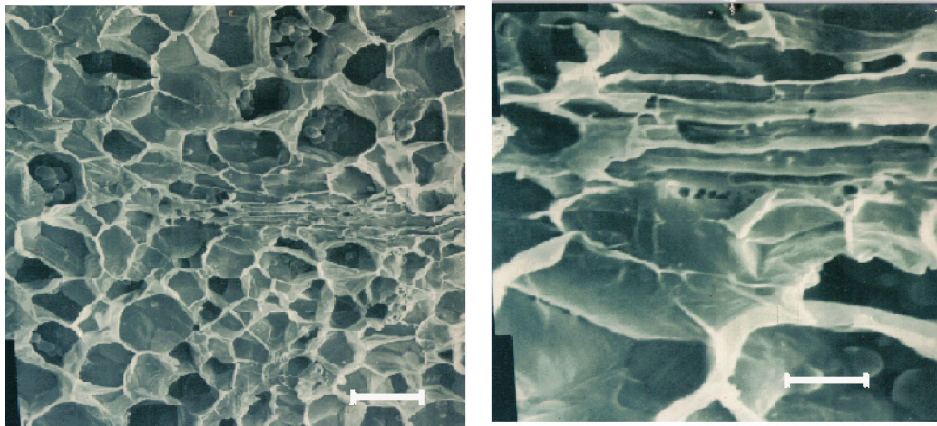
<center>a)</center>   <center>b)</center>

Fig. 2.37*. The shape of cells of conducting bundle in potato tuber parenchyma tissue. Longitudinal section. Magnification - X200; Bar 100 μm /A/. Magnification - X400; Bar 20 μm /B/.*
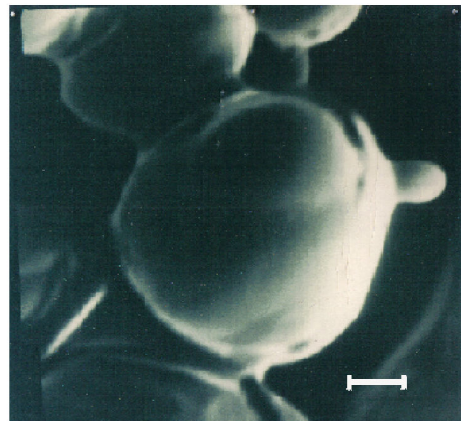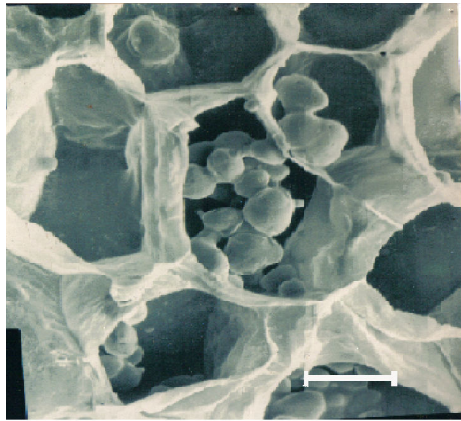
a)

b)

Fig. 2.38. Aggregation of starch granules within cells of parenchyma tissue of potato tuber cv. Irga at two magnification ratios - X 200 a), and X 600 b)
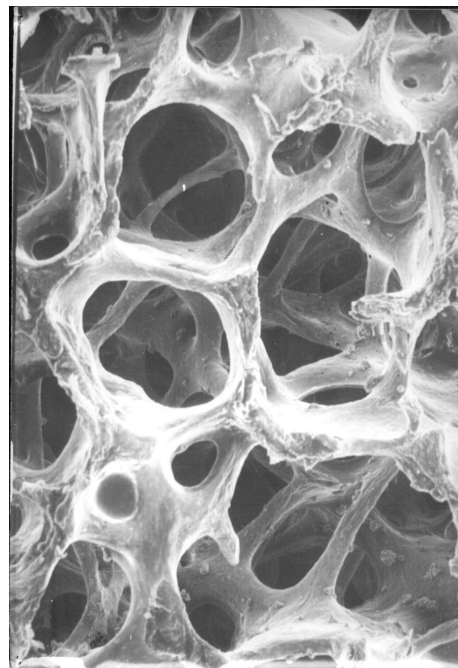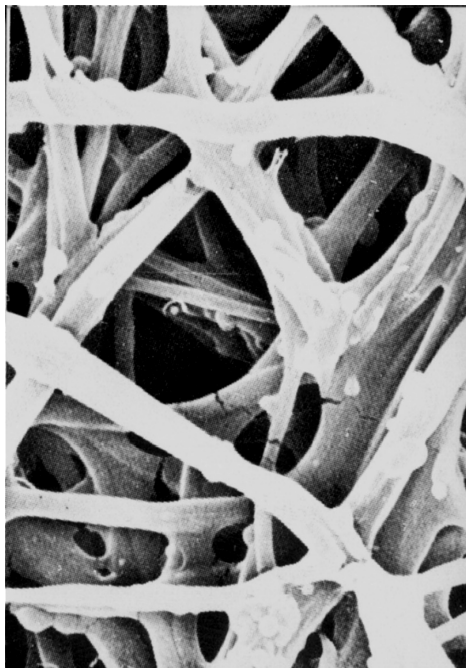
a)

b)

Fig. 2.39. Morphological similarity of images of two different specimens? Bird's egg shell a) and human heel bone b)

2.3.3. Limitations and development

The necessity of having high vacuum inside the columns with the electron beam control systems in electron microscopes /TEM and SEM/ restricted their application for studying the structure of materials containing even slight amounts of water which, introduced into the microscope, could cause extensive damage. Dehydration and metal coating of samples of agricultural materials (soil, materials of animal or plant origin) affect their structure to an extent that can be described as drastic. Preparation procedures consisting in specimen dehydration and imparting to specimens the required conductivity have been continually improved (Fig. 2.34 a) and b) in order to eliminate their effect on the parameters of the structure studied. Over the last two decades two significant changes were made in the design of SEM microscopes.

1.   Introduction of the technique of cryofixation.
2.   Implementation of the technique of variable vacuum.

Ad.1. In the method of cryofixation, the specimen studied is placed in a freezing apparatus and, once it is in the state of deep freeze (< 100 K), the specimen is transferred to a cryo-microtome, a sputter coater, or directly to the chamber of the microscope (Fig. 2.40). Both the sputter coater and the microscope must be equipped with refrigeration stages. Specimen temperature reduction rates obtained in the freezing apparatus are of the order of 10^2 - 10^4 $^{\circ}$K/s. Such a rate of refrigeration prevents the formation of ice crystals which are the main cause of changes in the structure. One of the leading centres that has been developing the method for over a dozen years and which has its own unique apparatus is the Max-Planck Institute in Dortmund where a group of researchers - Karl Zierold and others (7-10) –have developed a number of methods permitting the localization of ions in frozen cell structures, which allows the study of mechanisms controlling their transfer. The most recent designs have the possibility of controlled sublimation of water from specimen surface inside the microscope chamber, which permits successive layers to be uncovered and the internal structure to be recorded.
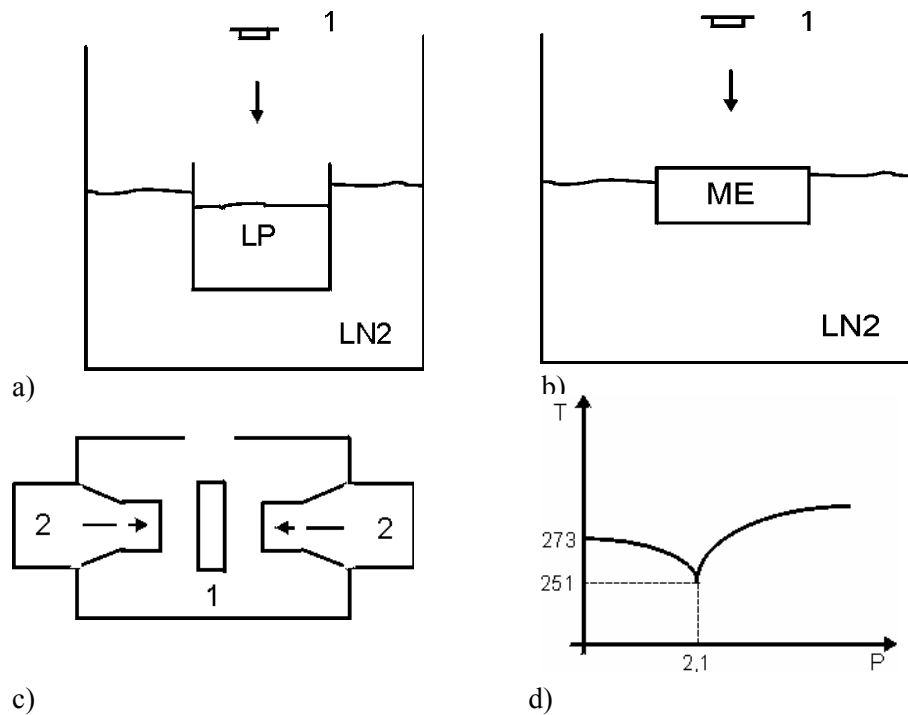
Fig. 2.40. *Schematics of the cryofixation method: Cryofixation in liquid propane a).*
Contact cryofixation b)/. Schematic of cryofixation chamber c) High-pressure
cryofixation d) Specimen /1/. Liquid propane nozzles /2/. Metal die /ME/.
Liquid propane /LP/. Liquid nitrogen /LN2/. Temperature /T/. Presure /P/.

Ad.2. The variable vacuum SEM /Environmental Scanning Electron
Microscope (ESEM) is one of the latest and most advanced technologically
designs in the field of electron microscopy. Foundations for this branch
of electron microscopy were created in mid 80's of the 20th century, at the Sydney
University, by a group headed by Danilatos. In the ESEM, the space surrounding
the specimen has a pressure of ~ 50 Tr, while the remaining section along the axis
have decreasing pressures that reach 10^{-7} Tr in the electron gun section
(Fig. 2.41). The relatively high pressure surrounding the specimen permits
observation of specimens in natural condition, like in optical microscopy, but the
magnification ratios achieved here are of the order of X 10^5. The ESEM
microscopes have also a new type of detector (Fig. 2.42) which makes use of the
interaction of secondary electrons with molecules of the gas surrounding the
specimen studied.
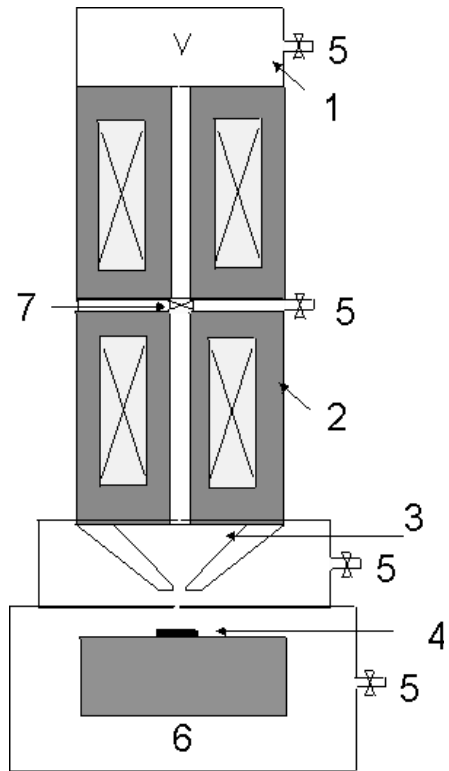
Fig. 2.41. *Schematic of the ESEM microscope. Electron gun /1/. Beam deflection coil area /2/. Focusing section /3/. Specimen /4/.Vacuum pump ports /5/. Intermediate chamber /6/.Vacuum lock /7/.*
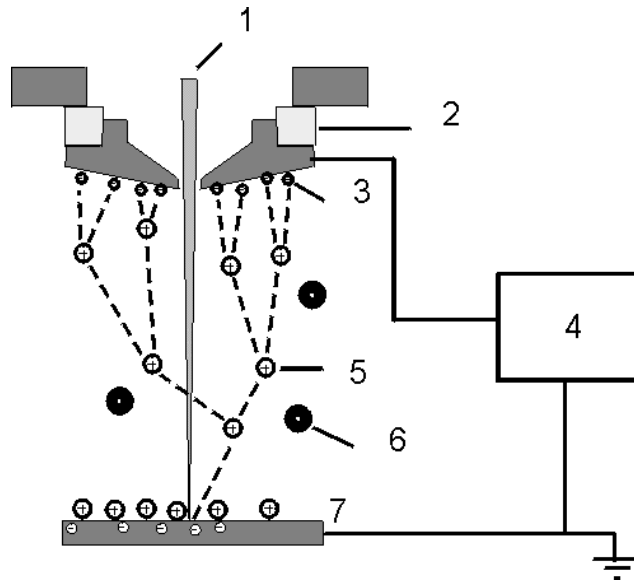
Fig. 2.42. *Schematic of ESEM detector. Primary beam /1/. Dielectric /2/. Electrons /3/. Current meter /4/. Positive ions /5/. Gas molecules /6/. Specimen /7/.*
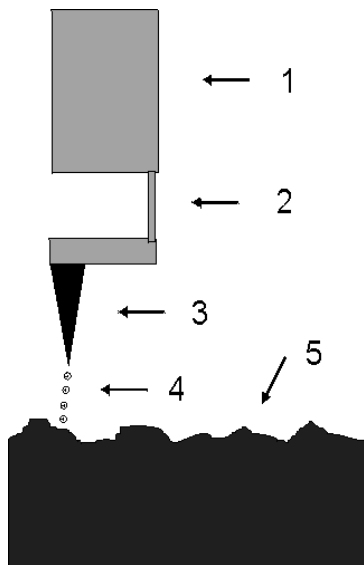
Fig. 2.43. *Schematic of tunnel microscope. Indexing 3D head /1/. Current measurement /2/. Blade /3/. Tunnelling electrons /4/. Surface of specimen /5/.*

Implementation of the phenomenon of cold emission of electrons permitted the design of a field microscope known as the tunnel microscope. Current intensity of tunneling electrons from the tip of the measurement blade reflects the topography of the specimen scanned (Fig.2.43). The ultimate solution in scanning electron microscopy is the close-effect or electron probe microscope in which the outer electronic shells of the atoms of the scanning probe are in direct contact with the outer electronic shells of the atoms on the surface of the specimen studied (Fig.2.44).
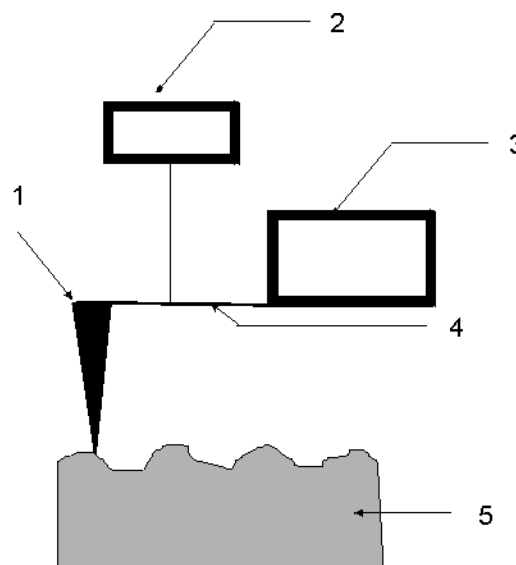
Fig. 2.44. *Schematic of the electron probe microscope. Micro blade /1/. Force (strain) meter /2/. /. 3D head /3/. Elastic element /4/. Specimen /5/.*

2.3.4. Conclusion

Over the last twenty years, scanning electron microscopy has reached the ultimate degree of resolution at the level of individual atoms of the specimens studied. The resolution of particular types of microscopes is presented in Table 2.1. The electron probe microscopes provide the possibility of shifting individual atoms and changing the structure of the surface. This makes the distinction between microscopy - as an observation technique - and nanotechnology to lose its significance.

Table 2.1.

TECHNOLOGY	LIMITING FACTOR	RESOLUTION
Human eye	Resolution of the retina	500 000 Å
Optical microscope	Diffraction of light	3000 Å
Scanning electron microscope	Diffraction of electrons	30Å
Transmission electron microscope	Diffraction of electrons	1 Å
Ion field microscope	Atom size	3 Å

REFERENCES

1. Bellare, J.R., Davis, H.T., Scriven, L.E. & Talmon, Y., 1988: Controlled environmental vitrification system: an improved sample preparation technique. J. Electron Microsc. Techn. 10, 87-111.
2. Danilatos, G.D., and Robinson, V.N.E., 1979: Principles of scanning electron microscopy at high specimen pressures. Scanning 2:72-82.
3. Danilatos, G.D., 1980a: An atmospheric scanning electron microscope (ASEM). Scanning 3:215-217.
4. Danilatos, G.D., 1980b: An atmospheric scanning electron microscope (ASEM). Sixth Australian Conference on Electron Microscopy and Cell Biology, Micron 11:335-336
5. Danilatos, G.D., 1981b: Design and construction of an atmospheric or environmental SEM (part 1). Scanning 4:9-20.
6. Danilatos, G., Loo, S.K., Yeo, B.C., and McDonald, A., 1981: Environmental and atmospheric scanning electron microscopy of biological tissues. 19th Annual Conference of Anatomical Society of Australia and New Zealand, Hobart, J. Anatomy 133:465.
7. Danilatos, G.D., and Postle, R., 1982a: Advances in environmental and atmospheric scanning electron microscopy. Proc. Seventh Australian Conf. El. Microsc. and Cell Biology, Micron 13:253-254.
8. Danilatos, G.D., and Postle, R., 1982b: The environmental scanning electron microscope and its applications. Scanning Electron Microscopy 1982:1-16.
9. Danilatos, G.D., and Postle, R., 1982c: The examination of wet and living specimens in a scanning electron microscope. Proc. Xth Int. Congr. El. Microsc., Hamburg, 2:561-562.

10. Danilatos G.D., 1983: A gaseous detector device for en environmental SEM. Micron and Microscopica Acta 14 307-319.

11. Danilatos, G.D., 1983a: Gaseous detector device for an environmental electron probe microanalyzer. Research Disclosure No. 23311:284.

12. Danilatos, G.D., and Postle, R., 1983: Design and construction of an atmospheric or environmental SEM-2. Micron 14:41-52.

13. Danilatos, G.D., 1986a: Environmental and atmospheric SEM - an update. Ninth Australian Conference on Elektron Microscopy, Australian Academy of Science, Sydney, Abstracts:25

14. Danilatos, G.D., 1986d: Improvements on the gaseous detector device. Proc. 44th Annual Meeting EMSA: 630-631.

15. Danilatos, G.D., 1986g: Specifications of a prototype emtironmental SEM. Proc. XIth Congress on Electron Microscopy, Kyoto, 1:377-378.

16. Danilatos, G.D., 1989b: Environmental SEM: a new instrument, a new dimension. Proc. EMAG-MICRO 89, Inst. Phys. Conf. Ser. No 98, Vol. 1:455-458. (also Abstract in: Proc. Roy. Microsc. Soc. Vol. 24, Part 4, p. S93).

17. Danilatos, G.D., 1990c: Theory of the Gaseous Detector Device in the ESEM. Advances in Electronics and Electron Physics, Academic Press, Vol. 78:1-102.

18. Danilatos, G.D., 1990d: Mechanisms of detection and imaging in the ESEM. J. Microsc. 160:9-19.

19. Danilatos, G.D., 1991b: Gas flow properties in the environmental SEM. Microbeam Analysis-1991 (Ed. D. G. Howitt), San Francisco Press, San Francisco: 201-203.

20. Danilatos G.D., 2000a: Radiofrequency gaseous detection device. Microsc_MicroanaL 6:12-J20

21. Danilatos G.D., 2000b: Reverse flow pressure limiting aperture. Microsc.MicroanaL 6:21—30

22. Hagler, H.K., Lopez, L.E., Flores, J.S., Lundswick, R. & Buja, L.M., 1983: Standards for quantitative energy dispersive X-ray microanalysis of biological cryosections: validation and application to studies of myocardium. J. Microsc. 131, 221-23

23. Hall, T.A. & Gupta, B.L., 1982: Quantification for the X-ray microanalysis of cryosections. J. Microsc. 126, 333-345.

24. Zierold K., Steinbrecht R.A., 1987: Cryofixation of diffusible elements in cells and tissues for electron probe microanalysis. Cryotechniques in Biological Electron Microscopy (ed. by R.A. steinbrecht and K. Zierold) 272-282 Springer-Verlag Berlin

70

3. DIGITAL IMAGES AND THE POSSIBILITY OF THEIR COMPUTER ANALYSIS

Leszek Wojnar[*]

Problems of computer image analysis presented in this Chapter constitute but a small fragment of the field. It appears that the Reader should first of all know that the tools of computer image analysis can be helpful in his work. For this reason, the greatest attention has been paid to the problems of image acquisition, and then to measurements. Elements of image processing have been introduced only to a limited extent, assuming that in the case someone undertakes studies in this field, persons with suitable experience in the subject will provide assistance in the development of image analysis algorithms.

3.1. Introduction - image analysis versus human sense of vision

Computer image analysis is not a tool that is totally new, as the history of its first commercial applications goes back to the sixties of the last century. However, for many years – primarily for economic reasons – the availability of the methods of image analysis was greatly restricted. Only now, in the era of digital cameras of all kinds, computer image analysis is a commonly available tool of research. Suffice it to say that over the last 20 years the price of a professional image analysis station has dropped by a factor of about 25. Nowadays nobody is surprised seeing a portable set consisting of a laptop computer with hooked up miniature camera and a suitable software package. Work stations of this type are frequently offered as auxiliary equipment kit for e.g. a research grade optical microscope.

Equipment and software suppliers are not willing to discuss the volume of sales, but one can assume that at present as many as several thousand computer image analysis stations are installed in Poland. We have, therefore, true availability of the tool, with a concurrent shortage of common knowledge on the possibilities of its utilization. What is meant here is not typical and routine

[*] Leszek Wojnar, Professor
Section of Computer Image Analysis
Institute of Computing Science, Krakow University of Technology
Al. Jana Pawła II 37, 31-864 Kraków
e-mail: wojnar@fotobit.net

applications, as in this respect the software provides step by step instructions, the operator being left to just follow the prompts and commands of the system. The lack of proper knowledge becomes apparent only when attempts are made at solving a specific problem. In this chapter we will try to at least partially fill the existing gap.

To avoid misunderstandings, let us first define the basic concepts – image, processing, and image analysis. The ASTM E7-99 standard defines image as the *projection of an object with the help of radiation, usually through a system of lenses or mirrors*. This definition is rather general, but it is sound. It covers a whole range of images, from those perceived by the human sense of vision, through images generated by microscopy[*], to images generated in X-ray or USG examinations, by CT apparatus, magnetic resonance, or by radio telescopes… If we analyze objects which constitute digital representations of images defined above, i.e. simply data sets (sets of numbers), the above definition of image implies that images have a certain content of information that can be recorded and processed. Therefore, images can be the subject of interest for computer science, as manifest in the creation of the field of computer image analysis.

Image processing can be defined as a *process of data processing in which both the initial and final (or: input and output) data sets are images or series of images*. Series of images are involved in e.g. video sequences which are sets of images recorded in a specific order. Almost every computer user has encountered, or at least heard of, image processing software. They are commonly used for processing photos taken with digital cameras – to reduce the level of noise, improve the contrast, enhance the „sharpness” or contrast, etc. Image analysis, in turn, can be defined in a very similar way – as a *process of data processing in which the input data set is an image or a set of images, and the output data set is not an image*. What is the output data set, then? It may be a number, a set of numbers, text, a logical variable, or a combination of those. A classic example of image analysis is a driver deciding to apply his brakes hard when his sense of vision recorded and analysed the image of a child running onto the road in front of his car. The differences between image processing and analysis are illustrated in Fig.3.1.

---

[*] Microscope examinations can be made with the help of a variety of devices, in which image is generated through the use of various physical phenomena; and thus we have optical microscopes, confocal microscopes, electron microscopes (scanning and transmission), atomic force microscopes, acoustic microscopes, X-ray microscopes, etc.

Fig. 3.1. *Image processing and analysis. Processing the image of pansies (top) we can obtain, as an example, an image of the contours of individual petals (bottom left), but only image analysis can provide the answer as to what the photograph actually shows (bottom right).*

The preceding paragraph included the example of image analysis performed by a human being. The example has its purpose, as image analysis is one of the fundamental sources of human knowledge. Reading is a very good example – it is but image analysis of printed text! This is a good moment to consider how complex a task image analysis really is. Reading texts can be reduced (if we restrict our considerations to the Latin or the Cyrillic alphabets) to the analysis of just a few dozen characters, yet it takes several years for a young human being to master that art. The above suggests a number of conclusions of great importance for the understanding of both the possibilities and the limitations of computer image analysis, understanding that will help to avoid in the future

many disappointments and that may assist in the selection of image analysis as an adequate tool of research:

- The history of computer image analysis goes back only a few dozen years and one cannot wonder why the analysis often loses against our sense of vision. By the way, we still do not fully know how the sense of vision works, and therefore encounter frequent problems when trying to imitate its operation effectively.

- Contrary to what one could think, effective utilization of the methods of image analysis requires not so much refined image processing as enormous knowledge that will permit the interpretation of information contained in the image analysed. To understand this it is enough to try to analyse a text written in an unknown - to us - language. We may recognize the letters, but the content will remain a mystery.

- Computer image analysis proves its worth the best in situations where we have to make multiple calculations or measurements, or to compare an image with a predefined model. These are tasks typical for research, diagnostics, or quality control. Usually the problems analysed are not very complex (at least superficially), but require multiple tedious and repetitive operations. And that is what computers can do better than us.

To recapitulate, we can say that computer image analysis is an interesting tool with notable capabilities that can be employed frequently and profitably. But like with any other tool, using it without the necessary skills can only lead to disaster. To facilitate the assessment as to when image analysis should be employed, Table 3.1 sets forth selected features of image analysis performed by man and by a computer system.

Table 3.1. Comparison of selected features of the sense of vision and of computer image analysis.

Analysed feature of image analysis method	Traditional analysis based on the sense of vision	System of computer image analysis
Change in efficiency (fatigue) after prolonged work	Very string effect on the results of analysis	No effect on the results of analysis
Susceptibility to illusion (we see what we want to see)	High, especially with inexperienced operators	No effect on the results of analysis
Repeatability of results (ability to obtain the same results from repeated analysis)	Poor	Full with automatic analysis, high with semi-automatic analysis
Reproducibility of analysis (ability to reproduce the analysis at another location)	Usually poor, therefore series of analyses should be made by one person	Full reproducibility
Qualitative assessment of structure (what we see)	Can be very good	Usually poor and hard to perform
Quantitative assessment of structure (all measurements)	Always highly time-consuming, often burdened with large accidental errors, sometimes impossible	May be very good
Costs of analysis	Relatively low with individual images, grow rapidly with the number of images analysed	Rapidly decrease with increasing number of images analysed, very high with individual analyses
Speed of analysis	Low, especially with quantitative analysis	May be very high, even *on line*, especially with routine analyses
Importance of operator experience	Has considerable effect on the results of analysis	Has negligible effect on the results of routine studies, but great importance in solving new problems

3.2. Digital images

In spite of the common presence of digital images, certain their features remain incomprehensible for the average camera user (especially one that has had some experience with conventional photography). We will try now to explain and clarify some of such problems.

Images processed by computer are datasets that describe the brightness (in the case of grey images) or colour (in the case of colour images) of individual dots called pixels. Pixels are located at the nodes of a square grid and, with sufficient

magnification, form a distinct mosaic (Fig. 3.2d). Of course, human eye cannot distinguish suitably small pixels, thanks to which we usually have the impression of viewing a continuous image with full details (Fig. 3.2a).

Characteristic parameters of a digital image are its dimensions, resolution, and depth. The dimensions specify how many pixels make up the image and this is the fundamental information about the image size, e.g. 512x512, 780x582, 800x600, 1392x1040 or 1200x1600 pixels. The number of pixels in the image depends on the type of equipment used and on its mode of operation. In the case of scanned images or of images being subsets of other images acquired earlier, the image dimensions can be practically chosen at will. Digital cameras most often provide images in the 3:4 size system (e.g. 1600x1200, 2560x1920 or 3264x2448). The product of the size values provides information on the total number of pixels in the image. Example: 3 264 x 2 448=7 990 272. Therefore, this kind of image can be obtained from a camera with an 8 million pixel matrix. It is worth noting that camera manufacturers frequently offer very high levels of image resolution, of course at a correspondingly high price. Often, however, such images are not suitable for computer analysis due to excess of details or even noise (example: in the image in Fig. 3.2d we will not identify too many objects even though the image contains almost 200 pixels). The number of pixels in the image should be as low as possible, but sufficient to permit recording of all the details that should be included in the analysis. Excessive number of pixels will only extend the time necessary for the analysis. For example – if we double the dimensions of the image, then the duration of the analysis (if the results are to be comparable) may be extended even by the factor of 16. This results both from the increase of the number of pixels to be analysed and from the matrix size of the filters used.

Another parameter that describes digital images, and causes considerable confusion, is their resolution. Most frequently, image resolution is given in dpi (dots per inch). Images generated by digital cameras usually have the resolution of 72 dpi. This results from the fact that this is the resolution value of most monitors. Thanks to this, an image recorded with a digital camera can be displayed without the need for any scale synchronization, so that one pixel on the monitor corresponds to one pixel in the image. If we had an XGA monitor (1024x768) and an image of 3264x2448 pixels, we would only see a small fragment of the photo on the monitor (slightly under 10%). With the resolution of 72 dpi, the image mentioned would have the physical dimensions of approximately 115x86 cm. To see the whole image, we have to change its scale. This, in fact, is not a problem. For printing with an inkjet printer we need about 150 dpi. In this case the image in question would have the size of about 55x41 cm. But when preparing it for top quality offset printing, we should select

300 dpi, which corresponds to the physical size of about 28x21 cm. Of course, we can always print the image smaller than it follows from the above calculations, as change in the resolution of the image (dpi) without changing its size in pixels has no effect on the amount and quality of information it contains. Therefore, the original resolution of the image in dpi is not that important as it can always be fitted to scale. It is the size of the image in pixels that is of fundamental importance.
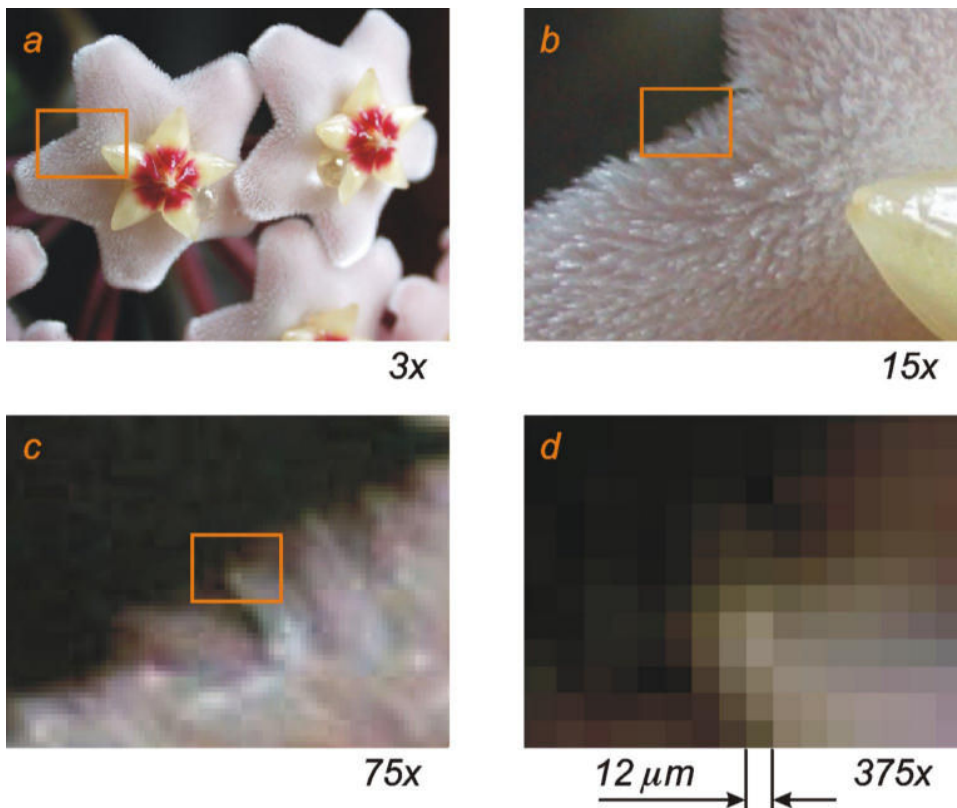

Fig. 3.2. *Digital image of wax-myrtle flowers. The first image presents the flowers magnified with relation to the original at approx. 3x (a). Successive images are at magnification ratios of 15x (b), 75x (c) and 375x (d). All the successive images (b, c, d) show the same fragment, marked with a box in the previous image.*

Persons having some experience with traditional recording of microscope images find it hard to accept that digital images have no magnification. By selecting a fragment of an image we can obtain any degree of magnification (see Fig. 3.2). In practice, the important thing is what linear value the size

of a single pixel corresponds to. This is another, much more significant for image analysis, measure of image resolution. In the case of the image in Fig. 3.2, the linear value of a pixel is 12 μm. As the resolution of the human eye is approximately 0.1 mm, the image in question will be perceived as good quality image up to a magnification ratio of about 10x. With greater magnification ratios (Fig. 3.2c, 3.2d) we will see individual pixels. This type of magnification is called empty magnification. Obviously, increasing the number of pixels of the recorded image cannot be used as a way of increasing the resolution of optical systems. Therefore, for purposes of computer image analysis, there is no sense in recording images at too high a level of resolution. One should keep in mind that image resolution, understood as the true linear value corresponding to a single pixel, is the most important parameter from the viewpoint of subsequent geometrical measurements.

Let us now take a closer look at the question of selecting the number of pixels for recording images from an optical microscope. We begin with the resolution of the objective lens. It is defined as the smallest distance between two points that can still be identified as discrete. It seems natural that the image should be recorded with a resolution (pixel size) close to that of the microscope. If we use significantly larger pixels (low resolution), some of the information discerned by the microscope will be lost. Small pixels, in turn, will create an image with empty magnification as mentioned above (a similar effect to that of images scanned at high interpolated resolution). Such a photograph will needlessly occupy a lot of memory space and will not contain more details than a photo taken at optimum resolution.

The resolution of an optical (light) objective lens can be expressed as:

$$d = \frac{0{,}61\lambda}{NA}$$

where λ is the wave length of light used for the observation (usually about 0.55μm), and NA – the numerical aperture of the objective. Knowing the resolution of the objective lens, we can determine the optimum resolution of the camera.

Considering the fact the field of view (FOV) of contemporary microscopes has usually the size of 22 mm, we can easily determine the number of pixels corresponding to the FOV diameter (Table 3.2). Likewise, we can calculate the necessary resolution of a typical camera with a CCD element of ½" diagonal (assuming the camera does not have any additional optical systems, that would affect the magnification ratio, installed between the camera and its lens).

78

If we consider a recording element of low resolution, 640X480 pixels, we get approximately 16μm per pixel. Comparing this value with the data in Table 3.2 (column 4), we can see that it will suffice for an objective lens with the magnification of 50X or higher.

Table 3.2. Resolution of objective lens and theoretical size of single pixel in CCD elements (data for Nikon CF160 objective lenses; objectives of other makes may have somewhat different values).

Objective magnification	Numerical aperture	Resolution of objective lens	Theoretical size of single CCD cell (pixel)	Number of pixels on diameter of 22 mm	No. of pixels on the diagonal of a ½" CCD element
		μm	μm		
5X	0,15	2,23	11,2	1964	1134
10X	0,30	1,12	11,2	1964	1134
20X	0,45	0,75	14,9	1476	852
50X	0,80	0,42	21,0	1068	605
100X	0,90	0,37	37,2	1048	341
150X	1,25	0,27	40,3	546	315
100X oil	1,40	0,24	24,0	917	529

CCD elements are composed of cells forming a square grid of pixels, as shown in Fig. 3.3. As can be seen in the Figure, the number of pixels along the diagonal (marked in grey) equals the number of pixels along the longer side of the image rectangle. Therefore, the number of pixels along the diagonal defines the required resolution of the CCD element. The optimum number of pixels at low magnification ratios is significantly greater (see Table 3.2), but we should remember about two factors:

- Frequently objective lenses with low magnification have lower aperture numbers than those given in Table 3.2. As a consequence, the required number of pixels will be lower.
- Observations under a microscope are usually conducted with the diaphragm partially closed to improve the depth of focus, which reduces the resolution.
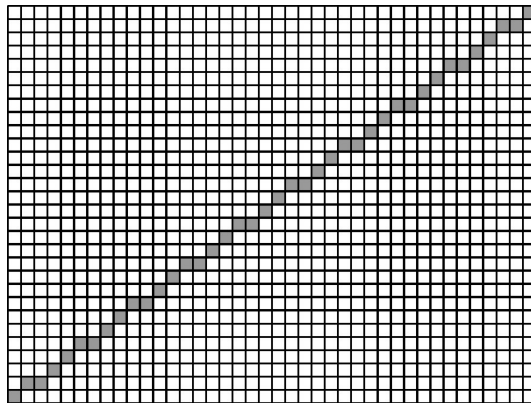
Fig. 3.3. *Fragment of the square pixel grid with the pixels on the diagonal filled with grey. Description in the text.*

To recapitulate, if a regular CCD camera is used without any additional optical systems, then the resolution of 640X480 or better, 800X600 pixels, seems to be acceptable. We should remember, however, that a CCD element of ½" in size is a rectangle with the dimensions of 10.16x7.62 mm, which gives only 20% of microscope field of view with FOV diameter equal to 22 mm (see Fig. 3.4).

It is possible to install an additional optical element between the camera and the microscope (usually with magnification of 0.4-0.7x), which permits the coverage of a rectangular area inscribed in the FOV and recording of about 70% of the field of view of the eyepiece (Fig. 3.4). If we use a camera with the resolution of 1600x1200 pixels, it will be sufficient to record all the information acquired by the objective of the microscope. Using a lower resolution will involve the loss of a certain part of the information. If the observations are rated as highly important, or if there is a need to reproduce the image in a large format (A4 or larger), it is possible to apply a higher level of camera resolution – 1.5 of that mentioned here. Further increase of image resolution will not provide any noticeable improvement in its quality, but will involve a needless growth of the memory space required for recording the image.

full field of view of the microscope,
as seen in the eyepiece

camera field of view
with additional optical systems used;
recommended CCD element
with a matrix of minimum 1024x768 pixels

half-inch camera field of view
with no additional optical systems used;
sufficient CDD element
with a matrix of 640x480 pixels
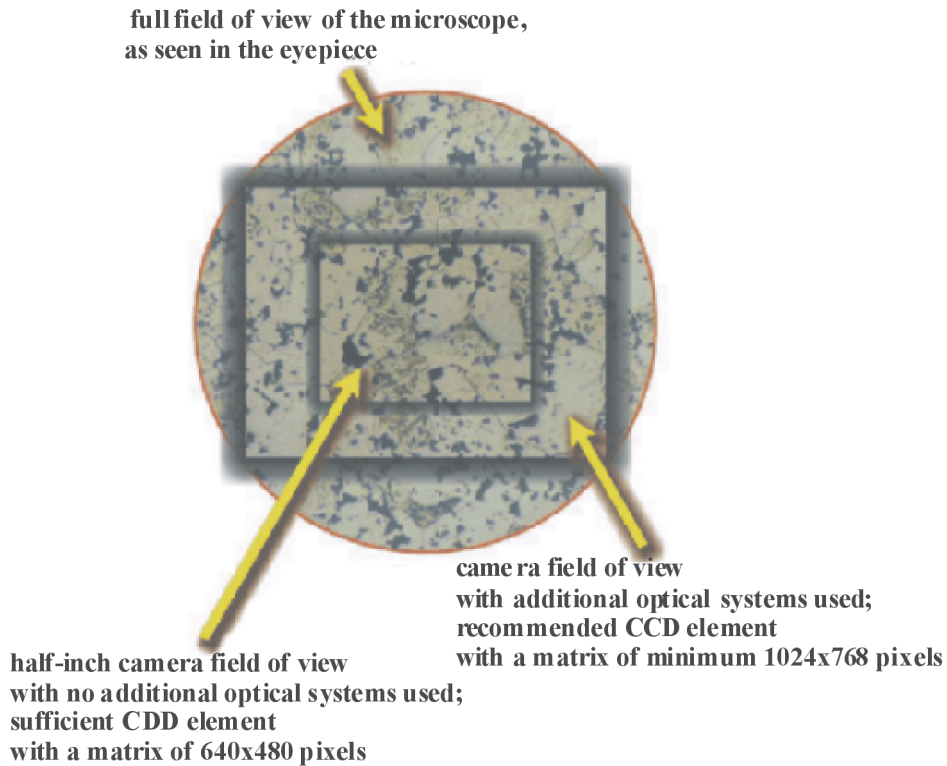
Fig. 3.4. *Comparison of a circular area visible through the microscope eyepiece and rectangular images captured with a digital camera.*

To recapitulate, when preparing images for automatic quantitative analysis we should remember that both too high and too low resolution may cause a deterioration of the results of our analysis (see Fig. 3.5).

Fig. 5a presents an example of image „over-sampling", i.e. a situation when its resolution is too high. All the details discernible in the image in Fig. 3.5a are also visible in Fig. 3.5b which represents the optimum resolution. If we analyse the microstructure from Fig. 3.6a, it is easy to arrive at erroneous results as digital filters often take into consideration the original proximity of pixels. Certain features in the image samples may be too large (or too thick as in the case of the cell structure boundaries) for correct detection. An "under-sampled" image (Fig. 3.5c) seems to lack contrast, but most of the detail features are still detectable. This example shows that usually we have a certain margin of resolution that permits correct detection. Further reduction of the resolution of images makes them unsuitable for automatic analysis (see Fig. 3.5d).
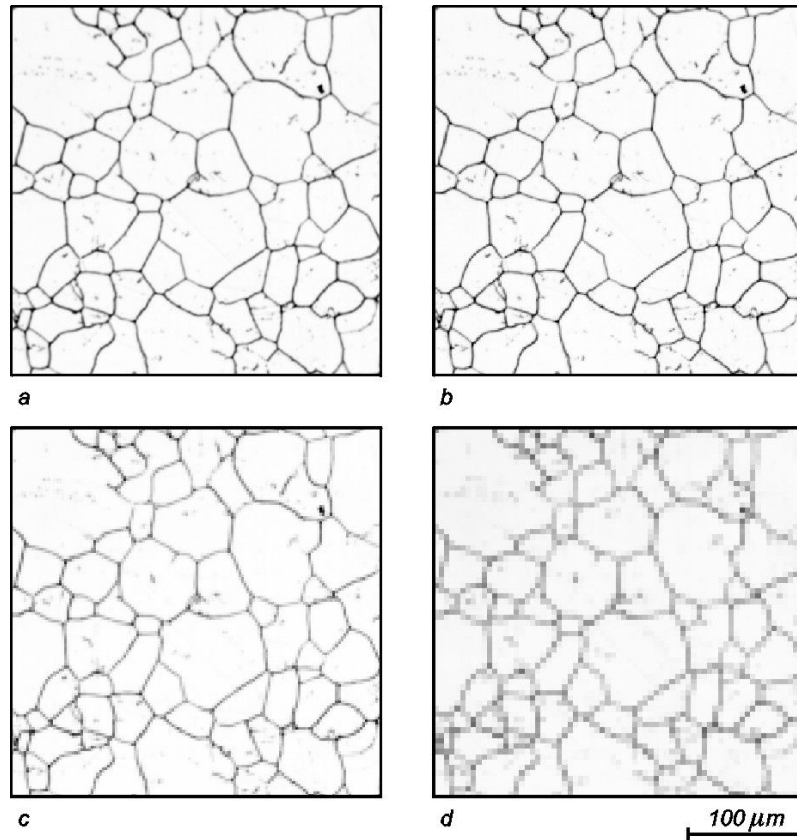
Fig. 3.5. *The same image recorded with decreasing resolutions. The pixel sizes of the image are, successively: a) 560x560, b) 280x280, c) 140x140, d) 70x70.*

If we analyse a system of isolated objects, we should apply somewhat different rules of image resolution selection. The upper limit remains the same as in the former case, i.e. excessive level of image resolution may lead to the detection of artefacts. The lowest acceptable resolution, on the other hand, depends on the size and shape of elements analysed. Firstly, the resolution should be sufficient for the detection of all required objects and their accurate counting. Secondly, if we need to analyse geometrical properties (dimensions, perimeter, surface area and form), then is appears to be the absolute minimum to analyse objects with surface area greater than 10 pixels (or, better still, 16 pixels, which corresponds to the square of 4x4 pixels). Consideration of smaller objects leads to serious errors in the appraisal of their geometry.
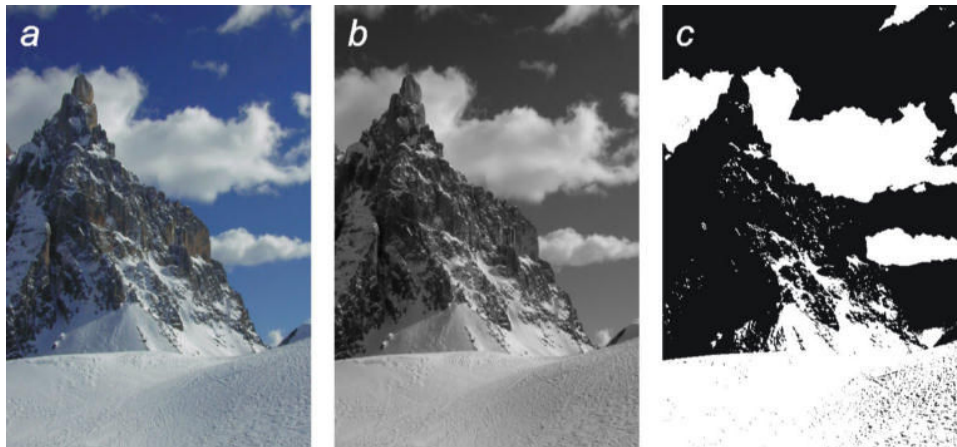
Fig. 3.6. *Changing depth of digital image: a) colour image (RGB) with 24 bits per pixel, b) grey image (monochromatic) with 8 bits per pixel, and c) binary image.*

Image-type information may have various forms and its recording will require different numbers of bits for individual pixels (this is what we call the depth of digital image) In practice, the user of an image analysis system will most frequently encounter three kinds of images – colour, grey (monochromatic), and binary. Examples of the three varieties of images are presented in Fig. 3.6, while more detailed information is provided in Table 3.3. We should remember that colour images can be obtained with the help of digital photography, cameras coupled with optical microscopes, and scanners. All images generated by electron microscopes, USG apparatus, or X-ray techniques, are monochromatic images. Colour can only be introduced artificially by the equipment, to highlight certain elements of the images.

It is worth noting that the number of bits used for encoding information on colours or shades of grey is actually greater than necessary to satisfy the requirements of the sense of vision. This is clearly seen in Fig. 3.7. The colours in Fig. 3.7a have been recorded using 24 bits, while the image in Fig. 3.7b required only 15 bits (32 shades for every RGB channel), which gives 32.768 colours. In practice, when comparing these two images we see no difference. At first sight there is no lack of colour also in Fig. 3.7c, although it contains only 216 colours, which can be coded with 8 bits (the number usually used for grey image encoding). Noticeable shortcomings are visible in Fig. 3.7d, but in this case the image has been created with just 27 colours that can be encoded using only 5 bits per pixel.

Table 3.3. Most common kinds of images used in computer image analysis.

Item	Type of image	Number of bits per pixel	Remarks
1.	Colour, RGB (example in Fig. 4a)	24	Most often used for recording colour images in digital still and video cameras and in scanners. RGB stands for the three component colours (Red, Green, Blue)
2.	Colour, CMYK	32	Used for colour image recording for printing where 4 colours of printer's ink are used to print colour pictures (Cyan, Magenta, Yellow, blacK). Images of this type are not used in computer image analysis. If necessary, such images are converted to the RGB components
3.	Grey (example in Fig. 4b)	8 (occasionally other numbers of bits per pixel are used, e.g. 4, 10 or 12)	Most often used for recording monochromatic images; frequently used in image analysis as interim images. An RGB colour image can be resolved into three grey component images.
4.	Binary (example in Fig. 4c)	1	Made up of only two kinds of dots, corresponding to black and white and marked as 0 and 1; used for recording line drawings and scanned texts and as auxiliary images in image analysis. Necessary for measurements taken on images.
5.	Labelled	most often 16	Specific images which are modifications of binary images. All pixels in successive cohesive areas of binary image (with values equivalent to one) are assigned values of successive natural numbers. This facilitates analysis of particular areas which are treated as separate objects.
6.	Float (Variable decimal point)	16 or 32	Used for saving the results of certain operations, e.g. division, finding the logarithm, etc. Often constitute components of composite images, e.g. being the result of Fourier transform
7.	Composite	depending on software and purpose	Used for recording image-type information that requires saving several separate images. Creation of a composite image prevents the loss of part of the information. Typical applications include recording the results of Fourier transform, edge detection, converted colour images, etc.

Fig. 3.7. *Change in the appearance of an image caused by change in the number of colours used for its recording: a) 16,777,216 colours (24 bits, 256 shades of grey for each RGB component), b) 32,768 colours (15 bits, 32 shades of grey for each RGB component), c) 216 colours (6 shades of grey for each RGB component), d) 27 colours (only 3 shades of grey for each RGB component).*

Analysis of Fig. 3.7 illustrates a serious problem, consisting in the fact that visual assessment of an image can be highly misleading. Our sense of vision does not discern certain differences in images that differ significantly from the viewpoint of their digital recording. Processing of such images may, in certain cases, lead to considerable differences in the results of analysis, in spite of using identical algorithms. Therefore, when conducting a study special care must be taken that all images under analysis be recorded in the same manner.

Another element that is important in the estimation of digital images is the format in which they are saved in computer memory. To permit exchange of information between different computers and software packages, several graphical formats have been developed, of which we will concentrate on four:

- **TIFF** (*.TIF files), i.e. Tagged Image File Format. This is probably the most common format used for raster graphics. The label of the file can be used to write comments concerning the magnification, the manner of image acquisition, etc, which facilitates subsequent analysis. The TIFF format has built-in mechanisms for data compression, which permits minimization of file size.

- **BMP**, i.e. bitmap. This format is often used in Windows. It is characterized by considerable simplicity, thanks to which it can be read by a great majority of software. A notable shortcoming of the format is the lack of data compression capabilities, which means that graphical files are big.

- **JPEG** (*.JPG files), i.e. Joint Photographic Experts Group. This format owes its popularity mainly to the Internet, where strong data compression is a necessity for speed of data transmission. Unfortunately, high rates of compression involve also deterioration in quality (Fig. 3.8). When recording in JPG format, we can select values of two parameters – rate of compression and degree of smoothing. If we want files saved in that format to be suitable for image analysis, we must select as low degrees of smoothing as possible. Data compression will then be weaker, but the quality of the image will be much higher. Low values of smoothing ratio in the JPG format permit the reduction of file size by a factor of more than 10 as compared to the TIFF format, while retaining high quality of images (differences between the two images exceed the level of about 5% only in the case of very few points).

- **GIF**, i.e. Graphics Interchange Format. Like in the case of JPG, this format gained popularity thanks to the Internet. It is characterized by a very high ratio of data compression with no loss of image quality. It is an excellent tool for recording line drawings, possibly also for images with low number of colours. It cannot be used for photographs, especially colour photos.
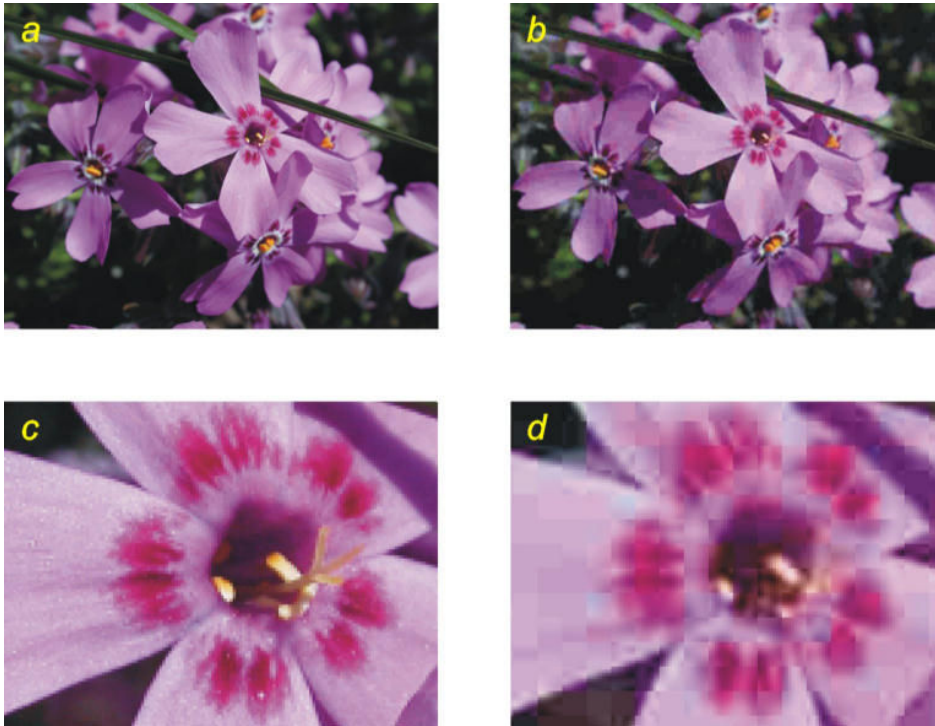
Fig. 3.8*. Comparison of an image in TIFF (a) and JPEG with medium degrees of compression and smoothing (b). Both images appear to be identical. However, observation of enlarged fragments reveals significant differences: the TIFF format retained small details that may be important in subsequent analysis (c), while JPEG generalized the image, creating large areas of uniform colour (e.g. the petal on the left side of image in Fig. d).*

3.3. Computer aided measurements

A very important element of computer image analysis is measurements of various kinds. One could even risk the thesis that in scientific research measurements are the fundamental objective of the research. Luckily, no deep knowledge of the construction of algorithms used for measurement purposes is necessary for solving practical problems. Therefore, we will concentrate only on the basic properties of digital measurement.

Probably the most fundamental and at the same apparently simple task is the counting of various objects. Making a count requires prior determination of the rules of connectivity. Two fundamental cases are distinguished in this respect:

- Each pixel has 4 closest neighbours, like the black pixel in Fig. 3.9a.
- Each pixel has 8 closest neighbours, like the black pixel in Fig. 3.9b.
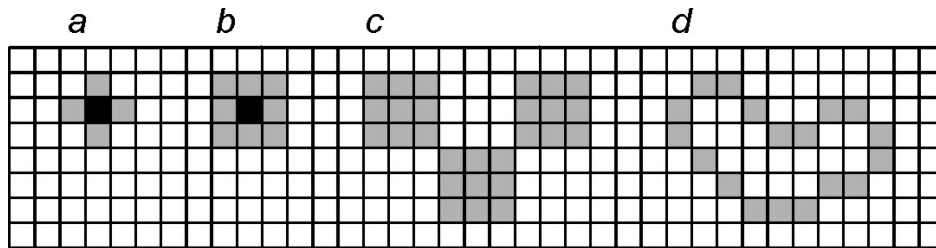
Fig. 3.9*. Effect of the choice of rule of connectivity on the result of a count of objects.*
Description in the text.

A single object in an image is recognized as a coherent group of connected pixels. In other words, every object is composed of all pixels arranged in such a way that we can freely move from any one pixel of the object to another without having to move onto the background pixels. The number of objects defined in this way will depend on the adopted rule of connectivity. If we want to count relatively large particles, the preferred choice will the rule of 4 closest neighbours. In this case the objects shown in Fig. 3.9c will be classified as 3 separate squares. In the case of the rule of 8 closest neighbours, all 3 areas will be treated as one object. In the case of thin curvilinear objects (Fig. 3.9d) it is better to adopt the rule of 8 closest neighbours. In such a case the object will be recognized as a closed circuit or loop. If we use the rule of 4 closest neighbours, the curve in Fig. 9d will be treated as 10 separate objects.

A separate problem is involved in the adaptation of the traditional methods of quantitative description (stereology) for purposes of computer image analysis. The first example is the point method of estimation of volume fraction:

$$V_V = P_P$$

where V_V is the estimated volume fraction, and P_P is the ratio of the number of points that hit the objects analysed to the total number of points included in the analysis. Sometimes persons without sufficient experience with image analysis try to implement this stereological equation by superimposing a grid of points onto the image analysed. Of course that is not necessary and we should simply count (in a binary image) all the pixels that represent the phase analysed and use the number of all the pixels of the image as the reference value:

$$V_V = N_P/N_O$$

where: N_P is the number of pixels that belong to the objects analysed, and N_O is the number of all the pixels of the image.

88
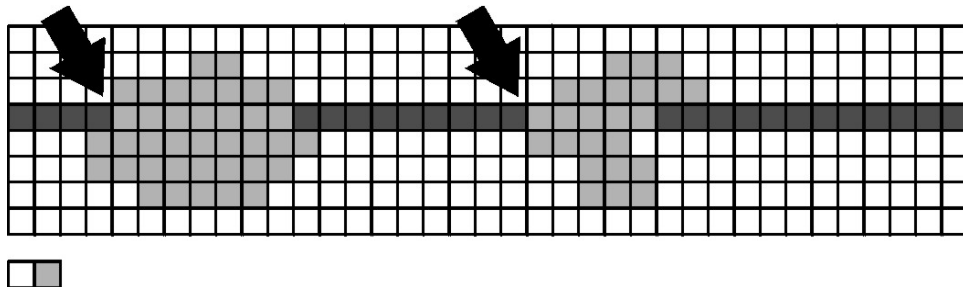
Fig. 3.10. Determination of the number of intersection points in image analysis. Description in the text.

Some problems can also be involved in the implementation of digital determination of the number of points of intersection of object edges with the secant, typical for the linear methods commonly used in stereology. Sometimes we draw (manually or automatically) a set of straight sections and search for points of intersection indicated with arrows in Fig. 3.14. Such a simulation of measurements taken manually is but unnecessary complication of the analysis.

We note that all the potential points of intersection have the following arrangement (see: the small, 2-pixel object in Fig. 3.10): 2 pixels along a horizontal line, one with the value corresponding to the matrix (usually 0), and the second with the value corresponding to the objects analysed (usually 1). This is sufficient for counting all such pairs of pixels existing in the image and hence we obtain the number of points of intersection though the test area.

Contrary to traditional stereology, the digital methods of analysis permit very rapid estimation of various geometrical features of individual objects. The basic parameters, most frequently used, are presented in Table 3.4 which also gives the basic properties of each of the values. They can be used as a basis for defining numerous complex parameters, e.g. form factors. The parameters presented in Table 3.4 are commonly known, but we must remember that they have been defined in Euclidean space, while image analysis is made on a simplified two-dimensional grid. This may be the source of numerous deviations from the expected values.

To determine the error of digital measurement, we must define a suitable test object. Most frequently it would be a circle, as its geometry is well known and its symmetrical form is well suited for error estimation in digital measurement. As shown in Table 3.4, surface area is calculated almost perfectly for all diameters, while the perimeter is estimated with a notable error beginning with the diameter of about 50 pixels. Perimeter measurement error is approximately

constant for diameters in the range of 10-25 pixels. Although the results shown in Table 3.5 have been obtained with the help of *Aphelion* v.3.2, similar results would be obtained by means of other image analysis software packages. These considerations suggest the conclusion that we should try to avoid the quantification of individual objects with surface area smaller than about 10 pixels. Moreover, the estimation of the perimeter of objects with curve radius smaller than 5 pixels may lead to serious errors exceeding 10% of the measured value.

Table 3.4. Basic geometrical parameters available in quantitative image analysis.

Parameter	Schematic	Properties
Surface area		In the case of non-calibrated images it equals the number of pixels making up the image. Surface area is one of the simplest and the most accurate parameters that can be determined in image analysis.
Perimeter		Should be used with special care as it often gives results burdened with considerable error. A good way of checking the accuracy of perimeter measurement is to use a strictly defined object for the test. Usually the best results are obtained when using the Crofton formula.
Feret's diameter (horizontal and vertical)		A very popular method for the estimation of the size of various objects, especially useful for the estimation of elongated objects oriented in parallel to horizontal or vertical directions in the image.
Feret's diameter (freely oriented)		Not available in all the software packages. As a result of measurement we obtain two parameters – length and angle. Usually the measurement is less accurate than in the case of the horizontal and vertical Feret's diameter.
Maximum chord		This is simply the longest of the Feret's diameters defined above. The measurement can be interpreted also as the longest projection of the object. The angle value is useful for orientation analysis, especially in the case of objects that are close to linear.
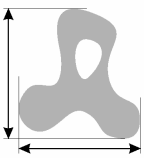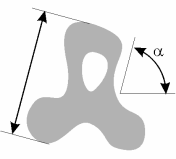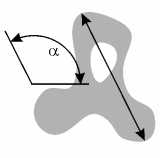
Maximum width		This measurement can be interpreted as the maximum diameter of a circle inscribed in the object analysed. Its value is approximately twice the maximum of the distance function (cumulated set of erosions of figure).
Centre of gravity		In this case we obtain a pair of values describing the position of the centre of gravity. The measurement is used in the analysis of the position of an object in space.
First point (point of origin)		These are the coordinates of a point located furthest to the left from among all the pixels belonging in the upper row of the pixels of the object. The position of the first point may be used for the separation of objects.
Convex surrounding area		Basically this is not a measurement but the creation of a new object based on the original object. It can be used for quantitative characterization of form. Often, due to the digital character of the image, it is only a rough approximation of the convex surrounding area.
Smallest circumscribed rectangle		A self-explanatory parameter with a character similar to that of the convex surrounding area. Its orientation can be useful for estimation of directionality of objects in the image. It can be used as the starting point for certain form factors.
Number of holes		An important parameter for the description of the topology of an object. Rarely used in practice.
Parameters of scale of shades of grey		These are parameters giving the minimum, maximum and average level of shade of grey or colour in the initial image, and its standard deviation. Can be useful for classification of objects, e.g. on the basis of their homogeneity.
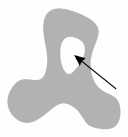
Table 3.5. Comparison of surface areas and perimeter values of circles of various diameters, obtained as a result of image analysis by means of the *Aphelion* software package.

Diameter [in pixels]	100	75	50	25	16	10	7
Relative error of perimeter measurement [%]	<1	-1	-6	-10	-10	-10	-14
Relative error of surface area measurement [%]	<1	<1	<1	<1	<1	+1	-4
Remarks: 1. Measurements with error estimated at less than 1% are considered to be error-free Values understimated and overestimated are described as „–„ and „+" , respectively							

3.4. Advanced analysis of features detected in digital images

Let us now concentrate on one of the most obvious tasks in image analysis, i.e. counting objects (these can be cells, nuclei, seeds, etc.). At the first sight it seems to be a very straightforward operation. However, even some of the commonly recognized standard contain errors related to object count. Counting objects visible in an image and division of the number by the surface area of the image gives the known stereological parameter of N_A which permits the estimation of the average surface area of an object:

$$\bar{a} = \frac{V_V}{N_A}$$

where $\bar{a}$ is the mean surface area of an object, V_V describes the volume fraction of the objects analysed, and N_A describes their density, i.e. the number of objects per unit surface area of the section.

Digital counting of objects (possible only in relation of binary images) is a very simple and rapid process that requires only the definition of the rule of connectivity (compare with Fig. 3.9). In practice, however, there appears a significant problem, as some of the objects are intersected by the border of the image (Fig. 3.11a). Particles or grains intersected by the border of the photo have no effect on the estimation of the volume fraction or of the number of points of intersection in the linear method.

92
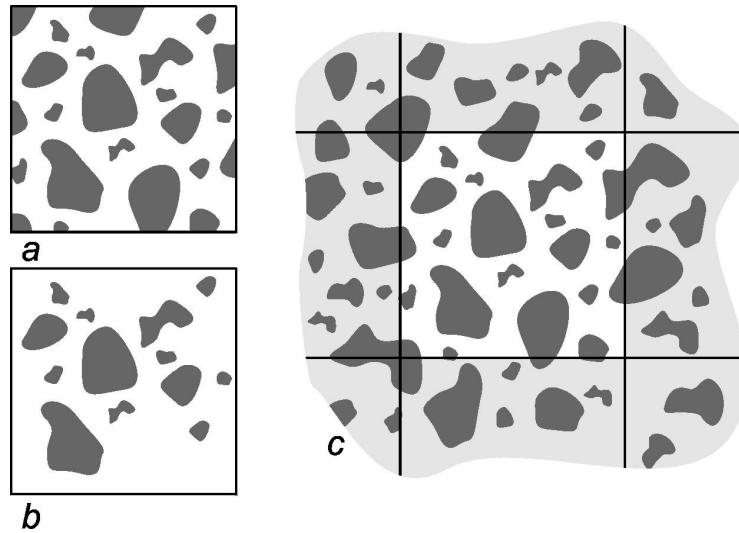
Fig. 3.11. *Counting particles visible in an image. Objects intersected by the image border must be counted with a suitable factor: a) image with objects intersected by image border, b) the same image after the application of elimination of objects intersected by image border (border kill), and c) analysed image treated as an element of a series of images. Description in the text.*

If we take into account both the objects within the image and those intersected by the image border, the number of object will be overestimated as the particles on the border belong also to another image, adjacent to that currently under analysis. Objects intersected by image border can be easily eliminated (the procedure is sometimes referred to as *border kill*), but this, in turn, leads to underestimation of the number of objects (Fig. 3.11b). The proper course of action can be explained on the example of Fig. 3.11c. The figure shows a series of adjacent images. The background of the images has been marked with grey, with the exception of the image currently analysed, whose background is white. We can observe that every particle located on the borderline belongs in fact to two images, while every particle located on the grid node belongs to four images. This leads to a universal formula that permits the count of particles in an image, known as the Jeffries formula:

$$N = N_i + \frac{1}{2} N_b + \frac{1}{4} N_c$$

where: N is the estimated number of particles (objects), N_i – the number of particles completely included in the image, N_b – the number of particles intersected by image border, N_c – the number of particles intersected by the image corners.

The method described permits unbiased estimation of the numbers of objects per unit surface area, N_A:

$$N_A = \frac{N}{A}$$

where: A is the surface area of the image under analysis.

Another problems appears when the objective of the analysis is particle size distribution. In such a case, for obvious reasons, we can take into account only those particles which are wholly contained in the image. A natural solution seems to be analysing the particles in the image after the application of the *border kill* procedure, as shown in Fig. 3.11b. Unfortunately, this leads to distortion of the distribution, as we will explain below.
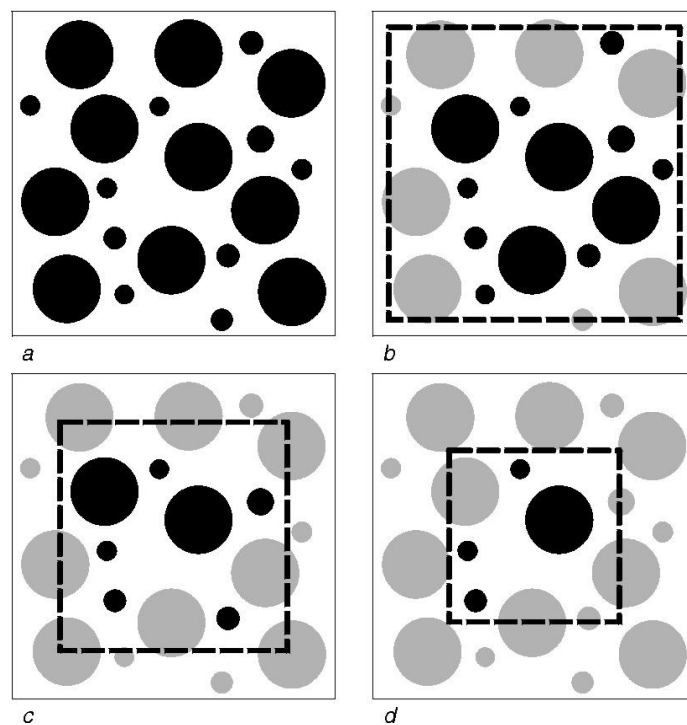
Fig. 3.12. The effect of elimination of particles intersected by image border or located outside the analysed area on the particle size distribution.

Let us analyse the distribution of circles simulating particles, shown in Fig. 3.12. Fig. 3.12a shows the same numbers of large and small circles. Figures 3.12b, c and d show gradually decreasing images, the borders of which are marked with broken lines. After the elimination of particles intersected by the borders (marked with grey), we are left with particles wholly contained within the images, marked with black. It is easily seen that the proportion between the large and small particles changes. As we select smaller and smaller images, the ratio of the number of large circles to that of small ones decreases. This is related to the fact that the probability of eliminating a particle is proportional to its size in a direction perpendicular to the border of the image. Therefore, the fraction of small objects is overestimated.
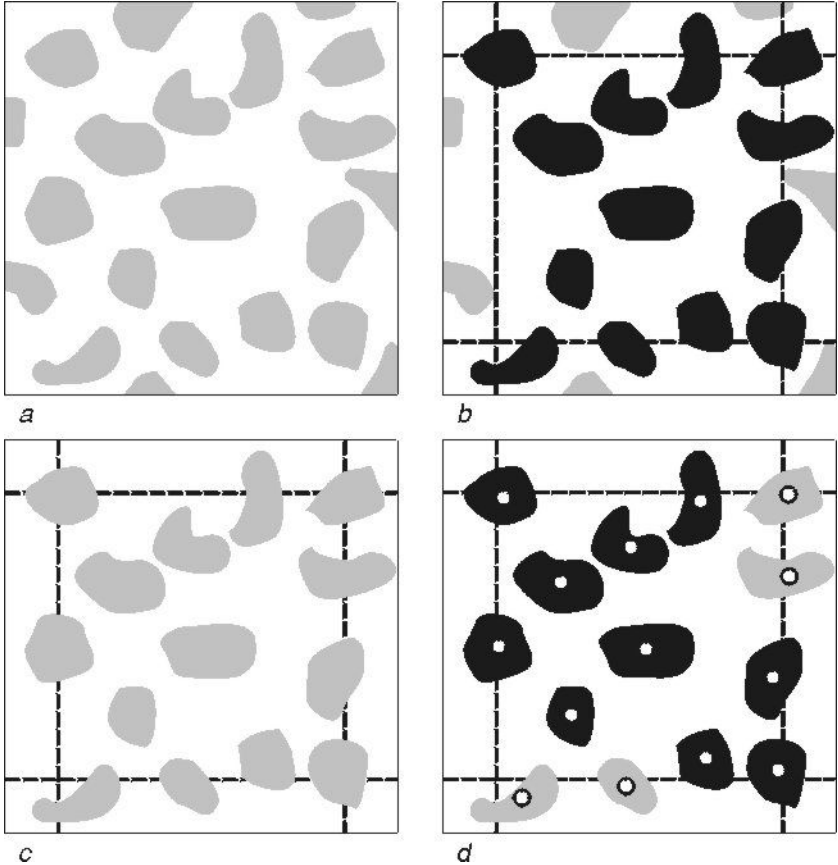
Fig. 3.13. *Schematic of correct selection of particles for size distribution with the help of the guard frame. Description in the text.*

Correction of the effects described is relatively easy with the use of the guard frame. We analyse an image containing objects intersected by the border (Fig. 3.13a). The guard frame is marked with broken line in Fig. 3.13b. The fundamental principle is that all the objects intersected by the border of the image should be outside the guard frame (in practice the principle can be slightly less stringent, but the solution described here is both safe and easy to effect by the automatic image analysis system). Next, we take into consideration all the objects wholly contained within the image (Fig. 3.13c). Each of the objects is assigned one and only one characteristic point, in this case the centre of gravity (the point can be chosen in any way, provided it is clearly defined). Only those objects are taken for further analysis (marked with black in Fig. 3.13d) whose characteristic point lies within the guard frame. Remaining objects (grey in Fig. 3.13d) are discarded. It is worth noting that if successive guard frames are adjacent to each other, every object will be analysed and none of them will be counted twice. In this way the application of the guard frame ensures estimation of object size distribution that is free of a systematic error.
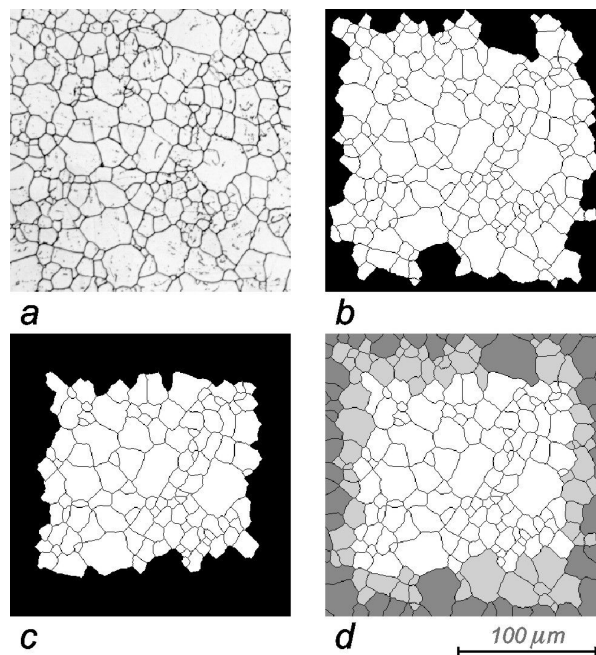

Fig. 3.14. *An example of cellular structure and its analysis: a) initial image, b) binary image after the elimination of objects intersected by image border (border kill), c) binary image after correction based on the use of the guard frame, d) comparison of various cell sets: dark grey – cells eliminated after the border kill operation, light grey – cells additionally eliminated after the application of the guard frame, white – the same set as in image (c).*

An example of the application of correction involving the use of the guard frame is presented in Fig. 3.14. As can be seen from the example, corrections based on the *border kill* procedure (Fig. 3.14b) and the guard frame procedure (Fig. 3.14c) give different sets of the objects under study. The procedures in question lead to different estimations of the object size distribution, as illustrated in Fig. 3.15. One can observe that the application of the *border kill* procedure leads, in accordance with the earlier remarks (Fig. 3.12), to an overestimation of the fraction of the smallest cells. This overestimation is a systematic error that can be encountered even in certain standardized procedures.
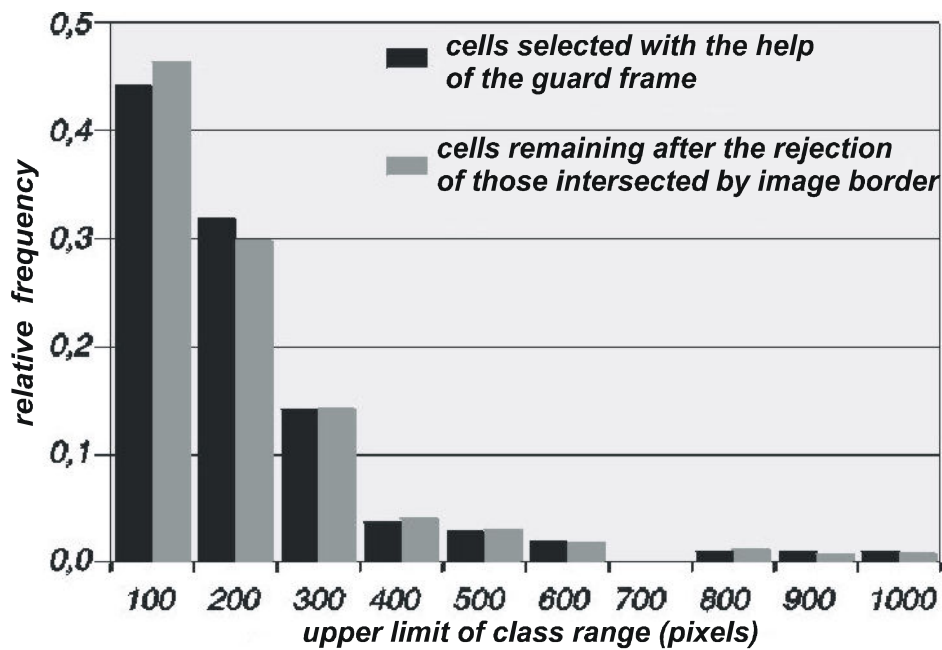
Fig. 3.15. *Comparison of the cell size distributions for the structure from Fig. 14, with the use of the guard frame and after the elimination of cells intersected by the image border. Description in the text.*

Images in which the guard frame has been used can be utilized for the determination of various stereological parameters, as shown in Table 3.6. It is worth noting that the fact of some objects protruding outside the border does not entail the introduction of systematic error into the result.

Table 3.6. Determination of selected stereological parameters in images with guard frame.

Symbol	Description	Calculation of value	Explanations
A_A	Surface fraction (also, estimator for volume fraction V_V)	$V_V = A_A = \dfrac{N_p}{N_O}$	N_P – number of pixels belonging to objects selected using the guard frame* N_0 – total number of pixels within the guard frame
L_A	Length per unit of surface area	$L_A = \dfrac{L_t}{A_0}$	L_t – total length of contour lines of all objects selected using the guard frame A_0 – total surface area of the guard frame Both the values should be calibrated**
N_A	Number of objects per unit of surface area	$N_A = \dfrac{N}{A_0}$	N – number of objects selected using the guard frame A_0 – total surface area of the guard frame (this value should be calibrated)**
* This parameter is best measured on the whole image, including objects intersected by the border.		
** Image is calibrated when we know what physical length is represented by a single pixel.		

3.5. Binarization - a step necessary for quantification

As has been mentioned before, measurements are taken on binary images, and the process of conversion of grey or colour images into binary images is called binary conversion, binarization or thresholding. The idea of the conversion is illustrated in Fig. 3.16. On the basis of preliminary analysis of a grey image (Fig. 3.16a) we select suitable threshold values. This can be done e.g. on the basis of the graph of changes in shades of grey (so-called profile), shown on the right -hand side of Fig. 3.16. In the graph three threshold values are marked, described as threshold 1, threshold 2 and threshold 3, respectively. If all the pixels with values between threshold 1 and threshold 3 are assigned the value of 1, and the remaining pixels the value of 0, we obtain an image of tablets (Fig. 3.16b). Selecting pixels with values from the range of from threshold 1 to threshold 3, we obtain an image of dark tablets (Fig. 3.16c). This image does contain certain elements of the light tablets, but this shortcoming can be easily corrected. Finally, selecting pixels from the range of from threshold 2 to threshold 3, we obtain an image of light tablets (Fig. 3.16d).
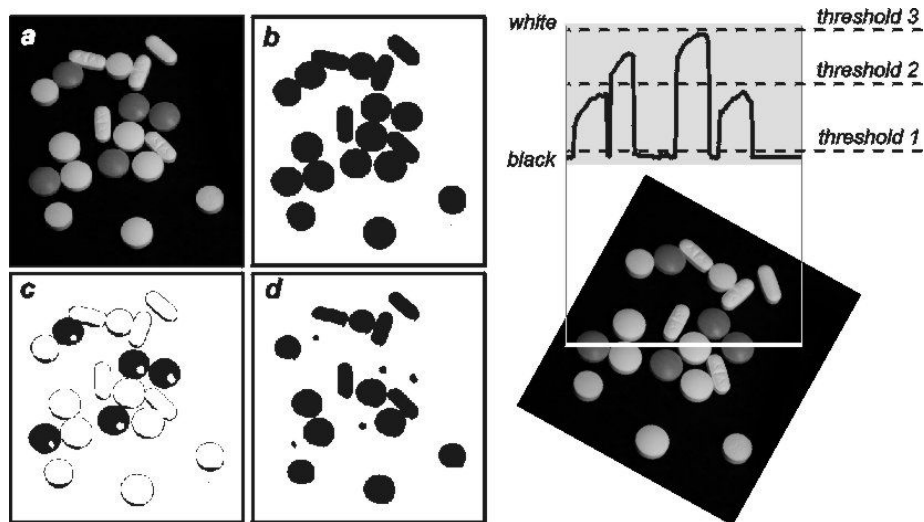
Fig. 3.16. *The process of binarization. Description in the text.*

    Image analysis software packages offer a variety of tools that facilitate work in the interactive mode. If we are to perform binary conversion of a given image (Fig. 3.17a), we simply use the mouse and slide controls to select the range of shades of grey that corresponds to the objects of our choice. The selected range can be controlled continuously, as the range selected is displayed in the image being converted, most often in red. Fig. 3.17b shows clearly that the parameters of the procedure are not selected correctly – the red area spreads outside the particles and covers most of the background area. Correct selection of parameters is presented in Fig. 3.17c, and the resultant binary image is shown in Fig. 3.17d. As can be seen in the image, many of the particles have holes – these can be filled (Fig. 3.17e), and particles intersected by the border can be eliminated (as we remember from earlier in the text, that latter operation may affect the result of subsequent measurements). The final result of detection is superimposed in the initial image in the form of yellow particle contours (Fig. 3.17f) to show how good is the effect of our work. In this example, all the operations with the exception of interactive selection of the threshold of detection can be performed fully automatically.
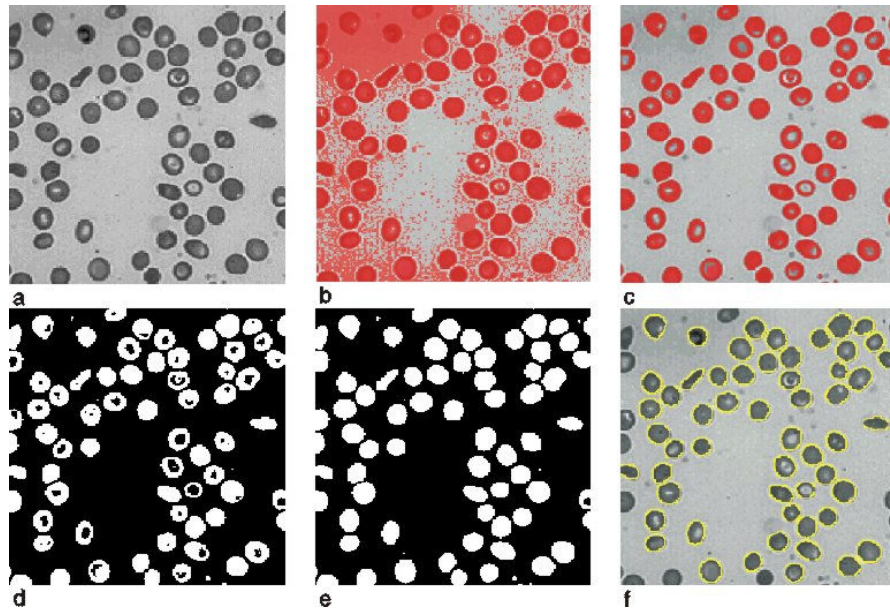
Fig. 3.17. *Interactive binarization: a) initial image, b)incorrect threshold of detection, c) correct threshold of detection, d) binary image, e) filling of holes, and d) final effect of detection superimposed on the initial image.*
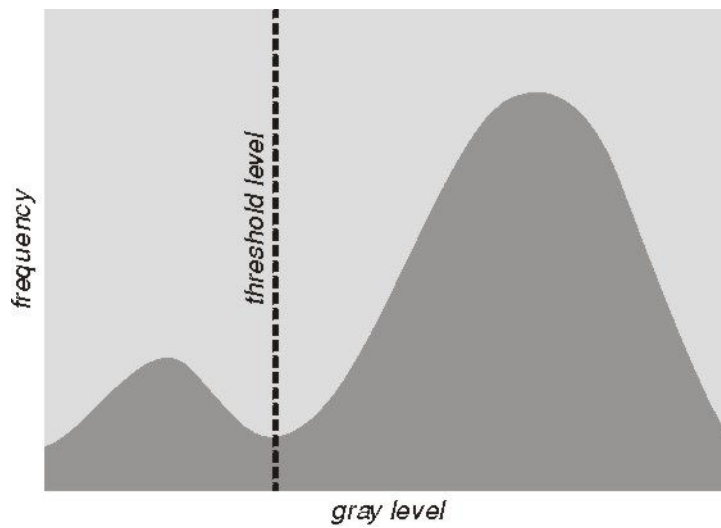

Fig. 3.18. *The idea of automatic binary conversion.*

Image analysis software packages frequently include procedures for automatic binary conversion. These cannot be used always, but in certain situations, e.g. having very dark objects on a very light background, they may prove highly useful and ensure rapid image analysis free of the subjective influence of the operator. Images of the type mentioned, containing dark objects against very light backgrounds, usually have distribution of shades of grey (histogram) with a character close to that shown in Fig.3.18. The threshold of detection can be then selected at the point of the local minimum of the histogram. Since this chapter, as has been mentioned before, is but an introduction to image analysis, the procedures of automatic binary conversion will not be discussed in detail.

3.6. Logical operations
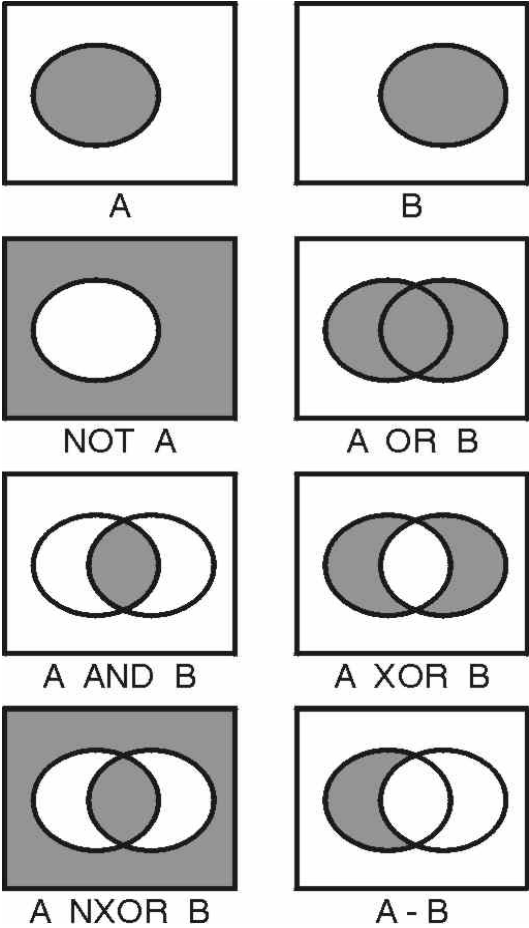
Fig. 3.19. *Logic transformations. Description in the text.*

Logic operations on images display full analogy to the known logic operations on sets. Fig. 3.19 shows a series of logic operations used in image analysis. Operations of this type are fairly often used in practice, e.g. for compilation of fragmentary results of detection. Various algorithms often lead to the detection of only a part of the necessary elements. Thanks to logic transformations we can add them together, search for common elements, or for differences. Attempts at the application of logic transformations should be limited to binary images only. Application of logic transformations in the case of grey images is burdened with very high risk of obtaining surprising results. The reason for this is the fact that the value of every dot in a grey image is converted to a binary code and the result of the transformation is generated as a result of operations performed separately for each position (digit) of the binary code.

3.7. Filters
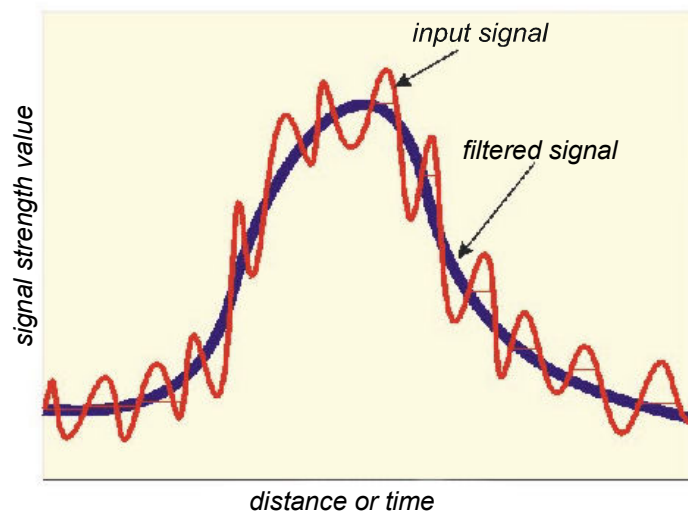
Fig. 3.20. *Schematic of the process if filtration.*

Before the process of binarization, discussed above, actually takes place, the image can be subjected to a variety of filtrations. The idea of the filtration process is presented in Fig. 3.20. Intuitively we assume that the run studied may include accidental interference, and we try to eliminate them, or at least reduce. Of course, there exists no single and universal method of filtration. Several examples of the application of various filters are presented in Fig. 3.21 (the initial

image is marked with the letter a). It should be pointed out here that particular filters may work with different levels of intensity. Generally speaking, the effect of the operation of a filter is most often simply the result of certain algebraic operations on numbers describing the colour or shade of grey of dots in the image, adjacent to the dot under analysis. The larger area is taken under consideration, the stronger the filter will modify the initial image. All the transformations illustrated in Fig. 3.21 were performed with high intensity to highlight the effects of their operation.

A task that we often have to face is the reduction of noise in an image. The simplest apparent method, by analogy to statistical analysis of results of a study, is the determination of a mean from the local environment of the point under analysis. Such a procedure will in fact smooth the image, but at the same time it will rob it of many details (Fig. 3.21b).

A much better filter for noise reduction is the median, i.e. medium value (the values of particular dots are arranged in a non-decreasing series and the value occupying the central position is selected). The median filter discards extreme values that usually constitute the noise, and moreover, as opposed to the former filter, it does not introduce new values into the image. Thanks to these features, it not only is an efficient tool for noise reduction, but also performs well in terms of preservation of the contours of the image under processing (Fig. 3.21c), without the "softening" effect like that of the filter based on the arithmetic mean.

It is also possible to create filters with reverse operation, i.e. enhancing the visual sharpness of images. An example of such filtration is presented in Fig. 3.21d. Filters enhancing sharpness are commonly used for artistic purposes and in the preparation of images for printing, but in image analysis their application is rather sporadic as they tend to generate noise which creates serious problem e.g. in subsequent binarization. For this reason they will not be discussed in greater detail here.

An interesting variety of filters are the minimum filter, also known as the erosion filter (Fig. 3.21e), and the maximum filter, also known as dilation filter (Fig. 3.21f). The result of operation of these filters is the minimum and maximum, respectively, from the local environment of the point analysed. Therefore, they cause simultaneous darkening or brightening of the image combined with detail reduction. The filters can be combined, i.e. perform suitable filtrations immediately one after another. Combination of erosion and dilation is called the opening (Fig. 3.21g), while that of dilatation and erosion – the closing of an image (Fig. 3.21h).
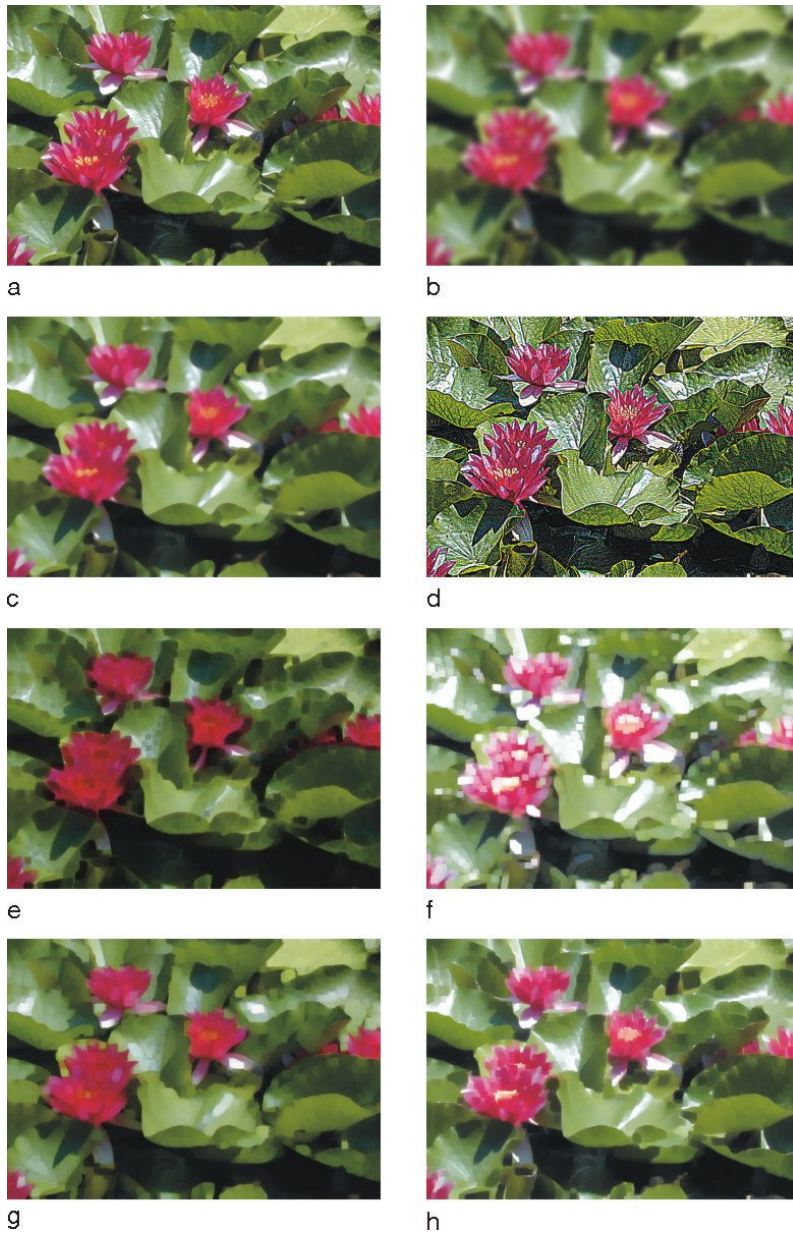
Fig. 3.21. *Examples of operation of filters: a) initial image, b) noise reduction through averaging, c) median, d) sharpness enhancement, e) erosion, f) dilatation, g) opening and h) closing.*

The effect of operation of these filters resembles, to a degree, that of the median filter (Fig. 3.21c). In essence, the closing and opening of images are sometimes used as noise reduction filters. Their primary application is the smoothing of edges of various objects visible in the image for better detection of their contours and, consequently, for better object detection. Therefore, the filters in question modify the shapes of objects analysed and for this reason are called simple morphological filters. Morphological operations will be mentioned again further on in this chapter.
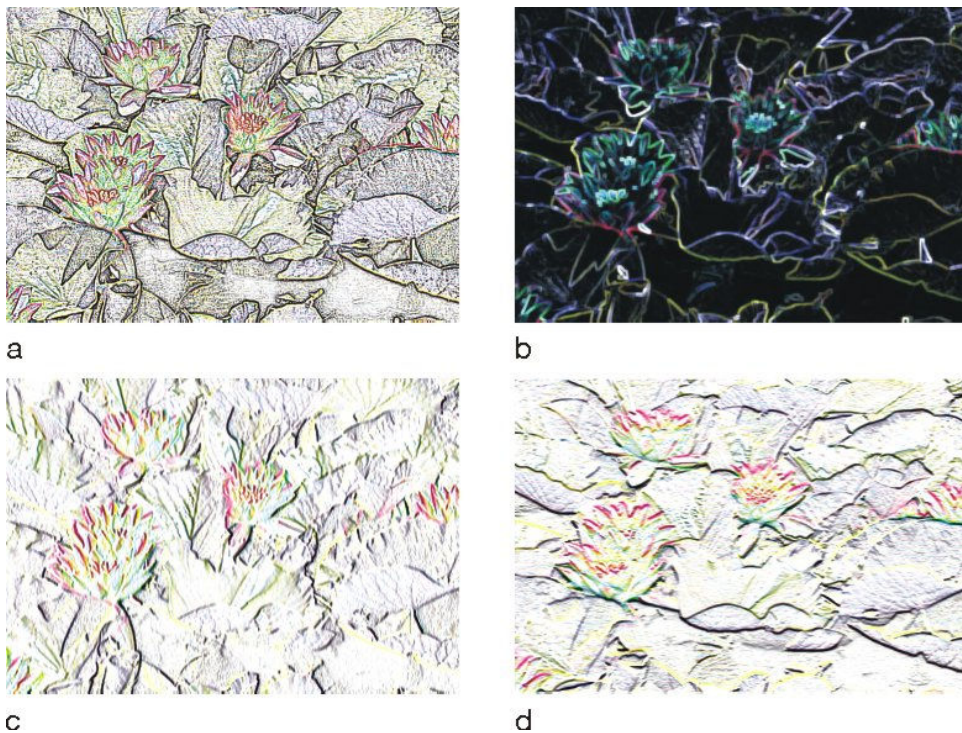
Fig. 3.22. Examples of edge detection: a) Laplacian, b) morphological filter, c) vertical edges and d) horizontal edges.

Filters are often used to enhance an interesting fragment of an image. Object edges are a classical example. Their detection is one of the most important (and at the same the most difficult) elements of the process of image processing. Dozens of filters for edge detection have been developed, and we will not go into a detailed discussion of those here. Let us only present a few examples to show how different the results of operation of such filters can be. Edges in Fig. 3.22a

have been detected with the help of the Laplacian which is very similar to filters enhancingsharpness. What is very important, the Laplacian helps to obtain continuous edge contours. A shortcoming of the filter is its great sensitivity to all traces of noise, which also can be seen in the figure. Another method of edge detection makes use of morphological operations. The image presented (Fig. 3.22b) is simply the difference between the initial image and the image subjected to erosion (discussed before) – as can be seen, applications of that relatively simple transformation can be varied. Finally, Fig. 3.22c and 3.22d present the results of operation of filters specifically designed for the detection of vertical and horizontal edge fragments, respectively. Combinations of similar filters for four different directions (0, 45, 90 and 135 degrees) constitute the basis for the operation of numerous filters for edge detection, including such well known ones as the Sobel, Roberts and Prewitt filters.

Usually, image analysis software contains a considerable number of predefined filters. It is always possible, however, to add user-defined filters designed for a specific problem of image analysis. The design of such filters can be learned through example solutions that usually form an integral part of professional image analysis systems.

Most commonly encountered are so-called linear filters, in which the value of the transformed pixel is a linear function of the values of the neighbouring pixels. Most frequently used are filters with a matrix like 3x3, 5x5 or 7x7, with the central pixel being the object of transformation. In practice, however, virtually any configuration of filters is possible.

Let us now examine several simple linear filters. Below is an example of a simple Laplacian.

-1	0	-1
0	4	0
-1	0	-1

If all the points have the same value, the response of the filter will be the value of 0 (we sum up four pixels with the weight of −1 and one with the weight of 4). It is enough for the central pixel to have a value other than its neighbours, and the response of the filter will be different from zero. A different value of the pixel analysed as compared to its neighbours suggests that it is located on the edge of an object.

And another example of a filter:

-1	0	1
-1	0	1
-1	0	1

which can be used for the detection of vertical edges. Using three points, modelling a short vertical section, prevents the detection of edges in the case of isolated pixels, and the column of zeros in the middle increases the sensitivity of detection of more differentiated pixels.
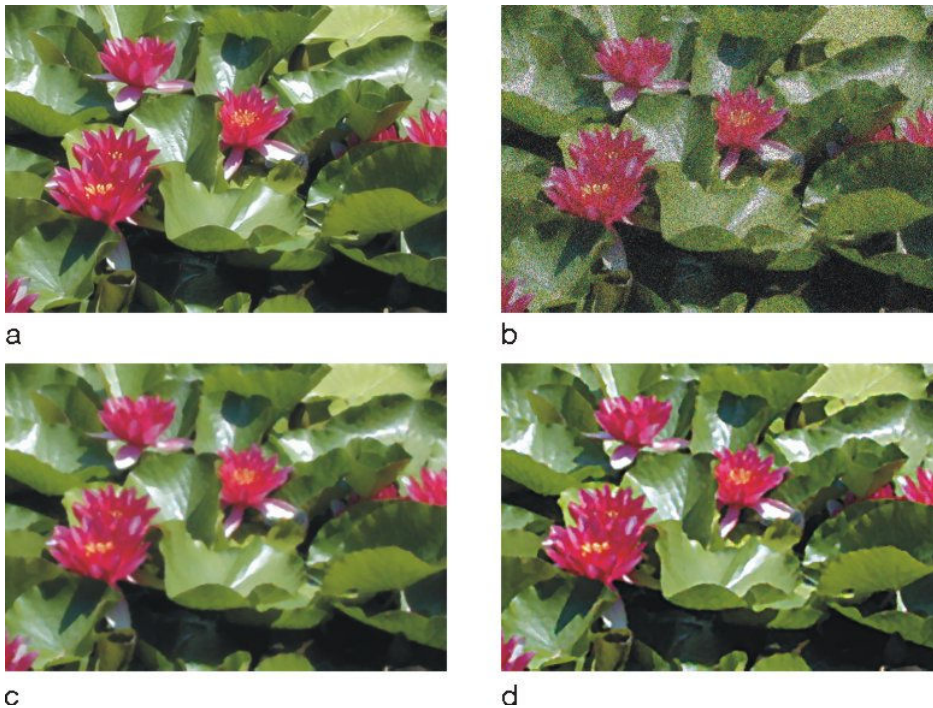
Fig. 3.23. *The initial image (a) can be reproduced on the basis of an image with noise (b) thanks to the median filter (c) and advanced sharpening (d).*

Let us now see how some of the filters mentioned can be utilized in practice. Fig. 3.23b presents an image the initial image (from Fig. 3.23a) with noise

interference (noise of this kind can appear e.g. when the image is recorded under poor light conditions). Then the noise is eliminated with the help of the median filter (Fig. 3.23c), and the whole image gets sharpness enhancement with the help of a very smart filter called "unsharp masking". Simplifying the issue, the filter in question consists in adding to the image we need to enhance the difference between itself and an image additionally artificially blurred. This type of procedure is sometimes called also the method of back-propagation. What is important for us is that the process of sharpening applied here generates virtually no noise, and the final effect (Fig. 3.23d) is really very close to the original from Fig. 3.23a.

When working with image analysis systems, it is worth keeping in mind that almost always it is possible to obtain the same or almost the same result using different methods. A very smart way of noise elimination is presented in Fig. 3.24. As can be seen, this method of noise elimination is characterized by very high efficiency. This results from the simple observation that noise generated by the camera under the conditions of poor light is of random character. It should be noted that this method of noise elimination is sometimes integrated in image analysis software packages which analyse images being means of several consecutive „frames" recorded by a video camera.
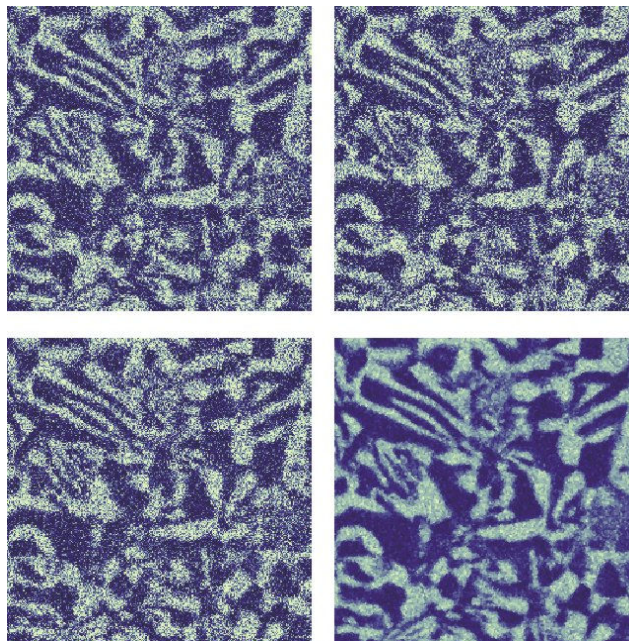

Fig. 3.24. *A smart way of noise reduction.*

108

3.8. Mathematical morphology

Morphological operations mentioned earlier can also be interpreted as filters. The basic difference consists in that the classical filters discussed so far transform all the pixels in an image, while morphological operations are more selective. The idea of morphological operations consists in the limitation of image transformation to those parts whose local pixel configuration corresponds to a certain model known as the structuring element. For example, the structural model presented below models an isolated point (with the value of 1) surrounded with a uniform background (with the value of 0):

0	0	0
0	1	0
0	0	0

It is now sufficient to give the program the command of „make a negative of all the points whose neighbouring pints correspond to the above model" to eliminate from a binary image all isolated points. The idea presented here is very simple, but it can be used for the construction of highly complex operations. One of them is filling the missing elements of the edge contours of grains, as shown in Fig. 3.25. An analogous procedure can be used e.g. for the separation of connected particles.
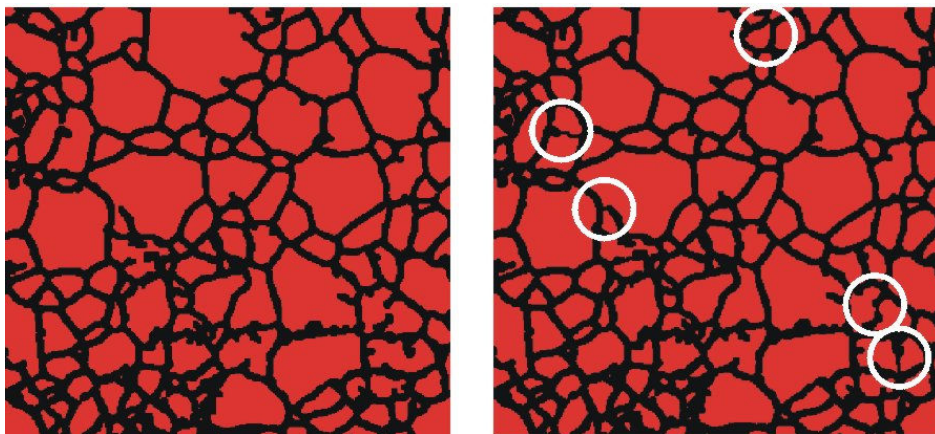
Fig. 3.25. *Example of filling in missing fragments of granule contours – areas of filling are marked with circles.*

An interesting example of morphological transformations is skeletonization which transforms figures into sets of thin lines. Theoretically, a skeleton is a set of centres of circles inscribed in a given figure, or (both definitions are equivalent) a set of all points equidistant from the two sides of a figure. Examples of skeletons are presented in Fig. 3.26.
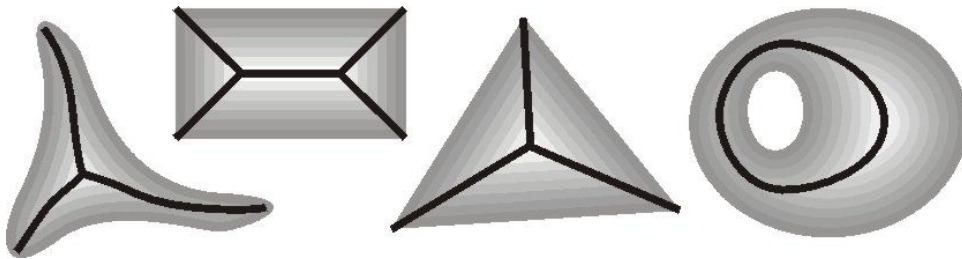

Fig. 3.26. *Examples of skeletons.*

As we can see, skeletons retain certain topological features of the figures. For example, the skeleton of the figure with a hole forms a closed loop. Moreover, the skeleton is always wholly contained within the figure, and the more developed the contour of the figure, the more complicated the skeleton. Digital realization of the idea of skeletonization is rather complex. It makes use of specific structuring elements, e.g.:

0	0	0
X	1	X
1	1	1

where X is a point whose value is disregarded. To create a skeleton, all the points that correspond to that point are eliminated. Next, the element is rotated by 90 degrees:

1	X	0
1	1	0
1	X	0

and the whole operation is repeated until the moment when the next step does not produce any changes in the image. Examples of figures with superimposed skeletons are shown in Fig. 3.27. It should be noted that in digital space (discrete) we sometimes obtain skeletons that differ from their mathematical models. For example, the theoretical skeleton of a circle is one point – the centre. Skeletons are utilized for analysis of the shape of objects, for separation of connected objects, for filling in missing fragments of cell borders or for purposes of modelling. In the latter instance we most frequently use the SKIZ (SKeleton by Influence Zone) transformation which is simply the skeleton of the negative of an image, with subsequently pruned extremities.
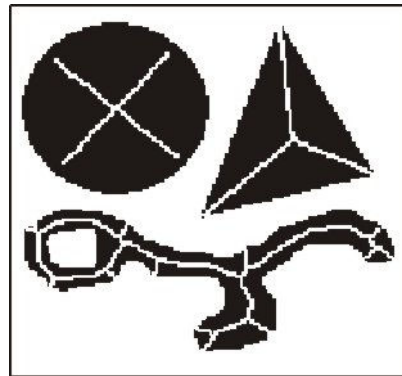
Fig. 3.27. *Figures with superimposed skeletons.*

3.9. Building image analysis algorithms

The transformations discussed so far constitute but a small part of transformations available in image analysis programs. More detailed descriptions of image analysis transformations can be found in software manuals and in literature of the subject.

Practice shows that understanding most of the transformations does not usually present any greater problems. The real problem lies in their skilful utilization and application. Luckily, one can more and more often encounter publications aimed at teaching the reader the practical utilization of image analysis software. An example of such a generalization of multiple algorithms is given in Fig. 3.28, where three types of image analysis problems, frequently encountered in practice, are presented.
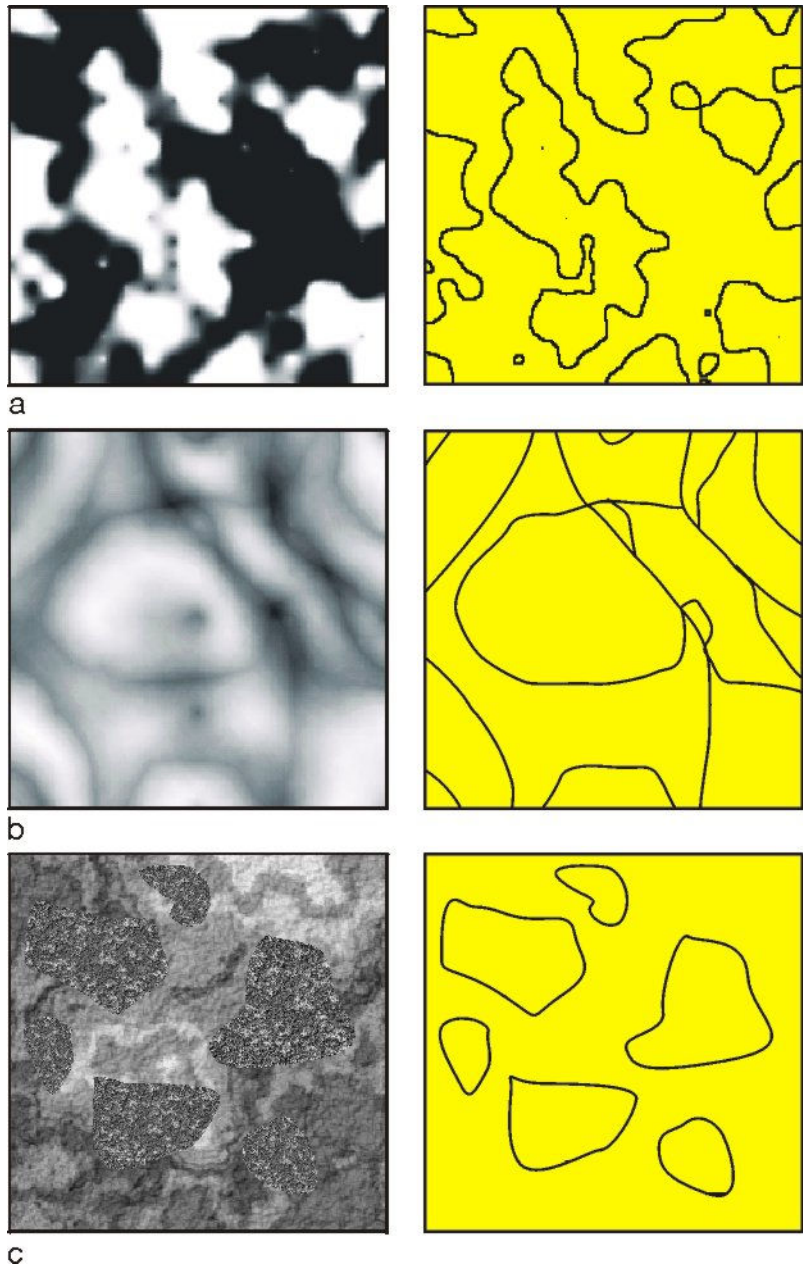
Fig. 3.28. *Various types of images and corresponding edge contour images. Description in the text.*

112

The simplest problem is presented in Fig. 3.28a, where particular elements of the structure clearly differ in the degree of blackness. Their separation can be achieved through simple binarization, and in the binary image the contours of the elements can be easily detected with the help of erosion (right side of Fig. 3.28a). In this case, the edges can also be effectively detected with the help of most edge detection filters.

A case that is distinctly more difficult and more frequent in practice is presented in Fig. 3.28b. The edges separating particular elements appear here in the form of local extremes (e.g. values locally the lowest) and, moreover, display considerable variation and often a lack of continuity. In such a case the edges can be detected with the help of gradient analysis (analysis of the rate of local changes in the degree of blackness) or through suitable combination of different filters. Good results can often be obtained by the determination of the difference between the initial image and the image after filtration. The case presented in Fig. 3.28b is characterized by a great variety of solutions that are often equally good even though based on highly differentiated operations (an example can be seen in Fig. 3.29 and the related commentary).

And finally, the third case, shown in Fig. 28c, represents differentiation in the texture of particular objects. This is somewhat similar to the problem of identifying individual fragments of various fabrics in „patchwork”-type decorative stuff. Edge detection in images of this type is a true challenge. The most sophisticated techniques are used for the purpose, like Fourier transform, correlation techniques, and neuron networks. Fortunately, in routine laboratory work, most often thanks to proper methods of specimen preparation and observation, images for analysis can be modified so that there is no need to resort to the most complex image processing techniques which at the same time usually are the least reliable.
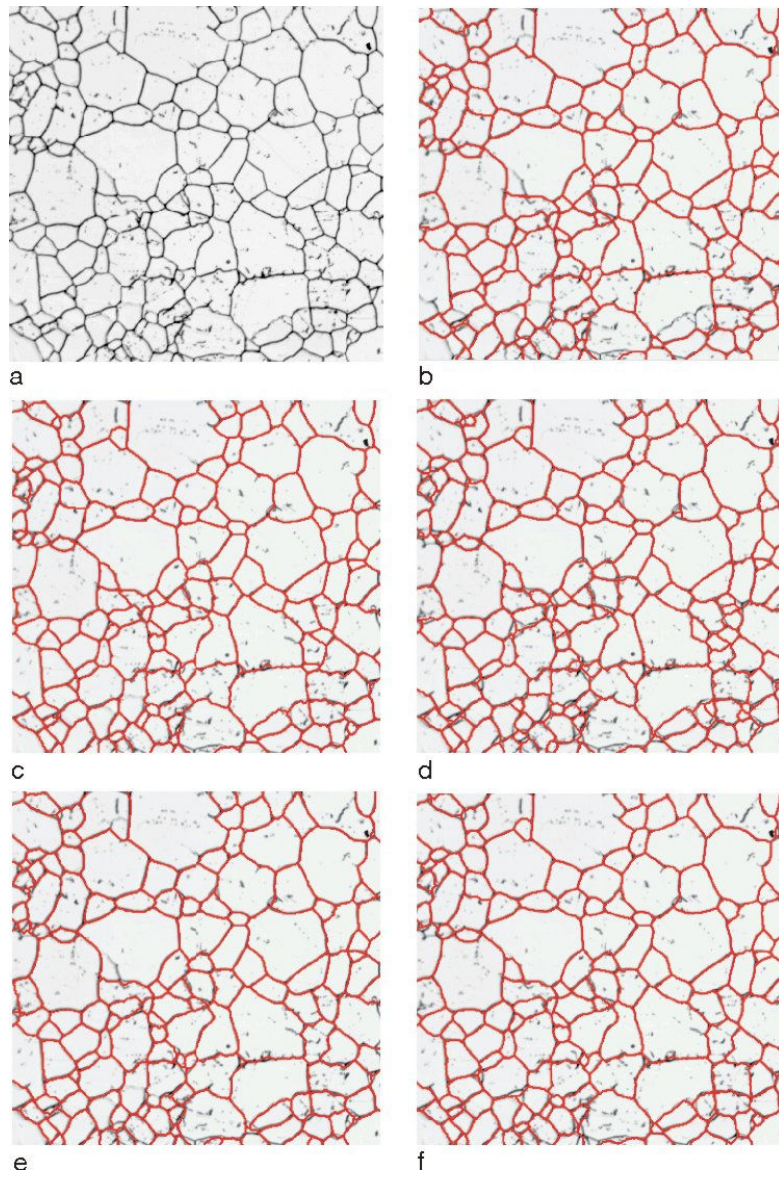
Fig. 3.29. *Comparison of various methods of grain edge detection. Description in the text.*

Fig. 3.29 illustrates the phenomenon, mentioned earlier and typical for methods of image analysis, of the existence of numerous virtually equivalent solutions for the same task. In our case the problem consists in the automatic detection of grain edges in the structure from Fig. 3.25a. To facilitate the estimation of particular algorithms, the results of their operation have been superimposed on the initial image in the form of red lines. The particular algorithms utilized distinctly different operations:

- The basis of the detection presented in Fig. 3.29b is the Laplacian. Areas in which it gave points with zero value formed the basis for the detection of grain borders.
- Detection of local minima (difference between the initial image and the image after closing) constituted the nucleus of the algorithm, the result of which is shown in Fig. 3.29c,
- Grains in Fig. 3.29d have been obtained as a result of binarization following the operation of shade correction (discussion of this operation exceeds the scope of this chapter)
- Grain borders in Fig. 3.29e have been obtained as the sum of edge contours detected with the help of three filters – Sobel's, Roberts' and Prewitt's,
- The final example, shown in Fig. 3.29f has been obtained with the help of automatic method of binarization, based on the analysis of a histogram of shades of grey for the whole image.

Without going into details, we can state that all of the five algorithms mentioned gave similar results. Although analysis of Fig. 3.29 reveals certain differences between the results obtained with the particular methods, the differences are slight and have no significant effect on the results of measurements. It is enough to say that the scatter of results obtained with those distinctly different algorithms is smaller than the scatter of results of analysis performed manually by several observers.

3.10. Fourier transformation

Fig. 3.30 presents an example of the application of Fourier transform. It is a very complex transformation, so we will not discuss it here in any detail. Since the Fourier transform approximates any function – in this case the shades of grey in an image – with the help of a series of trigonometric functions, it is especially suitable for the detection of objects that are periodic in character. Fig. 3.30a shows periodic noise originating from the printer raster, interfering with from the raster of the scanner. Periodic elements give clusters of bright points in the Fourier spectrum, marked with arrows in Fig. 3.30b. The clusters can

be filtered out. Then, performing reverse Fourier transform, we obtain an image that is free of the periodic noise (Fig. 3.30c). The result showed here cannot practically be achieved with any similar level of quality by using other filters. Unfortunately, practical utilization of the Fourier transform is very difficult, as it does not easily accept automation of parameter selection, and finding effective filters for Fourier image correction is also a hard task.
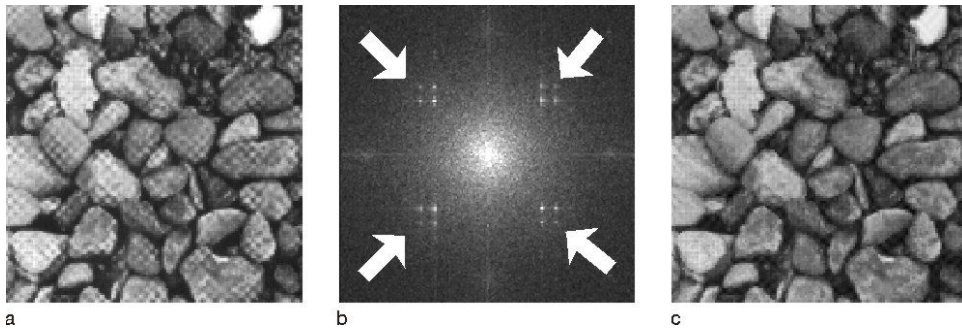

Fig. 3.30. Example of the application of Fourier transform. Description in the text.

3.11. Look-up tables and color image analysis

Some of the operations used in image analysis are very simple. Transformations utilizing so-called LUT (look-up tables) can be a good example here. To take a closer loot at this group of transformations, we need to concentrate for a moment on the way in which computers save data. And thus grey images (equivalent to black-and-white photography) are most often saved in 8-bit form, which means that information on the shade of grey of every dot in the image is written as an 8-bit number. Since $2^8=256$, it means that every dot in the image may assume one of 256 values. Usually, 0 is adopted for black and 255 for white. 256 shades of grey are enough to register most images, as the human eye discerns only 30-50 shades. In the case of colour images, three RGB component images are used (red, green, blue – see Fig. 3.31). The three components correspond to the sensitivity of the receptors of the human eye, and hence a mosaic of dots of three different colours reproduces colours fairly well – we experience this every day, whenever we watch TV or work with a colour computer monitor. Saving such three component colours requires 3*8=24 bits per pixel in the image. In practice it means the possibility of saving and reproducing about 16.1 million different colours, which in a great majority of cases satisfies our sense of vision.

116
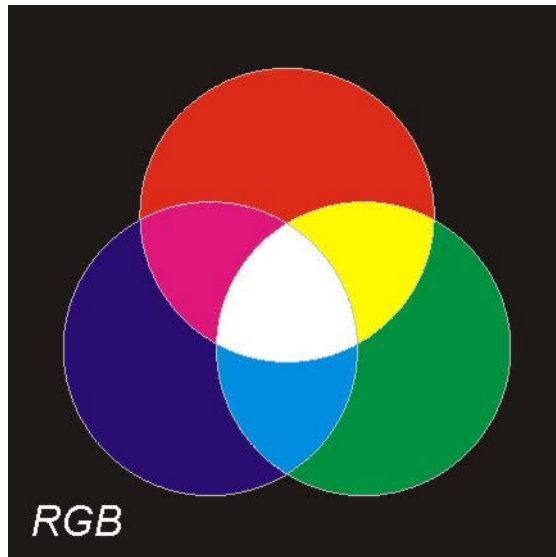
Fig. 3.31. *Model of RGB. Description in the text.*

The model of generation of RGB colours, shown in Fig. 3.31, demonstrates the difficulty involved in their analysis. As an example, the effect of composition of red and green is yellow, which does not correspond to our experience. The problem results from the fact that the RGB model simulates the way of colour reading by the human eye and not changes in the ability to reflect particular components of white light spectrum by mixtures of pigments. What is important here is that colour image analysis is reduced in practice to analysis of the three component images which in essence are grey images. A practical example of such component images is shown in Fig. 3.32.
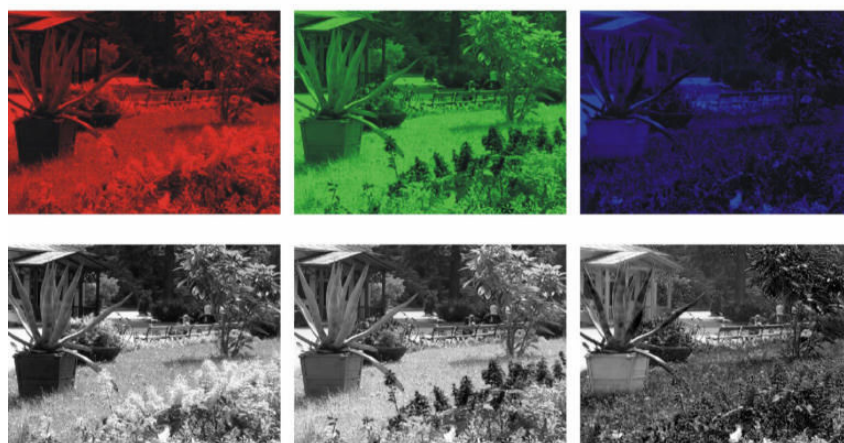
Fig. 3.32. *RGB colour image and its components shown in colour and as grey-tone images.*

Simple transformation of images can be performed both with the help of powerful (and correspondingly expensive) graphics software, e.g. Adobe Photoshop or Corel PhotoPaint, and of cheap, often shareware-type, software packages like the Paint Shop Pro. As can be easily guessed, simple transformation of images consists in assigning each dot a new value, calculated on the basis of the initial value with the help of a suitable selected function. Calculation of the function values, however, may by relatively time consuming, especially if it is a complex non-linear function. Since every grey image is composed of dots with maximum 256 shades of grey, we can covert earlier the values of the transforming function and write the new 256 values in the form of a table (hence the look-up tables) and proceed with the conversion by way of substitution.

And substitution is an operation that computers can perform exceptionally fast, often even in real time.

Let us now consider a few simple examples of transformations. They will be illustrated on schematic graphs and supported with examples of suitable transformations. If we do not change anything during a transformation, the result can be presented as a section marked with blue in each of the graphs. Position and shape changes to the section are marked as colour areas. Yellow spots correspond to slight changes, green areas – to an increase in the level of transformation, and red areas - to a reverse situation.
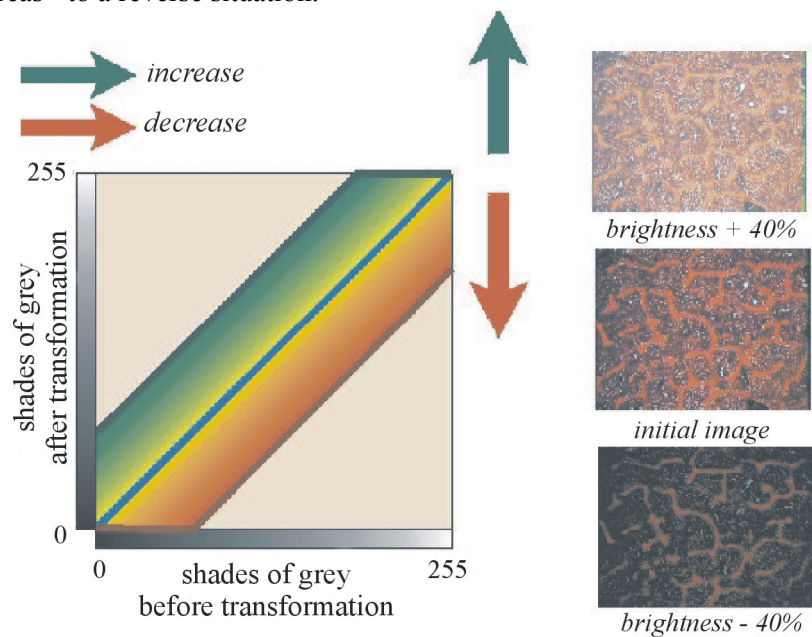
Fig. 3.33. *Schematic and examples of image brightness change operation.*

Probably the simplest transformation is the change of image brightness (Fig. 3.33). It consists in the addition or subtraction of a constant value with relation to every pixel value. As we can see in Fig. 3.33, this leads, in increasing image brightness, to exceeding the value of 255 in a certain range. In such a case the appropriate pixels are assigned the value of 255 (i.e. they are changed to white). Likewise, in the case of darkening an image, some pixels get changed to black. This is illustrated by the lines – dark-green and dark-red, respectively.
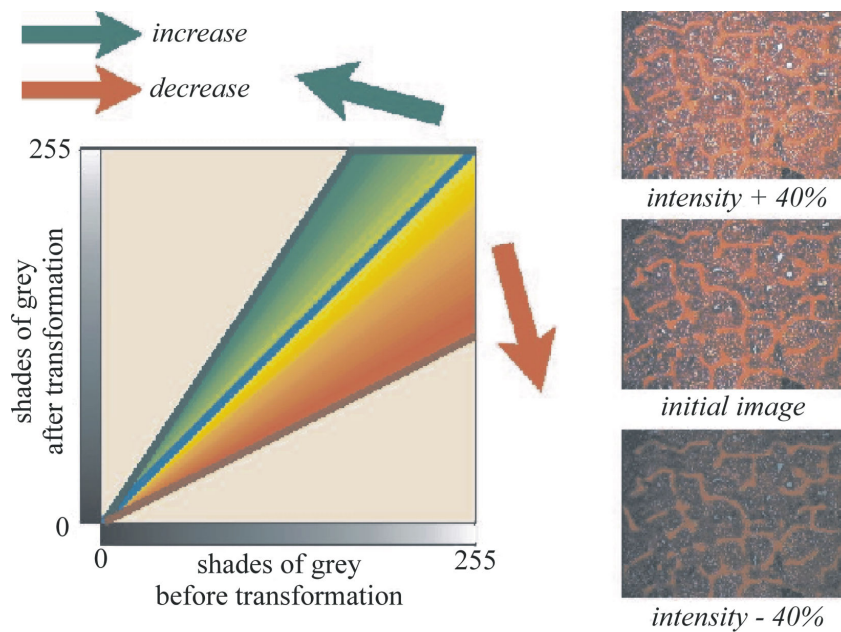
Fig. 3.34. Schematic and examples of image intensity change operation.

Change of image intensity is a very similar transformation (Fig. 3.34). It differs from the change of brightness in that instead of adding a constant value to each pixel value, the changing element is the slope of an appropriate line. Thanks to this black areas always remain black, and values exceeding the range of 0-255, replaced with the value of 255 corresponding to white, are obtained only with intensity increase.

In turn, a change in the slope of the line describing the manner of transformation of the values of particular dots leaving the centre dot unchanged (Fig. 3.35) leads to a modification of the level of contrast in our image. With increasing contrast, new pixels appear in our image, both black and white, while a decrease of contrast causes a narrowing of the range of shades of grey in the image.

120
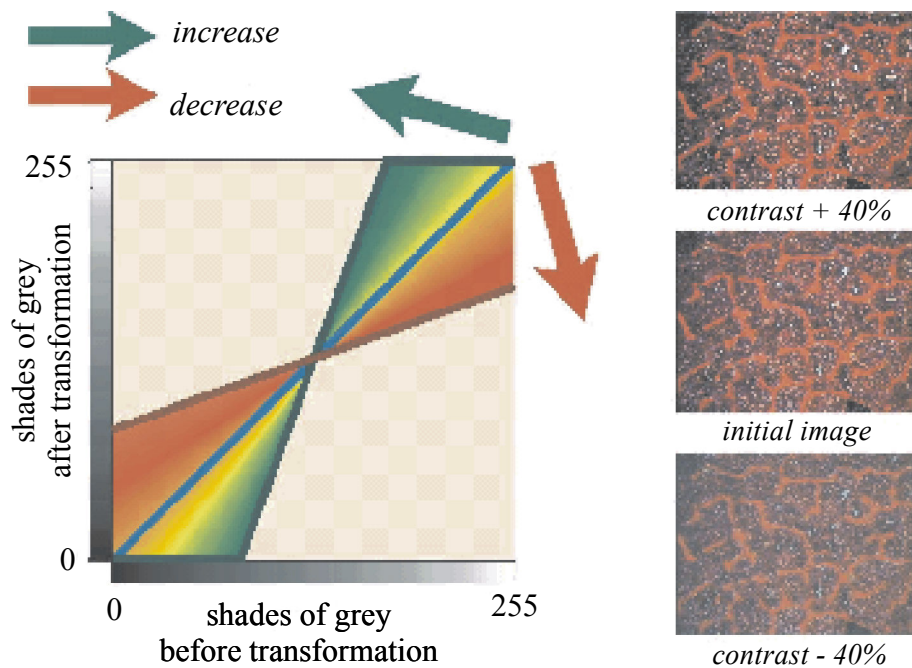
Fig. 3.35. Schematic and examples of image contrast change operation.

As we can see, each of the transformations discussed so far causes that, under certain conditions, some pixels – originally with varied shades of grey – are replaced with pixels with the same value corresponding to either black or white. In some cases this has no practical importance, e.g. when the initial image does not cover the full range of shades of grey from black to white. Frequently, however, transformations of this type cause the loss of a significant part of information contained in the image.

To avoid this shortcoming, non-linear transformations had to be employed. The most popular of those is the so-called gamma modulation which utilizes exponential functions as the basis for transformation. In the first publications describing the transformation the exponent of the function was denoted with the letter gamma, which gave the current name to the operation. Gamma modulation leaves white and black dots unchanged, while the remaining range of shades of grey is non-uniformly modified. For gamma values greater than one the image is brightened in the range of dark tones, while gamma values below one extend the range of bright tones and, consequently, darken the whole image (Fig. 3.36). A significant feature of gamma modulation is its monotonic run. This means that when we select two arbitrary dots A and B, such that A is brighter than B,

and then perform gamma modulation, A will sill be brighter than B. As a consequence, gamma modulation not only leaves unaltered white and black dots, but also modifies the image in a way that is perceived as natural and correct.
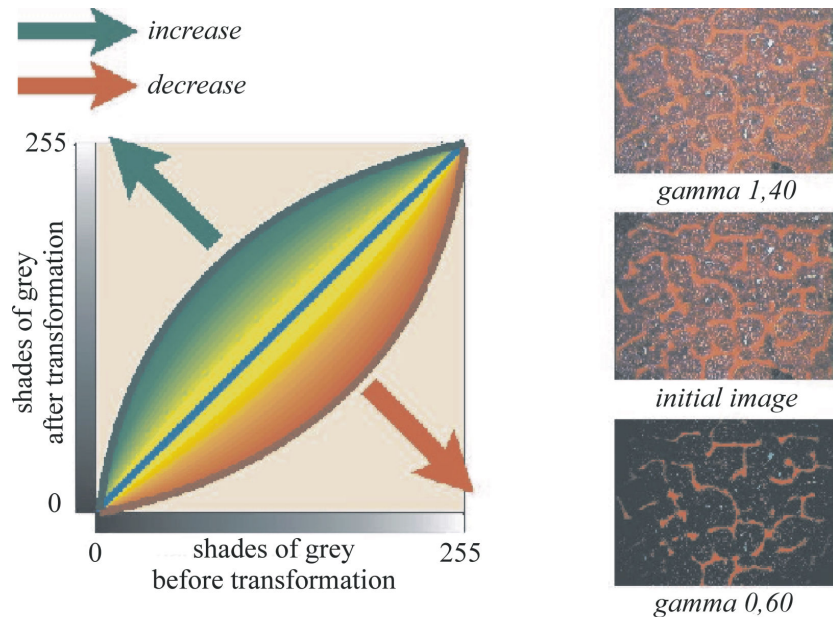

Fig. 3.36. *Schematic and examples of gamma modulation.*

The examples presented in Figures 3.33-3.36 utilized the transformations under discussion individually, so as to better present the effects of their operation. However, there is nothing to prevent their application in any combinations. An interesting variety of the transformations discussed here is the so-called normalization which can be used in relation to images that do not utilize the full tonal spectrum. Usually such an image (Fig. 3.37, top) is „flat", and its histogram of shades of grey shows a lack of values corresponding to the darkest and the brightest tones. Normalization consists in the extension of the range of shades of grey so as to cover the full tonal spectrum (Fig. 3.37, bottom). As a result of the transformation we obtain an image that is perceived as "more lively" and, though that is not really true, with better sharpness.
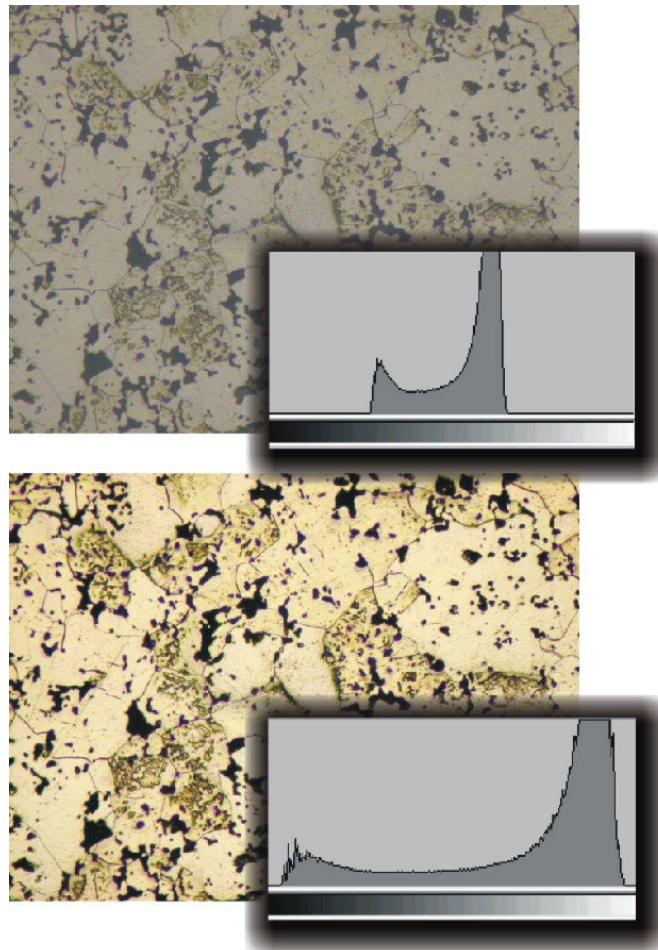
Fig. 3.37. *Application of normalization for enhancement of image perception. Corresponding histograms of shades of grey are presented against each image.*

The above simple methods for image transformation permit significant modification of images and allow the obtaining of satisfactory final images even from relatively poor quality initial material. Many people, however, are against the application of such methods, on the grounds that they provide the primary tool for falsification of results. Such signals can be heard even from reputable institutions. What the authors of such warnings tend to forget is that conventional photography provides just as many opportunities for result manipulation.

4. APPLICATIONS OF IMAGE ANALYSIS TO PLANT TISSUES

4.1. Analysis of plant tissue images obtained by means of optical microscopy

Henryk Czachor[*]

4.1.1. Introduction

The appearance and rapid development of new branches of microscopy (electron, confocal, acoustic) has not resulted in a decline of traditional optical microscopy, but rather in its further refinement. The optical microscope is still the primary research tool in many branches of science (biology, physics, medical sciences) and industry (metallurgy, geology). The fundamental objective of microscopy in those branches concerns the study of structure in its broad sense – of plant and animal tissues, of polished sections of metals and rocks. Contemporary optical/light microscopes have not only highly refined optical system of their lenses but are frequently augmented with accessories (photo and film cameras) which permit the acquisition of images in a digital form. The image of a structure studied can be then subjected to analysis for the determination of the occurrence of one of its elements, in both the qualitative and quantitative aspects. The development of computer technology and methods for digital recording of images has created the possibility of visual information processing, i.e. computer analysis of images. The principal advantage of this method as compared to the visual analysis lies in its objectivity and in the speed at which results can be obtained.

Presented below is the methodology of study of the cellular structure of potato tuber parenchyma tissue, using a program for image analysis. The method consists of three stages:

- Fixation of structure and preparation of tissue sections,
- Image acquisition and processing,
- Parametrization of the structure and extraction of geometric characteristics of the tissue.

---

[*] Henryk Czachor, Assistant Professor
Institute of Agrophysics, Polish Academy of Sciences
ul. Doświadczalna 4, 20-290 Lublin 27, Poland
e-mail: h.czachor@ipan.lublin.pl

4.1.2. Fixation of tissue structure

The structure of potato tuber meat tissue was studied by means of a BIPOLAR EPI BE-243 optical microscope, in which the light beam passes through the whole thickness of the slide before it arrives at the eye of the observer. To obtain an image of the cellular structure, the thickness of the prepared slide must be smaller than the cell size of the tissue under study. As the dimensions of the cells of potato tuber parenchyma tissue are approximately 100μm, it was decided to perform the study on tissue sections of a thickness of 25μm. Preparation of such extremely thin sections of potato meat tissue is very difficult and may lead to considerable deformation or even damage to the structure studied. One of the methods for avoiding the deformation or damage is the long-used fixation of the structure by means of paraffin [2] to a state permitting its machining. The fixation process involves several operations, the first of which consists in cutting, at specific locations on the tuber, of cylindrical cores 5 mm in diameter and 10 mm long. The cores were then deaerated under vacuum conditions and fixed for 24 hours in chromium fixer CrAF in a manner preventing excessive shrinkage of cell walls. The next stage of the process consists in dehydrating the cores in ethyl alcohol solutions of increasing concentrations - 10, 20,..., 100%. At that stage, apart from the dehydration of the cores, the dissolution and washing out from the tissue of the cores of lipids, small-particle compounds and ions takes place. Prior to the saturation with paraffin, the dehydrated cores were first washed in a mixture of ethyl alcohol and benzene, and then in pure benzene. The process of core saturation with paraffin, which lasted for 24 hours, was performed at the temperature of 37^0C and began with a 5% paraffin solution in benzene. In the next stage, paraffin was added in amounts equal by weight with benzene, and the whole lot was heated to 60^oC until total evaporation of benzene. Cores prepared in this way were then encased in paraffin blocks. Cores fixed in the manner can be stored for indefinite periods of time.

The next stage consisted in the preparation of slides for microscope observations. A cubicoid fragment of a core block, containing one sample of potato tissue, was placed in the grip of a Leica RM2155 microtome. The thickness of the section sliced off from the block was 25μm. Fragments formed in this manner were placed, using a brush, on a slide glass, their surface smoothed, and attached to the glass with Haupt adhesive. After the adhesive dried, the slides were heated up to the point of paraffin melting, which permitted excess paraffin to be removed from the slides.

Attempts at dying the cell walls with alum hematoxylin and safranine did not yield the results expected. Finally, for the study of tissue structure, images of non-dyed cores were used, obtained by means of a BIOPOLAR EPI BE-2403 microscope in transmitted light. Microscope images of the studied structures have to be recorded, which can be achieved with the help of digital cameras or CCD cameras working in combination with computer programs for image acquisition (e.g. Matrox Intellicam). Conventional photographs can also be analyzed, after their conversion to digital form.

4.1.3. Procedures of potato tuber parenchyma tissue image processing

A fundamental problem related to image analysis is the identification and highlighting of important elements in the image or the elimination of the remaining, unimportant elements. A digital image consists of pixels, the number of which is determined by the resolution of the image. Depending on what equipment has been used for image acquisition, the image can be saved in shades of grey or as a colour image. In the former case, individual pixels differ in their degree of greyness whose variability is, most frequently, 256 units. The value of zero corresponds to black, 255 – white, and the intermediate values – to various degrees of greyness.
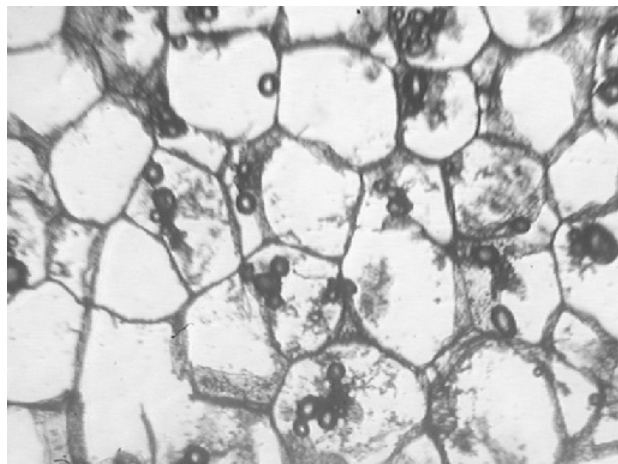
Fig. 4.1. *Cellular structure of potato tuber parenchyma tissue (image in shades of grey, 8-bit).*

126

The format most frequently used for colour images is the RGB format, in which the colour of each pixel is the resultant of superposition of three component colours: R-red, G-green, B-blue. The intensity of each of them assumes values within the range of 0-255.

An example of an image of the structure of potato tuber parenchyma tissue obtained in shades of grey is presented in Fig. 4.1. Apart from the cut cell walls, the image shows grains of starch in the form of dark circular spots which often touch one another making it impossible to determine the position of the cell wall. Moreover, some of the cell walls have not been cut square to their surface but at an acute angle, which resulted in the appearance of grey areas in the image. These features of the image, in conjunction with other intrusions and faults of the optical system, may severely restrict the possibility of automatic identification of cell structures.

Good detection of cell walls does not in itself mean that the structure characteristics obtained will be correct. The image in Fig. 4.1 comprises 30-40 cells. Almost one half of the number are intersected by the frame of the image and therefore should not be taken into consideration in the analysis. It should be emphasized that even the performance of a large number of analyses of such images may be burdened with a considerable error. The probability of cell wall intersection by the image frame depends on the ratio of the cell size to the frame size, which means that the probability grows for large cells [2, 3]. As cells intersected by the image frame are not taken under consideration, analysis of structures on the basis of small images has to yield results underestimating the share of large cells. Therefore, the correctness of analysis is conditional on having images of dimensions many times larger than the largest cell in the structure under analysis. To fulfil this condition, it was decided to merge 20-25 small adjacent images of the same cell structure, as shown in Fig. 4.2 where the image from Fig. 4.1 is indicated with a rectangle.

The analysis was performed using the Aphelion 2.3i program [1] which permits comprehensive processing and parametrization of any image.

Presented below is a description of the procedures of the program that permitted the determination of the geometry of cell walls and their further parametrization. It was assumed that the cell sections, visible in the image in the form of figures similar to polygons, completely fill the image area.
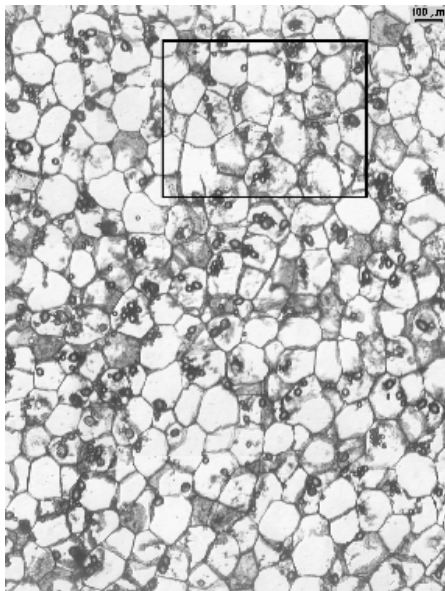
Fig. 4.2. *Image of potato tuber tissue in shades of grey obtained through merging a number of small individual images. Location of the image from Fig.1 is marked with a rectangle.*
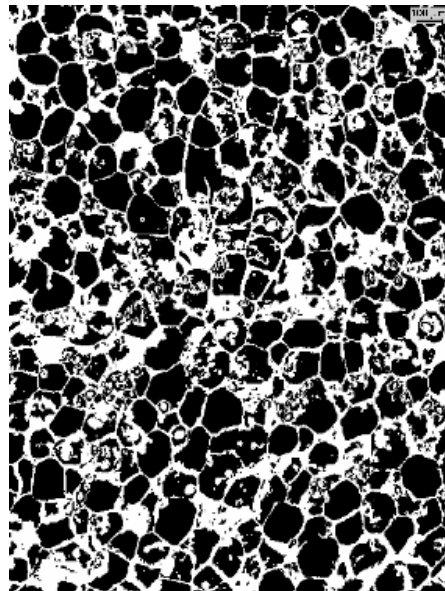
Fig. 4.3. *Image from Fig. 4.2 after binary conversion (Threshold procedure)*

The first step consisted in the removal of noise from the images, which was achieved through the use of a median filter with kernel size of 5x5 pixels [5].

The above operations preceded the binary conversion of the image, i.e. a procedure that would convert the image into a single-bit form. Pixels with values falling outside of the range limited by the upper and lower discrimination thresholds were assigned the value of zero, and the remaining pixels – the value of one. The correct determination of the thresholds is facilitated by the histogram of the image processed. Fig. 4.4 presents such a histogram, i.e. the share of pixels with different shades of grey, for the image from Fig. 4.2. The histogram is continuous, and the 1st maximum, related to the cell walls, is relatively weakly marked, which usually indicates poor image quality (poor optical contrast at cell wall boundaries).
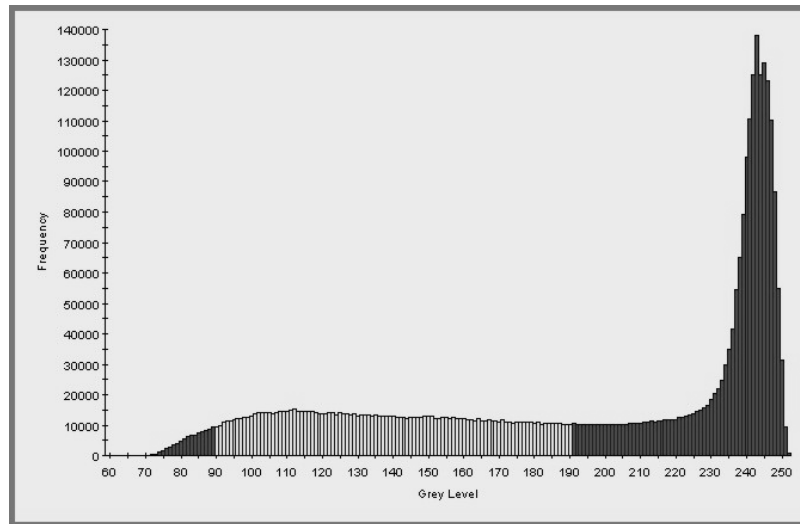
Fig. 4.4. *Histogram of grey levels of image from Fig. 4.2 with marked discrimination thresholds (lower and upper).*

Fig. 4.3 presents the result of binary conversion with double discrimination threshold for the image from Fig. 4.2. Pixels with a grey level value higher than the lower and lower than the upper discrimination thresholds were assigned the value of 1, and the remaining ones - 0. Even a perfunctory assessment of the image in Fig. 4.3 shows that the determination of the location of a considerable part of the cell walls would be difficult and that further conversion of the image is necessary. The image in Fig. 4.5 was created from the image presented in Fig 4.3 as a result of a sequence of four successive operations of the Aphelion program: inversion (Invert): (pixel with the value of 0 assumes the value of 1, and pixel with the value of 1- 0), "hole" filling (HoleFill), erosion (Erode) and separation

of concave areas into two or more convex areas (ClustersSplitConvex).

In Fig. 4.3 one can see a lot of small unwanted intrusions inside the cells. The application of the inversion and "hole" filling operations removes than from the image.

The operations of erosion and separation permitted the division of the image into a group of independent individual clusters. The shape of some of those, however, is still concave, which is contrary to the adopted assumption of cell convexity. The ClustersSplitConvex operator partially solves the problem, dividing a branched cluster into separate parts.
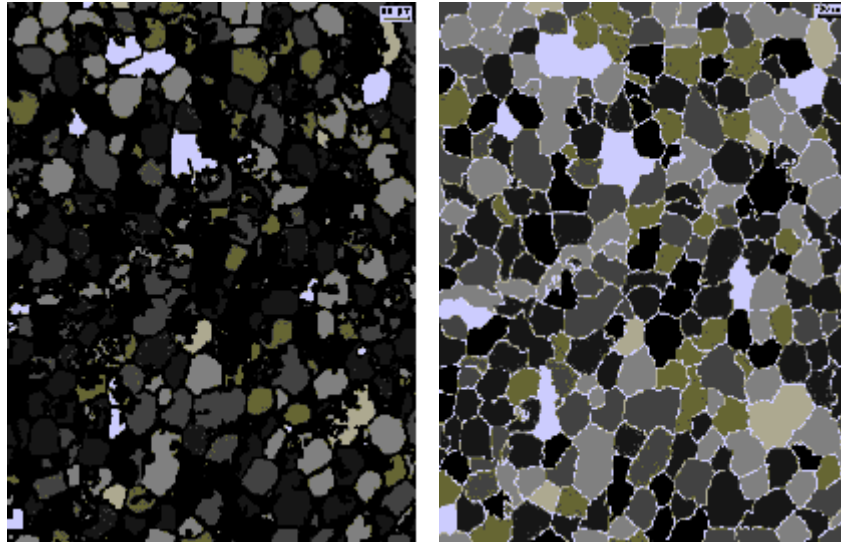
Fig. 4.5. *Objects (cells) identified in the image from Fig. 4.3 (ClustersToLabels).*

Fig. 4.6. *Image from Fig. 4.5 after removal of small objects (AreaOpen) and after watershed operation (ConstrainedWatershed).*

Its operation yields good results when the neck between the parts separated is clearly marked.

The image presented in Fig. 4.5 is therefore composed of clusters, each of which is a group of joined pixels. The ClustersToLabels operator assigns a label to each cluster, which allows it to be treated as a separate object in further operations.

After the application of the above transformations it turned out that the number of identified clusters is too large, that most of them are very small and bear no relationship with the cells. Therefore, they were removed from the image with the help of the AreaOpen procedure which eliminates clusters below a certain programmer-definable limit of area. The removal of small clusters, however, caused the appearance in the image of „empty" spaces not related to any of the clusters (cells). As the whole area of the image is filled with cells adhering to one another, it was decided to join the empty spaces to the nearest adjacent cells. If an empty space is located within a cell, the cell is extended by the value of the empty space area. Usually, however, the empty spaces are located at the

borderline of two or three cells. The division of an empty space between neighbouring cells can be accomplished using the watershed procedure (ConstrainWatershed). To illustrate the operation of the procedure, it can be compared to the determination of a line between two lakes along which they could be joined by rising waters in both the reservoirs. The image of the cells created with the help of the ConstrainWatershed procedure is shown in Fig. 4.6.
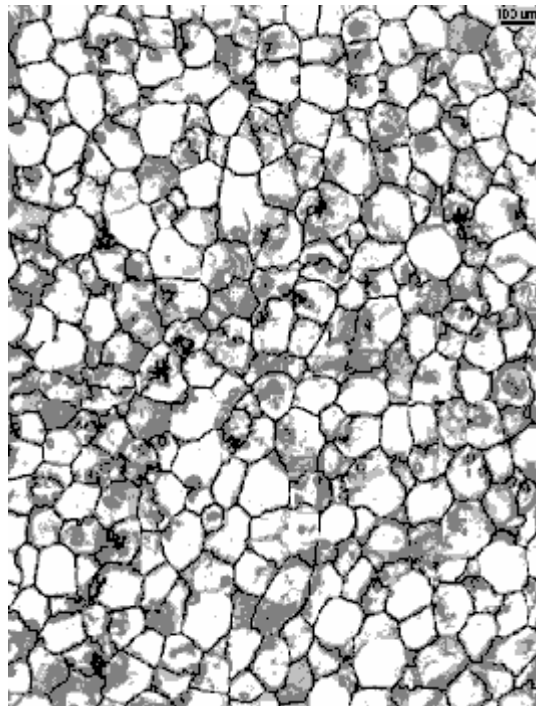

Fig. 4.7. Initial image with marked cell walls detected with the help of the procedures described (dark lines).

To determine the effect of all the procedures applied, the detected boundaries between cells can be superimposed in the initial image, i.e. the image presented in Fig. 4.2. Fig. 4.7 permits the evaluation of the results of cell walls detection. The course of the cell walls detected is marked with a dark line. As can be seen in the figure, most of the call walls of the potato tuber parenchyma tissue were determined correctly in spite of the relatively low quality of the initial image. The number of undetected call walls was at the level of 10-15%.

Cells intersected by the image frame should not be taken into consideration when analyzing the structure. As the image in Fig. 4.7 is made up of individual

objects, elimination of cells touching on the image frame can be easily performed considering the extreme values of pixel coordinates for each of the objects, which is made possible by the BorderKill procedure.

The program applied for image analysis permits combining all the selected procedures, together with their parameters, into so-called MACRO the execution of which results in sequential runs of the procedures, which reduces the duration of the analysis to from about a dozen to several dozen seconds.

4.1.4. Qualitative and quantitative characterization of structure under study

Cell sections visible in Fig. 4.6 are individual objects which means that each of them can be characterized by means of several dozen parameters, concerning the size, shape and direction, available in the Aphelion package. The parameters describing the size of analysed objects are the surface area, circumference, height, and width.

As the shape of cells differs from the rectangular, width and height relate to the smallest rectangle within which the object analyzed can be fitted (Minimum Bounding Rectangle - MBR) as it is shown in Fig. 4.8. Height and width determined in this manner are frequently referred to as Feret's diameters F_{min} and F_{max}.


Fig. 4.8. *Object parameterization by means of the minimum bounding rectangle (MBR).*

The ratio of Feret diameters F_{min}/F_{max} is the moist frequently used parameter describing the shape of an object.

Another parameter of the shape of an object/cell is its compactness C defined as

$$C = \frac{16 * surface\_area}{(perimeter)^2};$$

(1)

Its value equals 1 for a square and decreases for objects with developed and undulating shapes.

132

Shape can also be described by means of other dimensionless parameters, such as

- Elongation, E

$$E = \frac{(a-b)}{(a+b)};$$ (2)

where : a and b – axes lengths of the largest ellipse inscribed into the object,

- Circularity, Cr

$$Cr = \frac{(4*\pi*surface\_area)}{(perimeter^2)};$$ (3)

- MBR_fill – the degree of filling of the minimum bounding rectangle

$$MBR\_Fill = \frac{surface\_area}{MBR\_area};$$ (4)
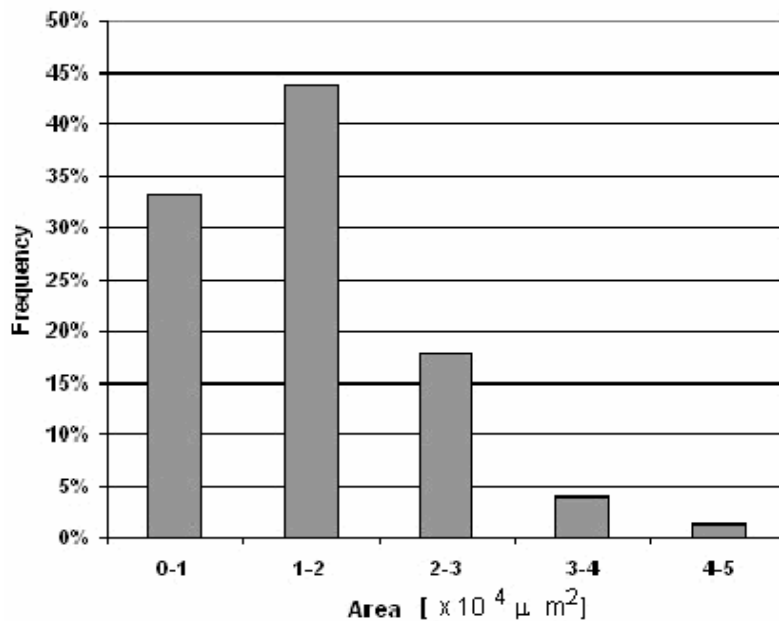
Fig. 4.9. Distribution of section area of potato tuber parenchyma tissue cells (variety Bila).

The number of parameters available in the program is much greater, which permits optimization of the description of structures under study. Data concerning

all the cells can be exported to Excel for generation of the characteristics required. Figs. 4.9 and 4.10 present two distributions obtained for the cell structure of the parenchyma tissue presented in Fig. 4.2.
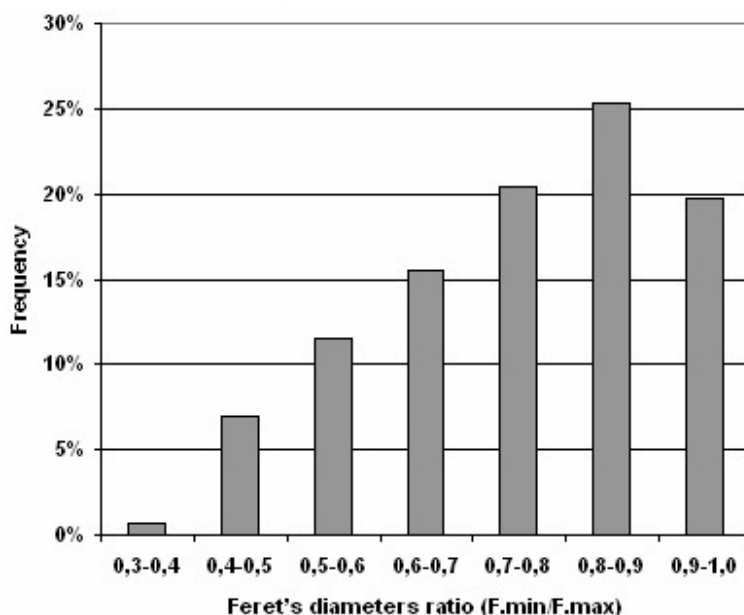
Fig. 4.10. *Cell shape distribution of potato tuber parenchyma tissue from Fig. 4.2 characterized by means of Feret diameter ratio F_{min}/F_{max} (variety Bila).*

The majority, ~75% of the cells of parenchyma tissue of the potato tuber under study (variety Bila) have section areas under 20 000 μm^2. Their shapes are close to irregular polygons characterized by considerable regularity – the elongation of the calls is relatively slight. Over 75% of the cells have shapes with Feret diameter ratio values >=0.7.

It should be emphasized that the MACRO developed is capable of automatically analyzing other structures of the same character within a very short time. It can, but not necessarily so – if successive images will be formed under different lighting conditions or the object studied will have different colouring from the preceding one the automatic analysis may be inaccurate. What is obvious for the human eye and brain may be very difficult or even impossible to perform for the image analysis system (camera plus image analysis program).
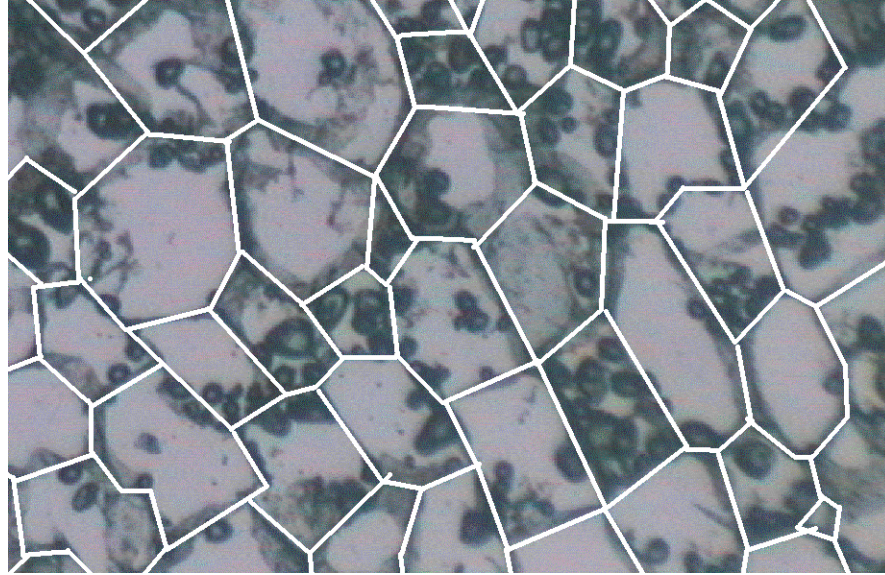
Fig. 4.11. *Image of the parenchyma tissue of potato tuber with cell walls marked out by hand*

If the quality of an image renders its automatic analysis impossible, the geometry of cell walls can be traced manually – directly on the image –by means of available graphic packages (CorelDraw, Paint). Fig. 4.11 presents an image in which the number of starch granules and intrusions was large enough to make it impossible to determine procedure sequences that would permit the determination of cell wall contours with the help of image analysis and therefore they were superimposed on the image with the help of the Paint package. Qualitative and quantitative analysis of an image cell network created in this manner is relatively simple, but also very time-consuming. It worth to mention that some lines are traced intuitively. In consequence the resulting cell network is depended on image quality and on the state of operator matter as well so it has no fully objective character.

Image processing and analysis is a highly useful method of studying the structure of any medium. The condition determining the correctness of the results obtained is having a good image of a section or a polished section, which in turn is determined by the method of sample preparation. The analysis must usually be preceded with a sequence of morphological transformations to a form

permitting the performance of correct binary conversion of the image. The selection of procedures depends on the quality of the image and on the knowledge of the person performing the analysis on the subject of the structure under study and the software used. The application of confocal microscopes eliminates a considerable part of the problems related with the obtaining of good quality images of parenchyma tissue of potato tubers, as the preparation of slides does away with paraffin saturation. This permits the removal of starch granules from the cells visible within the microscope field of view and thus enhances the quality of the images.

REFERENCES

1. Aphelion. Image Processing and Understanding Software v.2.3i, Help 1997, ADCIS SA and AAC Inc
2. Gerlach D. 1972: Outline of Botanical Microtechnology (in Polish). PWRiL, Warszawa
3. Konstankiewicz K., Guc A., Stoczkowska B., 1998: Determination of the structure parameters of potato tuber tissue using specialist image analysis program, Polish Journal of Food and Nutrition Sciences, vol. 7/48, no 3(S), 59(S)-64(S).
4. Pawlak K., Czachor H., 2000: Application of computer analysis of images for parameterization of potato tuber tissue structure (in Polish). Inżynieria Rolnicza, 7, 113-116
5. Wojnar L., Majorek M., 1994: Computer image analysis (in Polish), FOTOBIT-DESIGN S.C., Kraków

4.2. Analysis of images obtained with confocal microscopes

Artur Zdunek[*]

4.2.1. Introduction

In the preceding Chapter we emphasized the advantages of confocal microscopy in studies on living plant tissue, i.e. the speed of image acquisition, the high level of contrast of images obtained from a stable plane in a transparent material (3D analysis capability) and, consequently, simplified sample slide preparation procedure. The latter results from the fact that a slide used for reflecting confocal microscopy can basically have any thickness. The image is obtained from a thin layer which may be located beneath the sample surface at a depth limited by the degree of the material transparency for a given light source. All of these features of confocal microscopy hold true also for TSRLM and CSLM, described in the preceding Chapter. In this Chapter we will concentrate on one application of the microscopes, i.e. inspection of geometric features of the cell skeleton of plant tissues.

The mechanical skeleton of plant tissues is built of cells joined together with pectin lamellas. The structure can be different in various types of tissues. The most typical, and – first of all – one of the most important for agriculture, the parenchyma tissue is made up of regular-shaped or slightly elongated polyhedron cells joined together with pectins. A significant factor affecting the mechanical properties of plant tissue is the intracellular pressure which causes cell wall tension. The intracellular pressure is of the order of 0.3-1MPa, which results in cell wall tension values of about 100-250 MPa (Jackman and Stanley 1995). Certain parenchyma tissues, such potato tuber tissue, may have very small amounts of intercellular spaces (about 1%). Other tissues, like apple tissue, even up to 25% of the tissue volume. Cell cross sections can be up to several hundred micrometers in diameter, while the thickness of cell walls is of the order of several micrometers (1-10μm). Therefore, to be able to observe a cell wall under a microscope, the resolution of the microscope should be of a similar order. However, at this point we arrive at a certain problem. To examine the mechanical skeleton the image observed must contain at least several or around a dozen cells, which means an area of about a millimeter in diameter, while the resolution

[*] Artur Zdunek, PhD
Institute of Agrophysics, Polish Academy of Sciences
ul. Doświadczalna 4, 20-290 Lublin 27, Poland
e-mail: azdunek@demeter.ipan.lublin.pl

should be sufficient for the cell walls to be visible. In other words, the field of view of the microscope should be as large as possible while retaining the high resolution required. As we remember, according to the Lukosz law the resolution can be increased through increasing the scan field. Therefore it appears that confocal microscopes are perfectly suited for this type of studies. Contemporary optical microscopes are equipped with cameras which also permit this type studies. However, only the confocal microscope provides images with sufficient level of contrast to permit the development of automatic procedures of image analysis for the extraction of geometric parameters of the cell skeleton of plant tissues. Another advantage of confocal microscopes which deserves repeat emphasis is the simple slide preparation procedure which will be described further on in this chapter.

4.2.2. Analysis of images obtained with TSRLM

At this point we shall concentrate on the analysis of images obtained with TSRLM for the purpose of extracting geometric parameters of cells. The analysis will be discussed on the example of potato tuber tissue.

As we mentioned above, sample slide preparation procedure is very simple. It consists of the following:

1. Sample slicing. The size of the slice can be freely chosen; what is important is for the slice surface to be as flat as possible. This provides for a uniform image as the depth of the focal plane with relation to the surface is constant and light diffusion is uniform within the scan zone. It is also important that the slice surface be perpendicular to the optical axis. Therefore, good results are obtained by slicing samples of a thickness of about 1 mm using two parallel cutting blades.

2. Washing with water. A cut through the tissue causes the intracellular liquid, cell organelles and, in the case of potato, starch to remain on the slice surface. This makes the washing of slices with water necessary. The washing should not be too long, as through equalization of concentrations the tissue may absorb water and thus increase the intracellular pressure with the resultant increase in cell wall tension.

3. Positioning on slide glass and observation. The slice should be placed on a slide glass on the microscope table at perfect squareness to the optical axis of the microscope (item 1). In the case of lenses with large magnification ratio, the slice should be covered with cover glass, following a principle similar to those applicable to sample preparation procedures in conventional optical microscopy. In the case of immersion lenses, a suitable medium should be provided between the sample and

lens. However, the realization of the objective described above does not require this type of measures. For the observation of the cell skeleton a 10X lens is sufficient. In this case the slice can be placed on the slide glass without the need for the cover glass or for any additional medium. It is important, however, to carefully drain excess water remaining on the slide after the washing or to wait a while for the excess water to evaporate. What should be kept in mind is that is such a case the time for the observation is limited. At room temperature, after about 5 minutes the sample slice begins to shrink and the observation should have been completed by then.

Examples of images if potato tuber tissue prepared in the manner described above are shown in Fig. 4.12.
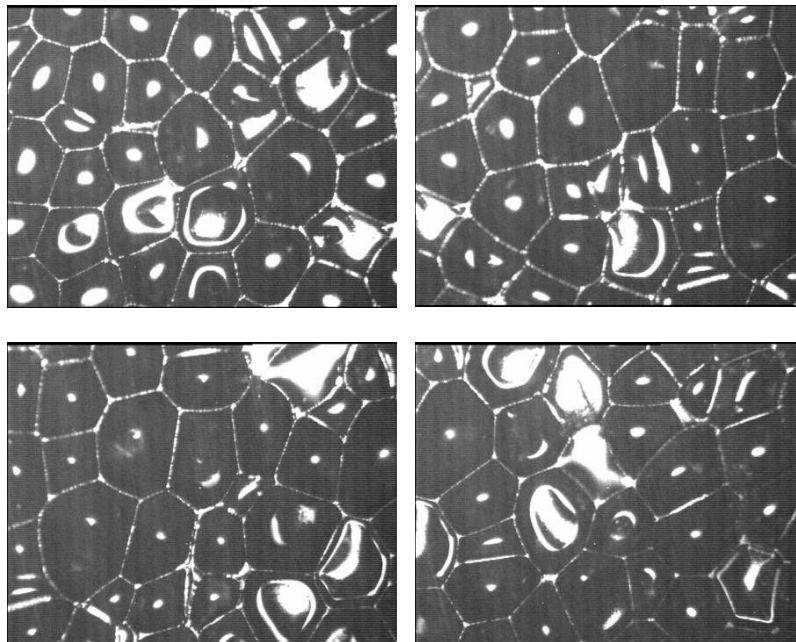
Fig. 4.12. *Examples of images of potato tuber tissue obtained with TSRLM. Lens used - Plan 10/0.24. Sample slides prepared according to the procedure described in the text.*

The images presented in Fig. 4.12 show the principal advantages of confocal microscopy. The image, recorded by the camera in 256 shades of grey, is composed solely of sharply defined areas and the observer can clearly identify

the location of the cell walls in a given section. The resolution of the 10/0.24 lens, in conjunction with an image recording camera with the resolution of 752X582 pixels (equivalent to linear dimensions of 0,82 mm X 0,65 mm), is sufficient for the cell walls to be visible in the image. Of course, the images have their shortcomings as well, especially is we want to apply computer procedures for image analysis. From this point of view, the basic drawbacks are the following:

1. Gaps in the cell walls. These result from poor utilization of light in microscopes using the Nipkov discs. Another reason may be local irregularities of sample slide surface and the resultant "falling out" of parts of the surface from the focal plane.

2. Bright objects within the cells. The image generated is a random section through the tissue. Therefore the positioning of the cell walls with relation to the optical axis can also be random. The image can show, apart from the thin sections of cell walls, also whole walls located approximately perpendicular to the optical axis, visible as brighter spots. Also, bight dots in almost every cell are most probably membranes of fully hydrated cells from the next layer. This element of the image may also be the result of water remaining in the cells after the washing.

As has been mentioned before, the observer will easily spot the cell wall section in the images. However, the extraction of geometrical parameters of the cell skeleton would require manual measurement of a huge number of cells, which appears to be a tedious and difficult task. Therefore, an attempt has been undertaken to develop semi-automatic procedures of quantitative computer analysis of images obtained with TSRLM. The two methods described below have been developed at the Institute of Agrophysics, Polish Academy of Sciences in Lublin.

In the first stage of semi-automatic image analysis, the observer, with the help of a graphics software that has the functionality of layer management (e.g. Corel Draw), traces the contours of cell walls in an additional layer projected in the input image (Fig. 4.13). This makes use of the fact that most cell walls (especially in potato tuber tissue) form straight lines. Therefore, a useful tool is the drawing of lines from point to point where two or more cell walls meet. For the next stage of the analysis it is desirable that the lines join one another, as this renders additional operations on the image unnecessary. This method of image analysis is not applicable when the tissue studied contains a high percentage of intercellular spaces or when there are other cell organs, such as vascular bundles etc. In such a case the cell walls in the section are not straight lines which renders their manual tracing inaccurate or even impossible. However, when such analysis is possible, then the cell wall contours can be exported to a .BMP file (Fig. 4.13) and subjected to further automatic analysis. The automatic analysis

140

is now extremely easy, as all the walls are continuous, have the same thickness, and the pixels in the image have only two values - 0 (for the walls) and 1 (for the cell interior), i.e. the image is binary. In the next stage of the analysis we should divide the image into objects, i.e. cells, and to make the measurements. A useful tool for the purpose is provided by image analysis software packages, e.g. the Aphelion. Using the Watershed morphological operator, we can divide the image into zones or areas (Fig. 4.13). Then the computer will take the geometrical measurements according to given algorithms, separately for each cell.
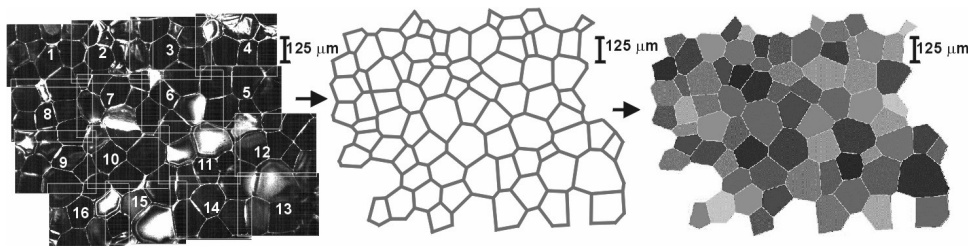
Fig. 4.13. Semi-automatic analysis of images obtained with TSRLM. Example for an image obtained by merging 16 images. The input image (on the left) is traced in a separate layer using Corel Draw, then exported to a .BMP file (middle) and processed, in Aphelion, to the Watershed operator (on the right) which divides the image into objects that are the cells.

The method presented above can be used for image analysis when there is no need for large tissue areas to be examined, as it is tedious and largely dependent on the experience and skills of the operator. Therefore, parallel attempts were made at developing procedures of fully automatic image analysis.

Due to the imperfectness of images obtained with TSRLM, the procedure of their automatic analysis should cover the following operations:

1. Image enhancement, i.e. performance of such transformations that will join the cell walls and that will eliminate from the image all elements which are not cell walls.
2. Conversion of the image into binary form.
3. Identification of objects which are cells.
4. Measurement of the cells.

At present, intensive work is in progress on the development of just such a method. The results are still not quite satisfactory – however, for illustration purposes, one of such methods is described below. The procedure, developed by a Team at the Laboratory of the Mechanics of Agricultural Materials, Institute of Agrophysics, Polish Academy of Sciences, is based on the utilization of morphological operators and logical transformations available in the

141

Aphelion® image analysis software. Figures 4.14 – 4.19 present the successive stages of analysis giving the names of operators applied. The operators, which are operations on the pixels of the image, are clearly defined. However, the parameters of particular operators have to be adapted for each image so as to obtain satisfactory results.
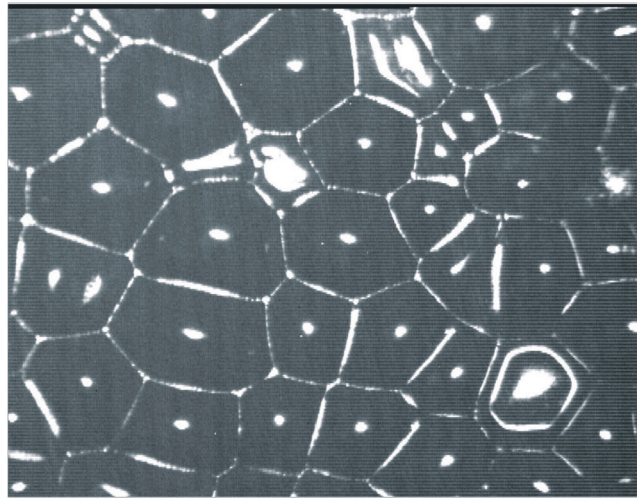

Fig. 4.14. *Example of input image obtained with TSRLM.*
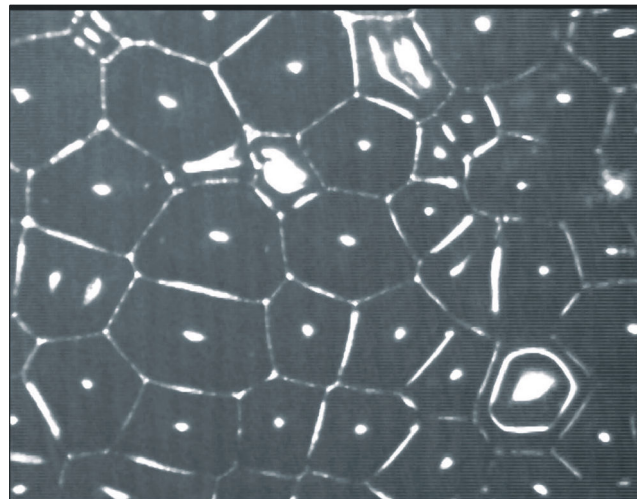
Fig. 4.15. *Smoothing (averaging) of microscope image to eliminate defects resulting from imperfections of the process of acquisition (AphImgMedian5x5).*
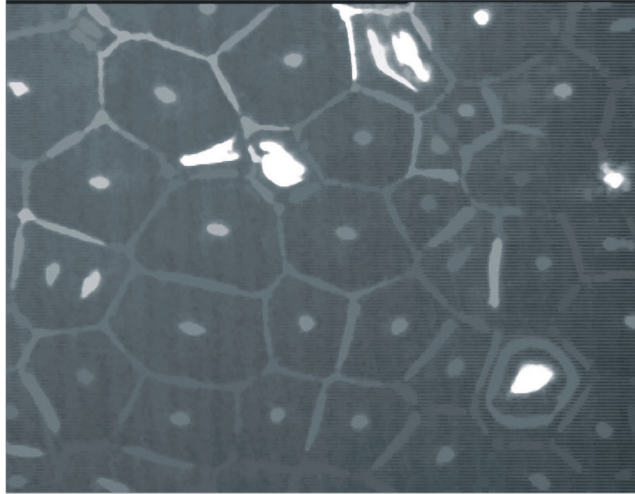
Fig. 4.16. *Combination of erosion, reconstruction and opening up, aimed at the isolation of large bright objects that are not cell walls (AphImgErodeReconsOpen)*

Fig. 4.17. *Difference between images from Fig. 4.15 and Fig. 4.15. Elements highlighted by the preceding transformation have been eliminated from the image analyzed (AphImgSubtract). Additionally, noise inside the cells has been eliminated.*
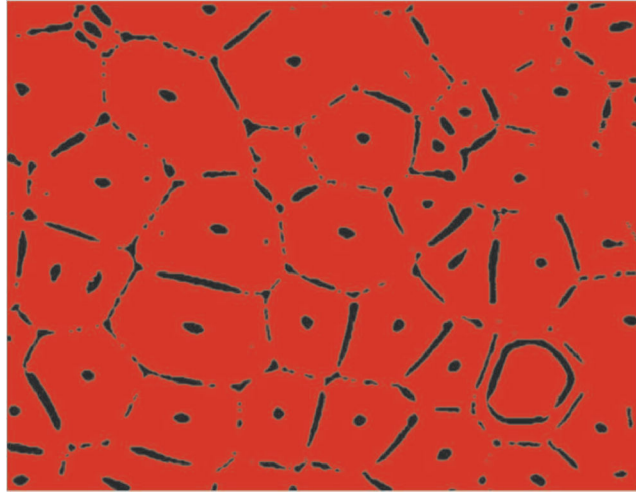
Fig. 4.18. *Binary conversion*

Fig. 4.19. *Erosion*

144
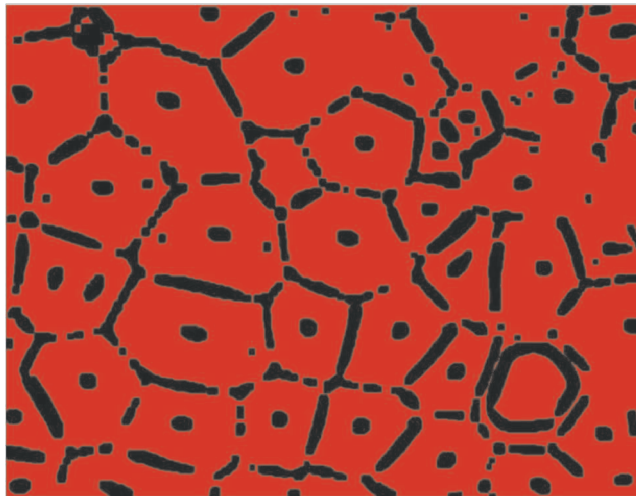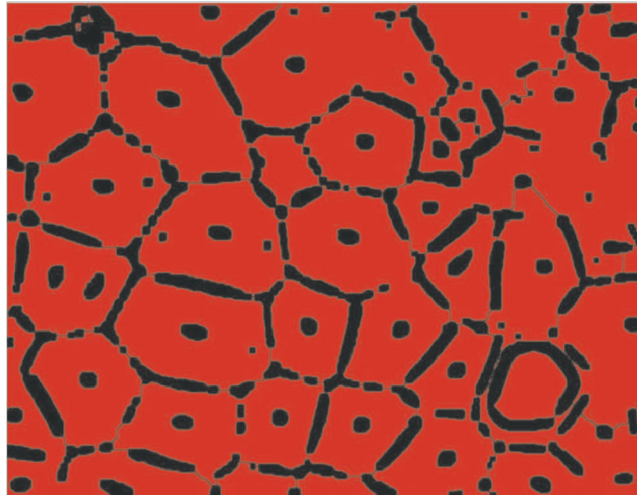
Fig. 4.20. *Division of binary image into convex areas. This transformation yields isolated areas which are „sources" of cells sought in the microscope image. (AphImgClustersSplitConvex)*
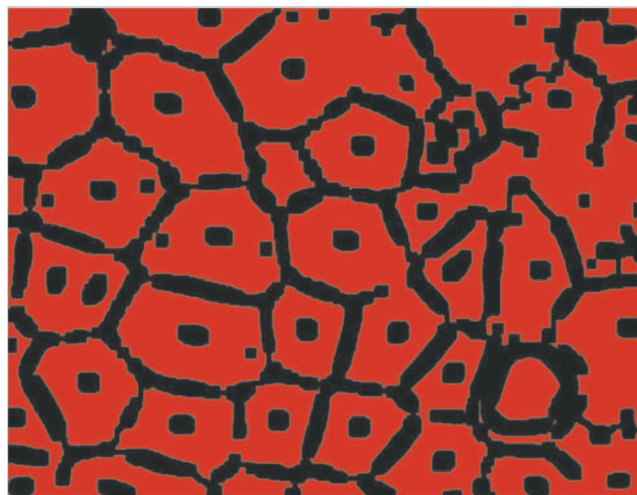

Fig. 4.21. *Repeat erosion.*
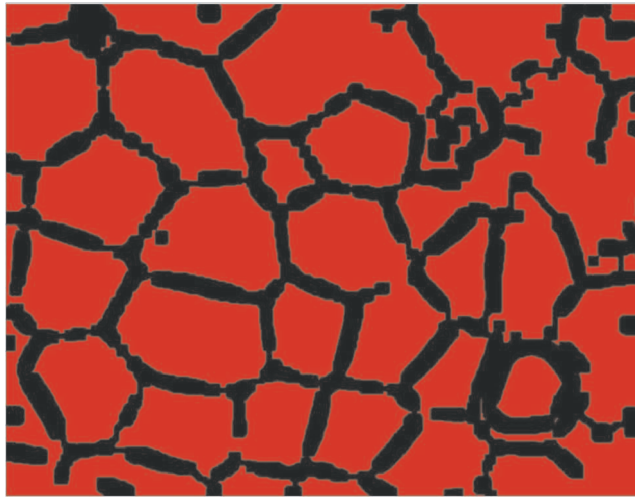
Fig. 4.22. *Hole filling (AphImgHoleFill).*
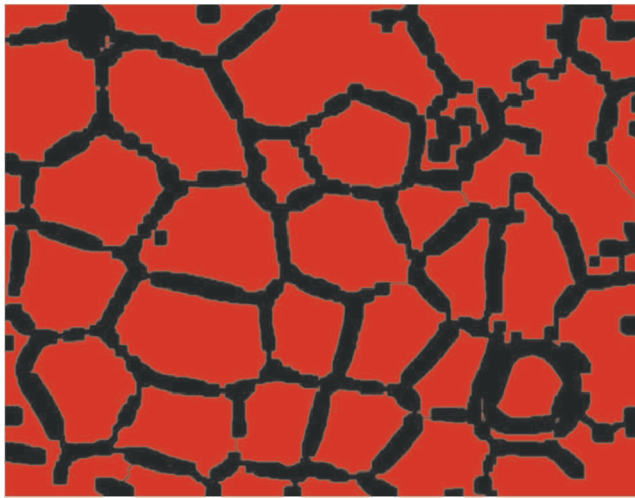
Fig. 4.23. *Repeat division of binary image into convex areas. This transformation yields isolated areas which are „sources" of cells sought in the microscope image. (AphImgClustersSplitConvex).*

**Fig. 4.24.** *Image labelling (AphImgClustersToLabels).*

Fig. 4.25. *Effect of application of the Watershed procedure.*
*(AphImgConstrainedWatershed)*
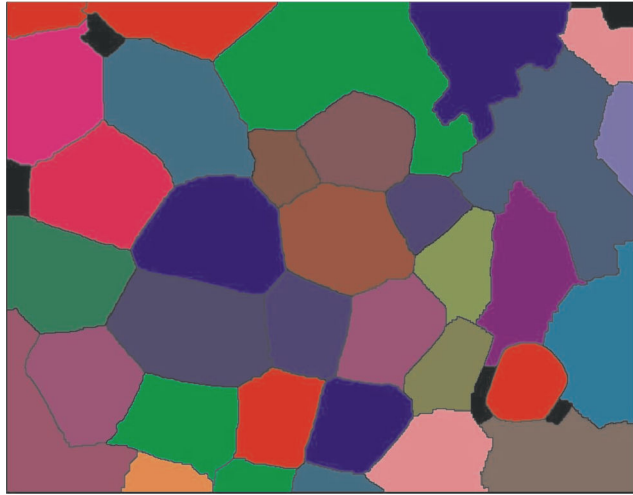
Fig. 4.26. *Elimination (with the opening function) of small objects (AphImgAreaOpen).*
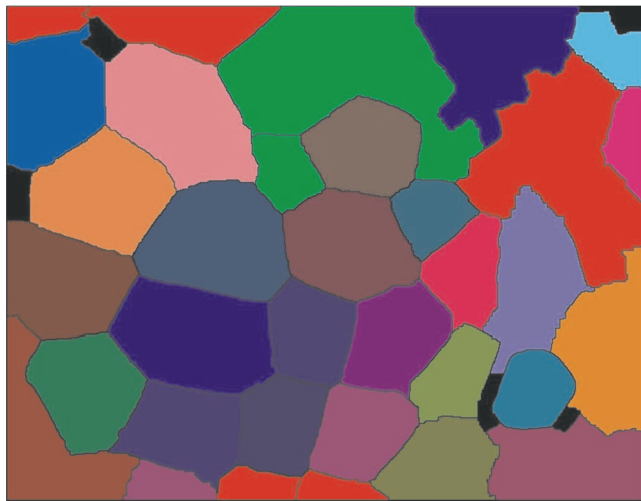
***Fig. 4.27.*** *Repeat labelling (AphImgClustersToLabel).*

148
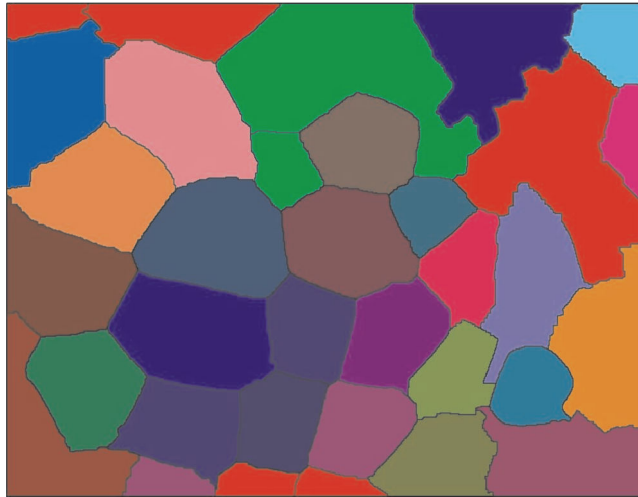
Fig. 4.28. *Repeat watershed detection (AphImgConstrainedWatershed).*

Fig. 4.29. *Elimination of objects not fully contained in the image (AphImgBorderKill).*
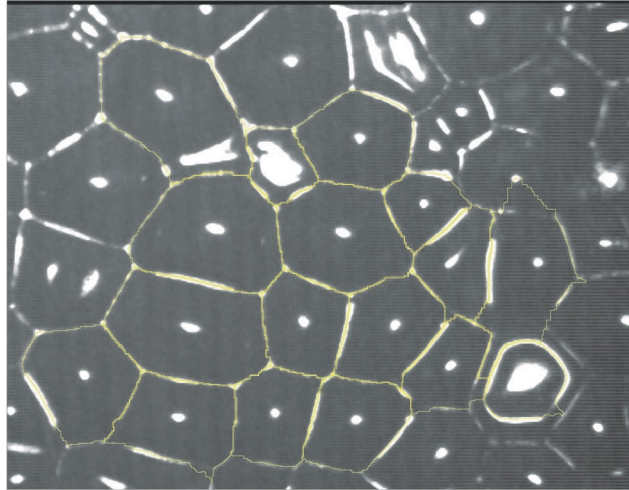
Fig. 4.30. *Cells detected as a result of operation of the automatic image analysis procedure (yellow lines).*

As a result of the analysis, the image from Fig. 4.29 is divided into objects that are to represent cells and measurements can be taken for each of the objects individually, as is the case in the semi-automatic procedure. The image presented in Fig. 4.30 shows the accuracy of the automatic reconstruction. It can be seen that most of the cells in the image have been represented correctly. In other words, the lines of the computer reconstruction coincide with the lines that would be drawn by the observer. Unfortunately, several cells have been omitted by the computer and several objects have been added.

It is possible to assess quantitatively the accuracy of the automatic reconstruction by comparing its results with the results of the semi-automatic analysis. For the potato tuber tissue, where the cell walls in the sections form straight lines, it can be assumed that the semi-automatic method is the reference method due to its high accuracy. Such a comparison was made for 50 different images of potato tuber tissue, obtained with TSRLM. In the automatic analysis, the parameters of the particular operators were the same for all 50 images. The results are presented in Table 4.1 and Fig. 4.31. It can be seen that even such a complex automatic method does not ensure accurate results, as the mean values obtained vary by as much as 30%, and the number of cells (objects identified) is 60% lower that that obtained by the observer! This, however, suggest a promising conclusion: If the mean value - which is the most frequently used estimator of distributions of geometric features of cell sections - differs by "only" 30% as compared to the difference in the number of cells identified (as much

as 60%), then the source of error is not in the loss of cells in the course of the analysis, but rather in wrong routing of lines in the course of the reconstruction. Therefore, if the objective of the study is to obtain reliable mean values of the distribution of geometric parameters of cells, a solution to the problem may be found in the elimination of erroneously reconstructed cells and leaving them out of further measurements. Providing, of course, that the "erroneous" cells do not represent some selected and important type of tissue.

Table 4.1. Mean values of cell area and perimeter in tissue section images obtained with the automatic and semi-automatic methods.

Parameters of cell		semiautomatic analysis	automatic analysis
Area [μm^2]	mean value	12011	17813
	standard deviation	*6134*	*9441*
Perimeter [μm]	mean value	521	712
	standard deviation	*138*	*223*
Number of detected objects		1049	426
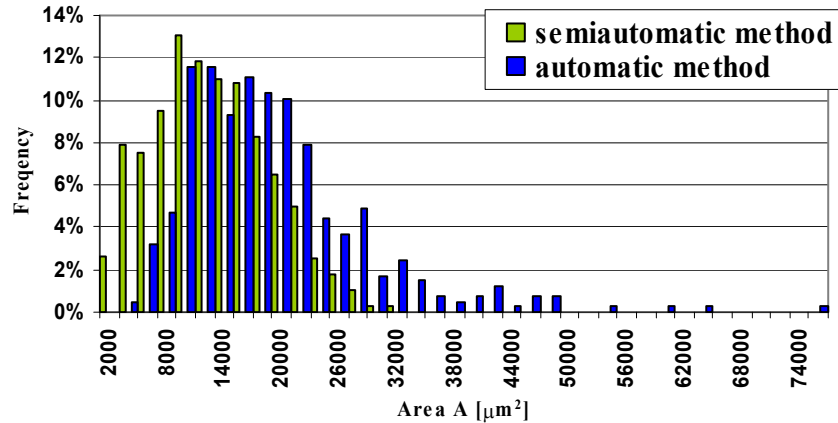
Fig. 4.31. *Distributions of cell sizes in potato tuber tissue sections obtained with the semi-automatic and the automatic methods.*

4.2.3. Analysis of images obtained with CSLM

(On the basis of the publication: Zdunek Z., Umeda M., Konstankiewicz K. with the original title: Method of parenchyma cells parametrisation using fluorescence images obtained by confocal scanning laser microscope. Electronic Journal of Polish Agricultural Universities, Agricultural Engineering, Volume 7 Issue 1, 2004).

Let us stay with the same research objective, i.e. quantitative analysis of the geometric parameters of the cell skeletons of plant tissues. In this Chapter we will concentrate on images obtained with the Confocal Scanning Laser Microscope (CSLM).

In this research a Laser Scanning Confocal Microscope (Olympus Fluoview B50) was used. The microscope uses fluorescence for obtaining images. As it was described before, the application of special fluorescence dyes to cell walls increases the amount of light coming from walls and contrasts with objects inside the cells. In this microscope, the source of light used for excitation was Argon-Ion laser (450-515nm). The observation was carried out using an Uplan FI 10X/0.30Ph1 lens. Images were recorded by digital camera and then transferred to a computer with the resolution of 512 x 512 pixels. At 10X magnification, it corresponds to field of observation of 1.4 mm x 1.4 mm. The magnification can be increased both by changing the lens and by changing the size of the field of observation while resolution remains the same.

4.2.4. Sample preparation and taking images in unbiased way

In order to develop and test the method, potato tuber and carrot were chosen as examples of soft plant materials. Potato samples were taken from the centre of the tuber, i.e. inner core, and carrot samples were taken from the outer part of the root, about 5mm from the skin. These tissues have significant differences in cell size and textural parameters that are important from the point of view of sample preparation, microscopic observation and image analysis. Thus they are suitable for test the method for reconstruction quality. On the other hand, these tissues contain only about 1% intercellular spaces of tissue volume, thus they will not influence results significantly.

A procedure of sample preparation was found experimentally where the criterion was cells distinction as clear as possible. Following settings of sample preparation have been found for parenchyma tissue:
1. Cutting cylindrical samples with dimensions of 7 mm X 10mm (diameter X height) and gluing to microslicer table.
2. Slicing by razor blade (using microslicer D.S.K., DTK-1000) into cylindrical slices with diameter equal to 7 mm and thickness of 300 micrometers for carrot and 500 micrometers for potato. This thickness is optimal for samples

in natural state maintaining high slice stiffness in order to prevent its folding and mechanical damage to cells during handling.

3. Staining in aqueous *Coriphosphine O* solution (excitation wavelength - 460 nm, emission wavelength - 575 nm) for 10s and next washing in tap water for about 10s. This dye is used for pectin staining that in the case of parenchyma tissue bond cell to cell. The time of dying and washing should be the shortest possible to avoid slices swelling because of water transportation between tissue and external aqueous media.

4. Drying the slice and mounting on microscopy slide. The slice is placed on microscopic slide and carefully drained off by tissue paper that causes its sticking to the slide as well. Cover slides are not used, thus maximal observation time cannot be longer than 5 minutes. After this time changes in geometry and size of the cells are visible under the microscope.

It should be emphasized that the above procedure takes no longer than 1 minute for one slice.

In order to test the quality of reconstruction, 10 slices of potato and 10 slices of carrot were analyzed.

The Confocal Scanning Laser Microscope allows obtaining 2D grey (0-255) images from different layers, however images taken from the slice surface are the most suitable for automatic analysis. According to Stereology, images should be taken (sampled) in unbiassed way if we would like to describe 3D structure by 2D images. Therefore, in the present experiment images are taken in 3 parallel rows, but the distances between rows and between images in rows are random. 10 images are taken from each slice, which takes about 4-5 minutes (Fig. 4.32).
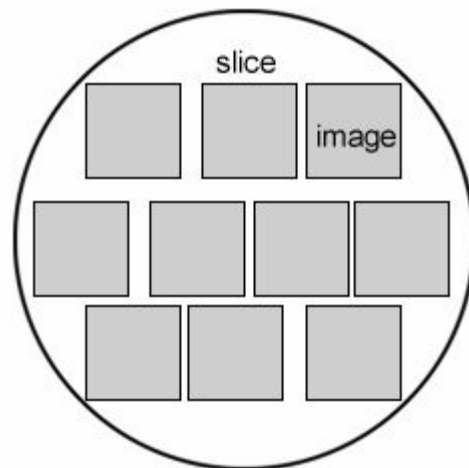
Fig. 4.32. *Method of unbiased taking of images from tissue slice. Rows are parallel, but distances between rows and between images in rows are random.*

4.2.5. Procedure of image analysis

Examples of obtained microscopy images of potato tuber and carrot root are shown in Fig. 4.33. In order to show problems during computer analysis, the presented images have average quality and they are relatively difficult for computer analysis.
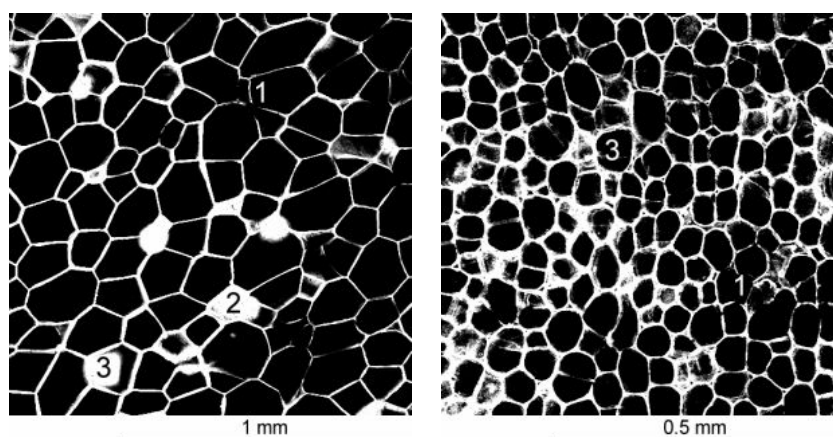

Fig. 4.33. *Images of potato tissue (left image) and carrot root (right image) obtained by Confocal Scanning Laser Microscope. 1 - "broken" walls, 2 - cells bottoms, 3 - nonparallel walls to observation axis.*

Dye used in the experiment stains pectins between cell walls, hence only the walls should be visible in the images. These walls create polygonal (for potato) or round objects (for carrot) that are cells or intercellular spaces. It is not possible to distinguish these two different structures in this method. However, potato and carrot contain small amount of intercellular spaces, thus we can assume that cells are visible in images, mainly. Most of the cell walls are clearly seen (grey level close to 255) and contrast with the remaining area (grey level close to 0) of the image is high. Unfortunately, there are walls whose grey level is close to background or they are completely invisible ("broken" walls shown in spot No. 1 in Fig. 4.33). This can be a result of bad fluorescence or uneven slice surface in these places. Other areas difficult for computer analysis are bottoms of cells (spot No. 2 in Fig. 4.33) or walls nonparallel to observation axis (spot No. 3 in Fig. 4.33). If a cell bottom or a nonparallel wall is located in the focal plane, these will look in images as oval white areas or unusually thick walls. This problem appears especially for carrot tissue where cells are very small, thus even for thinnest focal layer there is high probability that nonparallel walls and cell bottoms will be visible in images.

Therefore, the tasks of the computer procedure are: 1) to link "broken" walls, 2) to remove oval white areas that are not cells but to retain the adjacent walls, 3) to separate cells and to measure their geometrical parameters. According to this, a special computer procedure was developed containing series of morphological operators [13]. A combination of four operators was used in this research, in the following sequence: *DilateReconsClose*, *ThinSkeleton*, *Watershed*. Each operator is already defined and available in commercial software for image analysis. In this research the Aphelion® image analysis software was used. *DilateReconsClose* (Fig. 4.34) works similar to the *Close* operator, but has the advantage of preserving shape contours since the *Reconstruction* step recovers part of what was lost after *Dilation* [13]. In this operator, the size and shape of a structural element can be adjusted according to analyzed images. The structural element is applied to each pixel and changes it according to conditions defined in *DilateReconsClose* operators. Thus, breaks between walls can be linked in this way if the structural element is big enough. Undesirable result of this operator is filling small cells too. We have found experimentally for tested images that square structural element with side equal to 4 pixels is optimal for analyzed images. *ThinSkeleton* (Fig. 4.35) operator finds image skeleton of thickness of 1 pixel [13]. The purpose of this operator is to find borders between cells and to change oval white areas into elements with branch appearance. Next, *Watershed* (Fig. 4.36) operator detects only closed regions in images thus branches (previously oval white areas) disappear in this step. After this, each remaining object shown in Fig. 4.36 in different colour is labelled and is treated separately. Objects divided by image border are removed from further analysis. The procedure works in a loop thus it can be applied for any number of images automatically.
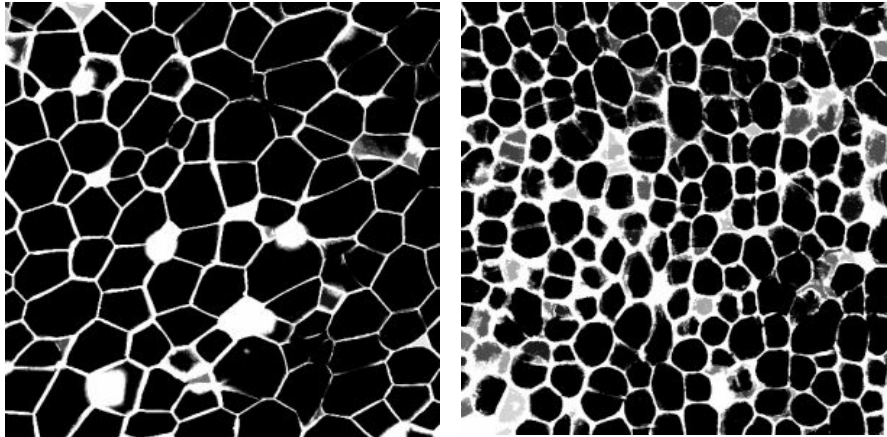
Fig. 4.34. *Result of DilateReconsClose operator application to images of potato (left image) and carrot (right image). The structural element is square with side equal to 4 pixels.*
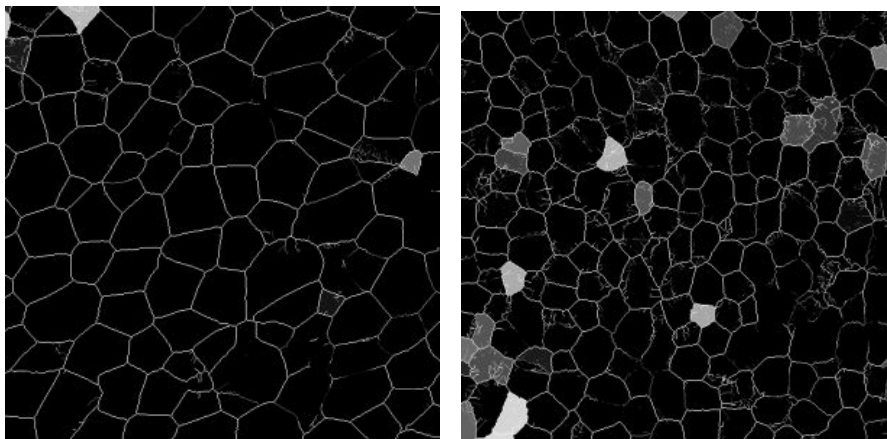
Fig. 4.35. *Result of ThinSkeleton operator application to image of potato (left image) and carrot (right image).*
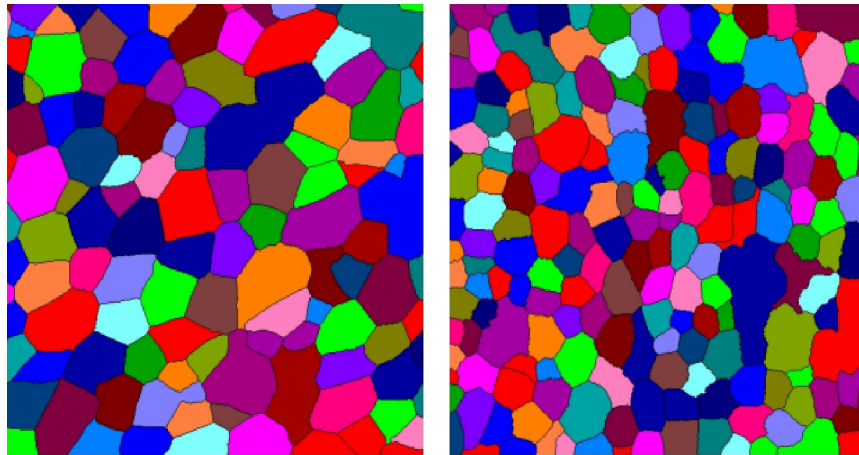
Fig. 4.36. *Result of Watershed operator application to image of potato (left image) and carrot (right image).*
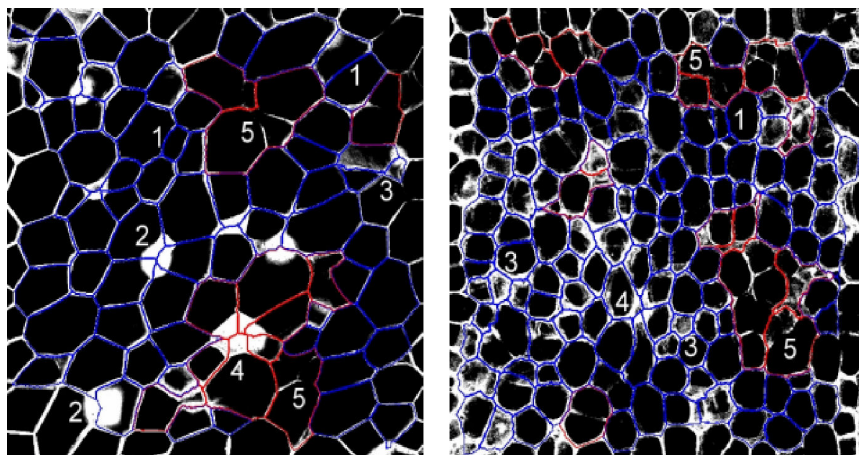

Fig. 4.37. *Cell reconstruction for potato (left image) and for carrot (right image) shown as blue lines. Objects in images not correctly reconstructed and deleted from further analysis are shown in red. Places in images correctly reconstructed: 1 – linked walls, 2 – oval white areas changed into lines, 3 – cells filled by pixels of low grey level. Places in images incorrectly reconstructed: 4 – polygonal shapes, 5 – objects containing more than one cell.*

In Fig. 4.37 the final cell reconstruction sketch is shown. Most of the cells are reconstructed correctly for both tested materials. Lines of the reconstruction lie on the original walls and some of the breaks are linked (example: No. 1 in Fig. 4.37, please compare with Fig. 4.33). Oval white areas like No. 2 in Fig. 4.37 are changed into lines lying around their middle. Another positive aspect of the procedure is correct cells separation filled by pixels of low grey level, seen in images as grey points (places No. 3 in Fig. 4.37).

However, despite image processing and improving, there are still cells not correctly reconstructed. Big objects containing two or more cells being a result of long breaks in walls are the most important for result of analysis (No. 5 in Fig. 4.37). Other problematic places are objects completely white with a polygonal shape (No. 4 in Fig. 4.37). These objects are probably cells, too, but their bottom is placed in focal layer of the microscope. These objects are incorrectly recognised as thick walls. Therefore, neighbouring cells become bigger than in reality. Because the aim of this work is analysis as fully automatic and efficient as possible, these problems cannot be completely avoided. Each image is different and taking into consideration all the cases by changing operators or changing their sequence is very difficult. Therefore, we have decided to introduce into computer procedure the possibility of manual checking and correcting of reconstruction quality. After cell labelling, reconstruction sketch is displayed over the original image (like in Fig. 4.37). Now the observer can decide which object is reconstructed incorrectly and delete it from analysis by clicking on the object and choosing the proper option. Examples of objects deleted in the case of presented images are marked in red in Fig. 4.37. It should be stressed here that not each image requires correction, but if any correction is necessary, the time of this operation is about 30 second per image for an experienced observer.

4.2.6. Geometrical parameters distribution and estimation of reconstruction error

For the remaining objects, the procedure measures their geometrical parameters. Similar to the work of Konstankiewicz et. al. (2001): *cell area*, *elongation*, *Feret's Max.diameter* and *Feret's Min. diameters* were chosen as the basic geometrical parameters of cells. *Elongation E* is given by the equation $E = (a - b) / (a + b)$, where a and b are longer and shorter axes of ellipse of best fit inside the cell, respectively. *Feret's Max.* and *Min.* d*iameters* are defined as longer and shorter sides of rectangle of best fit outside the cell, respectively. In order to estimate error of incorrect cell reconstruction, measurements were done before correction and after correction. For potato, the number of reconstructed cells from 100 images (size 1.4 x 1.4 mm) is 5763 before correction

and 5617 after correction. For carrot, the number of obtained cells from 100 images (size 0.7 x 0.7 mm) is 5144 before correction and 4520 after correction.

Results of measurements are shown in Fig. 4.38 for potato and Fig. 4.39 for carrot in the form of histograms. They have normal distribution: symmetrical for *Feret's diameters* and little skewed to the left for *area* and *elongation*. Mean values of cell geometrical parameters before and after correction with standard deviations are shown in Table 4.2. Comparing mean values from Table 4.2, it is clearly visible that potato is built of bigger cells than carrot. Linear dimensions (*Feret's diameters*) of potato cells are more than twice longer. However, the shape parameter *elongation* of potato cells is similar to that of carrot cells.

Figures 4.38 and 4.39 show that histograms after correction are similar to histograms before correction and it is difficult to estimate any changes. Especially potato reconstruction looks correct; only few points of histograms are not covered completely (Fig. 4.38). For carrot, the influence of correction is more significant. Points of left side of histograms obtained after correction lie higher and some points of right side lie lower than before correction (Fig. 4.39).

Table 4.2. Mean cell geometrical parameters, standard deviations and λ values of Kolmogorov-Smirnov test. Non-significant differences of results distributions are marked as "*" when $\lambda < \lambda_\alpha$. $\lambda_\alpha = 1.358$ ($\alpha = 0.05$).

| Cell parameter | Mean | | Std. Dev. | | λ |
	before correction	after correction	before correction	after correction	value of K-S test
	Potato				
Area [micrometer^2]	15383	15188	7655	7253	0,419*
Elongation	0,302	0,297	0,155	0,152	0,470*
Feret's Max.diameter [micrometer]	160	159	43,2	40,5	0,280*
Feret's Min.diameter [micrometer]	126	126	35,5	34,7	0,562*
	Carrot				
Area [micrometer^2]	2462	2230	2099	1151	1,266*
Elongation	0,332	0,320	0,174	0,168	1,384
Feret's Max.diameter [micrometer]	66,0	62,8	24,1	17,5	1,729
Feret's Min.diameter [micrometer]	50,1	48,4	16,5	13,2	1,284*

In order to test the hypothesis that cells geometrical parameters before and after correction have the same distributions, the Kolmogorov-Smirnov λ test at critical value $\lambda_\alpha = 1.358$ (where $\alpha=0.05$) was used. In Table 4.2, λ values are shown and non-significant differences of distributions are marked as "*" when $\lambda < \lambda_\alpha$. Analysis has shown that differences of histograms are not significant for all potato cells parameters, however for carrot *elongation* and *Feret's Max. diameter* have been changed significantly after correction.

Table 4.2 shows that mean values of all geometrical parameters decrease after correction for both potato and carrot, even if the Kolmogorov-Smirnov test does not show significant differences of histograms. It means that in correction process mainly big objects were deleted as a result of "broken walls". However, changes for carrot are bigger. For example, mean cell area has decreased by about 10% after correction comparing to 1% for potato. This is a result of the overall quality of carrot images that are worse than potato images. If we compare the number of cells after and before correction, we will see that the number of deleted objects for carrot is much higher: 624 (12%) deleted objects for carrot and only 146 (2,5%) for potato. The above result shows that correction would be not necessary when source images have relatively good quality, like in the case of potato tuber inner core where the change in results after correction is only about 1%. On the other hand, results after correction are shifted always towards lower values, therefore it can be considered as a systematic error of the method that is about 1% for potato tuber inner core and lest than 10% for carrot tissue of external part of root. However, this error is different for different tissues and thus should be estimated for every kind of tissue individually if we decide not to correct images.
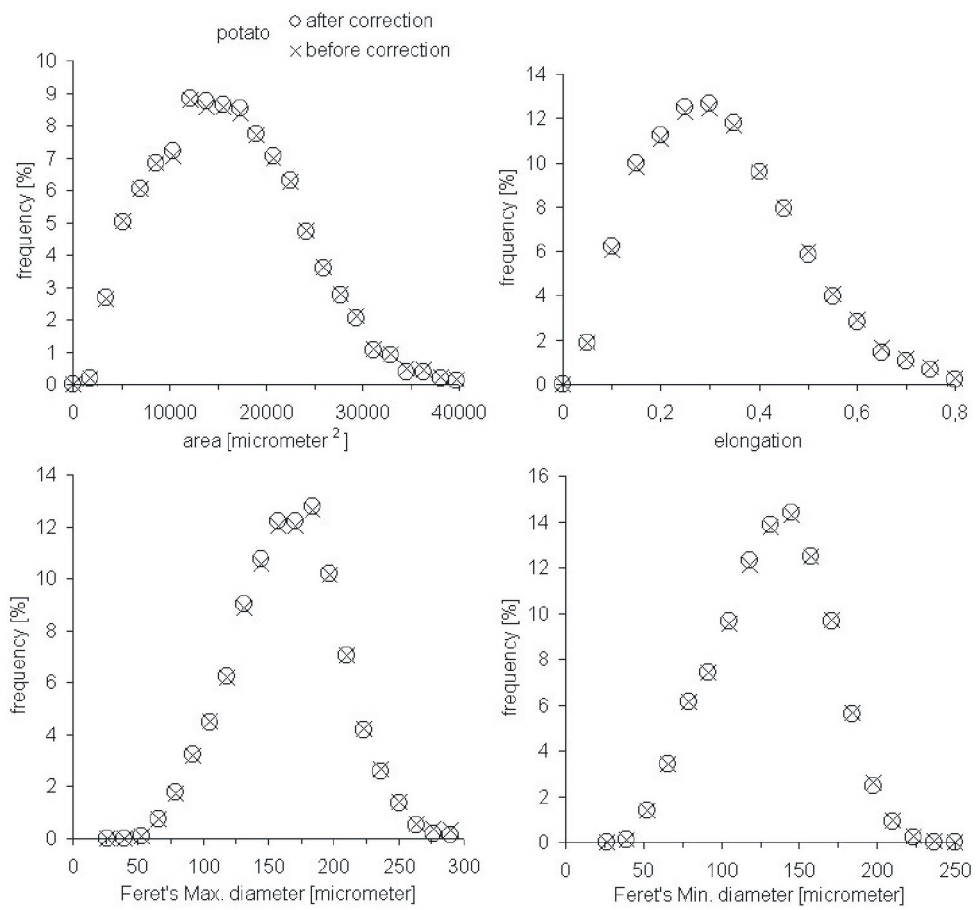
Fig. 4.38. *Histograms of cell area, elongation, Feret's Max. diameter and Feret's Min. diameter before and after correction obtained for potato.*
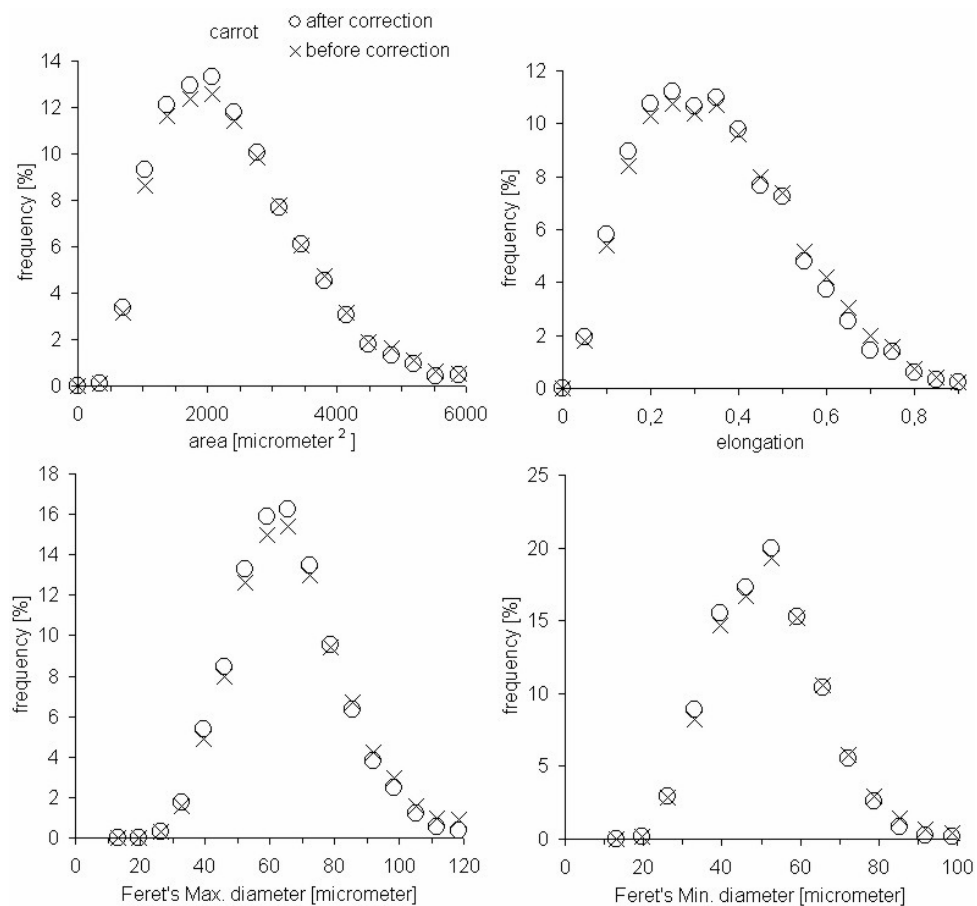
Fig. 4.39. *Histograms of cell area, elongation, Feret's Max. diameter and Feret's Min. diameter before and after correction obtained for carrot.*

4.2.7. Reconstruction of highly heterogeneous parts of tissue

Tests with different types of tissues have shown that the properties of investigated materials play an important role for reconstruction. When a tissue is relatively homogenous, slicing in natural state by razor blade gives good results. Unfortunately, when the tissue consists of objects like vascular bundles with different mechanical properties, for example, cutting does not give a smooth surface. In this case, it is difficult to obtain proper image for analysis. Additionally, having big differences between sizes of objects in the same image or among a group of images makes is difficult to choose a universal structural element of *DilateReconsClose* operator. Thus, images or even their fragments

162

should be analyzed separately. An example is shown in Fig. 4.40 for carrot tissue taken from centre of root where the structure is very heterogeneous. When structural elements of *DilateReconsClos* operator equal 4 - big cells are reconstructed correctly (No. 1 in Fig. 4.40), but small object like vascular bundles in the left side of image (No. 2 in Fig. 4.40) are reconstructed poorly. On the other hand, applying the same operator with structural element equal 2 improves the reconstruction of small elements (No. 2 in Fig. 4.40) but some bigger cells are divided into smaller objects (No. 1 in Fig. 4.40).
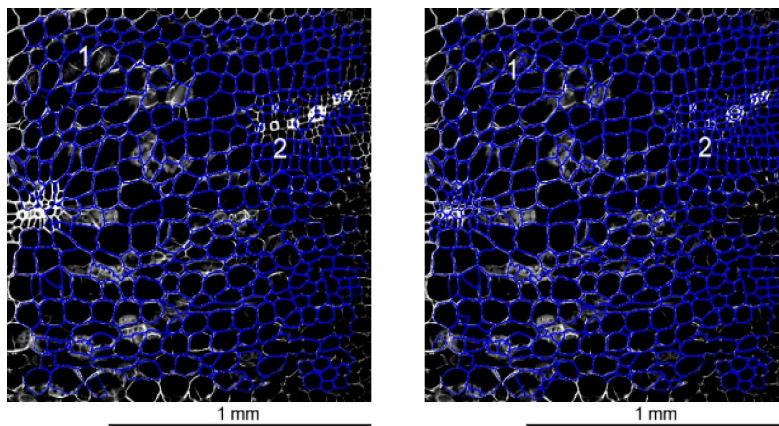

Fig. 4.40. *Reconstruction of carrot tissue taken from centre of root with DilateReconsClos square structural element with side equals 4 pixels (left image, 1 – cell reconstructed correctly, 2 – cells reconstructed incorrectly) and side equals 2 pixels (right image, 1 – cell reconstructed incorrectly, 2 – cells reconstructed correctly).*

Generally, an image analysis procedure does not depend on image size. Therefore, similarly to what was shown for images from TSRLM, the procedure for CSLM can be applied for stitched images. In this case, the unbiased way of collecting images from a slice is replaced by taking overlapped images in a raster pattern, as in Fig. 4.41. The images can be merged manually or automatically by computer using for example Aphelion® or Adobe Elements® software. An advantage of analysis of larger areas is the possibility of observation of homogeneities or non-homogeneities within a tissue. This is clearly visible in Fig. 4.42 where merged images after image analysis are shown.

163
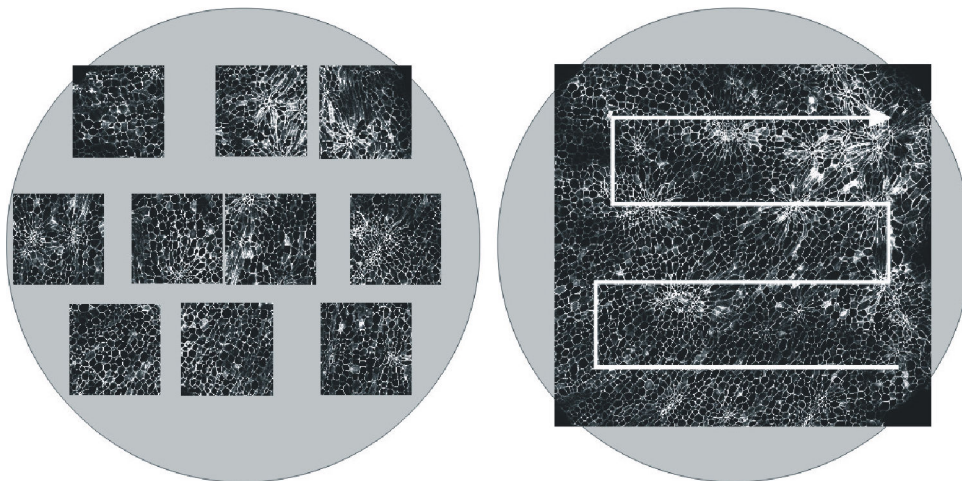
Fig. 4.41. *Two ways of collecting images for analysis: unbiased way (left image) and raster pattern (right image).*


a) ⎯⎯⎯ 1 mm ⎯⎯⎯

b)
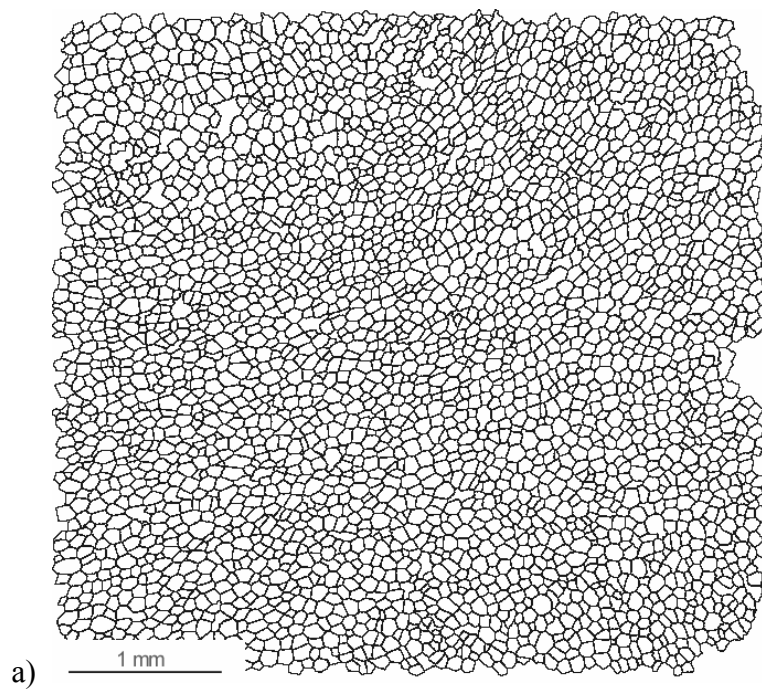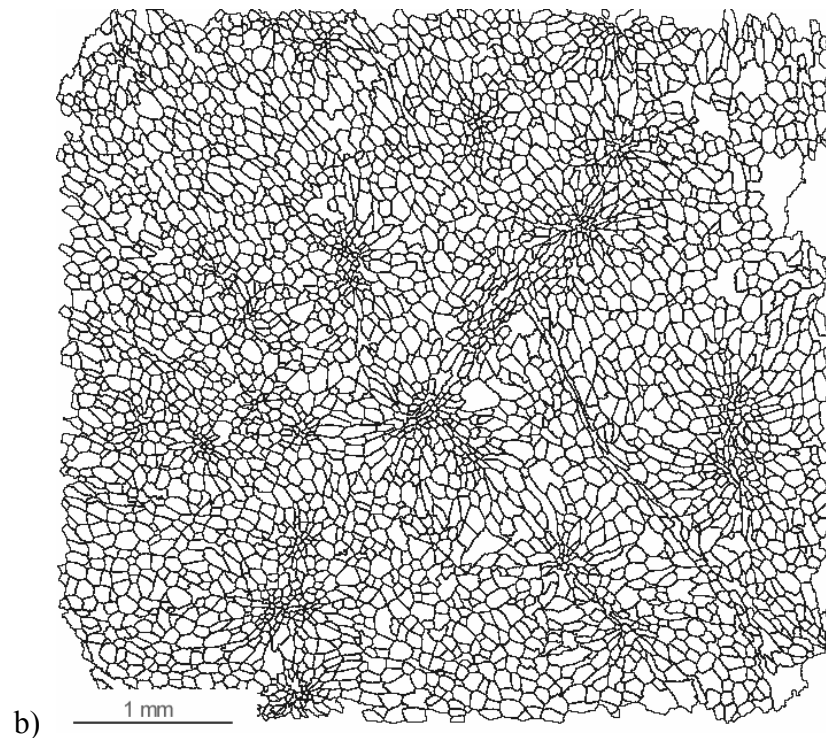
Fig. 4.42. Result of reconstruction of potato tuber tissue (a) and carrot tissue (b) as examples of homogeneous and heterogeneous structures of plant tissues.

The presented method of reconstruction and parameterisation of plant tissue cellular skeleton for images obtained by CSLM is a unique combination of sample preparation, image obtaining and image analysis. Advantages of the developed method are:

1. Correct cell reconstruction because of proper combination of image quality and automatic computer image analysis.
2. Error of automatic cell reconstruction is about 1% for potato tissue taken from inner core of tuber and 10% for carrot tissue taken 5 mm under the skin of root. Manual correction of reconstruction allows avoiding this error.
3. Method is universal for materials with different structures like potato and carrot. Only one parameter is adjusted to improve reconstruction of more heterogeneous parts of tissues.
4. Fast image obtaining. It takes only about 1 minute for slice preparation and about 4-5 min per one slice to take 10 images.

165

5. Automatic image analysis of high number of images. Analysis of 100 images and obtaining parameters of about 5000 cells takes no more than 40 minutes with correction and only about 5 minutes without correction for P4 class computer.

REFERENCES

1. Konstankiewicz K., Pawlak K., Zdunek A., 2001: Quantitative method for determining cell structural parameters of plant tissues. *Int. Agrophysics* 15, 161-164.
2. Wojnar L., Majorek M., 1994. Computer analysis of images (in Polish). Fotobit-Design.
3. Konstankiewicz K., Czachor H., Gancarz M., Król A., Pawlak K., Zdunek A., 2002: Cell structural parameters of potato tuber tissue. Int. Agrophysics, 16, 2, 119-127.
4. Konstankiewicz K., Guc A., Stoczkowska B., 1998: Determination of the structure parameters of potato tuber tissue using specialistic image analysis program. Pol. J. Food Nutr. Sci., Vol.7/48, 3, 59
5. Konstankiewicz K., 2002: Determination of geometrical parameters of plant tissue cellular structure (in Polish), Acta Agrophysica, 72, 61-78.